

AD-A256 400

## REPORT DOCUMENTATION PAGE

Form Approved

GSA No. 0704-0188

Please reporting burden for this collection of information is estimated to average 1 hour per response, including the time for reviewing instructions, searching existing data sources, gathering and maintaining the data needed, and completing and reviewing the collection of information. Send comments regarding this burden estimate or any other aspect of this collection of information, including suggestions for reducing this burden, to Washington Headquarters Service, Directorate for Information Operations and Reports, 1215 Jefferson Davis Highway, Suite 1204, Arlington, VA 22202-4302, and to the Office of Management and Budget, Paperwork Reduction Project (0704-0188), Washington, DC 20503.

1. AGENCY USE ONLY (Leave blank)

2. REPORT DATE

3. REPORT TYPE AND DATES COVERED

ANNUAL 15 May 91 TO 14 May 92

4. TITLE AND SUBTITLE

CYTOCHEMICAL ORGANIZATION OF THE RETINO-SUPRACHIASMATIC SYSTEM

5. FUNDING NUMBERS

AFOSR-90-0072

61102F

2312

A3

AUTHOR(S)

DR VAN DEN POL

PERFORMING ORGANIZATION NAME(S) AND ADDRESS(ES)

Dept of Neurosurgery  
Yale University School of Medicine  
333 Cedar Street  
New Haven, CT 06520

AFOSR-TR-

6. PERFORMING ORGANIZATION REPORT NUMBER

92 0909

SPONSORING/MONITORING AGENCY NAME(S) AND ADDRESS(ES)

Dr Genevieve M. Haddad  
AFOSR/NL  
Building 410  
Bolling AFB DC 20332-6448

7. SPONSORING/MONITORING AGENCY REPORT NUMBER

11. SUPPLEMENTARY NOTES

DTIC  
ELECTE  
S OCT 14 1992 D

12a. DISTRIBUTION/AVAILABILITY STATEMENT

Approved for public release;  
distribution unlimited

12b. DISTRIBUTION CODE

13. ABSTRACT (Maximum 200 words)

One of the approaches that we have spent alot of energy on is the analysis of the calcium behavior of cultured cells from the SCN. Using digitally enhanced video imaging, we have studied the responses of both neurons and glial cells to glutamate and to several other substances found in the SCN. It has been taken several years to get the apparatus functioning, but we are now in a good position to make use of both the low light computer enhanced video system and the confocal laser scanning microscope to study the behavior of living SCN cells. One of the strong advantages of this approach is that single cells can be studied, or interacting groups of cells can be studied simultaneously.

92-27030 39



pgs

425639

14. SUBJECT TERMS

15. NUMBER OF PAGES

16. PRICE CODE

17. SECURITY CLASSIFICATION OF REPORT

(U)

18. SECURITY CLASSIFICATION OF THIS PAGE

(U)

19. SECURITY CLASSIFICATION OF ABSTRACT

(U)

20. LIMITATION OF ABSTRACT

(UL)

# Yale University

Section of Neurosurgery  
Research Laboratories  
School of Medicine  
333 Cedar Street  
P.O. Box 3333  
New Haven, Connecticut 06510-8062

Campus address:  
LSOG 221  
333 Cedar Street  
Telephone: 203 785-2597  
Fax: 203 737-2159

Dr Genevieve Haddad  
Program Director  
Chronobiology Program  
Air Force Office of Scientific Research

Aug. 3, 1992

Dear Dr. Haddad:

This letter is in part a Progress Report at the end of the second year of support from the Chronobiology Program of the AFOSR.

One of the approaches that we have spent a lot of energy on is the analysis of the calcium behavior of cultured cells from the SCN. Using digitally enhanced video imaging, we have studied the responses of both neurons and glial cells to glutamate and to several other substances found in the SCN. It has been taken several years to get the apparatus functioning, but we are now in a good position to make use of both the low light computer enhanced video system and the confocal laser scanning microscope to study the behavior of living SCN cells. One of the strong advantages of this approach is that single cells can be studied, or interacting groups of cells can be studied simultaneously.

We have an extensive report which was just published (Journal of Neuroscience, 1992) describing the calcium response of both neurons and glia to glutamate, serotonin, and extracellular ATP. The data in the following abstract of that paper describe some of our findings there.

To study the calcium responses of the cellular components that make up the clock in the SCN, computer-controlled digital video and confocal scanning laser microscopy were used with the  $\text{Ca}^{2+}$  indicator dye fluo-3 to examine dispersed SCN cells and SCN explants with repeated sampling over time.  $\text{Ca}^{2+}$  plays an important second messenger role in a wide variety of cellular mechanisms from gene regulation to electrical activity and neurotransmitter release, and may play a role in clock function and entrainment.

SCN neurons and astrocytes showed an intracellular  $\text{Ca}^{2+}$  increase in response to glutamate and serotonin, two major neurotransmitters in afferents to the SCN. Astrocytes showed a marked heterogeneity in their response to the serial perfusion of different transmitters; some responded to both serotonin and glutamate, some to neither, and others to only one or the other. Under constant conditions, most neurons showed irregular temporal patterns of  $\text{Ca}^{2+}$  transients. Expression of regular neuronal oscillations could be blocked by the inhibitory transmitter GABA. Astrocytes, on the other hand, showed very regular rhythms of cytoplasmic  $\text{Ca}^{2+}$  concentrations with periods ranging from 7 to 20 seconds. This periodic oscillation could be initiated by in vitro application of glutamate, the putative neurotransmitter conveying visual input to the SCN critical for clock entrainment. Long distance communication between glial cells, seen as waves of fluorescence moving from cell to cell, probably through gap junctions, was induced by glutamate, serotonin, and ATP. These waves increased the period length of cellular  $\text{Ca}^{2+}$  rises to 45 to 70 sec. Spontaneously oscillating cells were common in culture medium, serum, or rat cerebrospinal fluid, but rare in HEPES buffer.

One source for cytoplasmic  $\text{Ca}^{2+}$  increases was an influx of extracellular

12 SEP 1992

$\text{Ca}^{2+}$ , as seen under depolarizing conditions in about 75% of the astroglia studied. Neurotransmitter-induced  $\text{Ca}^{2+}$  fluxes were not dependent on voltage changes, as  $\text{Ca}^{2+}$  oscillations could be initiated under both normal and depolarizing conditions. Since neurotransmitters could induce a  $\text{Ca}^{2+}$  rise in the absence of extracellular  $\text{Ca}^{2+}$ , the mechanisms of ultradian oscillations appear to depend on cycles of intracellular  $\text{Ca}^{2+}$  fluxes from  $\text{Ca}^{2+}$  sequestering organelles into the cytoplasm, followed by a subsequent  $\text{Ca}^{2+}$  reduction.

In the adult SCN fewer astrocytes are found than neurons, yet astrocytes frequently surround glutamate immunoreactive axons in synaptic contact with SCN dendrites, isolating neurons from each other while maintaining contact with other astrocytes by gap junctions.

Neurons and glia respond to neurotransmitter application with a variety of  $\text{Ca}^{2+}$  responses; both may play a role in the function of the SCN, and their interaction may explain several aspects of mammalian clock physiology not easily explained solely on the basis of our current understanding of axonally mediated neurotransmission.

We have also finished several studies on amino acid neurotransmitters in the SCN, based on immunogold cytochemistry. In one we found that almost 50% of all axons making synaptic contact with SCN neurons contain GABA immunoreactivity. Similar findings were made with antisera against the GABA synthesizing enzyme glutamate decarboxylase (Decavel and van den Pol, 1990). Along similar lines, we found high densities of immunoreactive glutamate in presynaptic terminals in the SCN (van den Pol, 1991). The SCN sends efferent axons to several loci; one of these is the paraventricular nucleus. As in the SCN, GABA immunoreactivity is found in about half of all presynaptic terminals in the paraventricular nucleus (Decavel and van den Pol, 1991). With intracellular recording, we found that glutamate may be the dominant excitatory transmitter in the paraventricular nucleus: most of the postsynaptic response to release of the endogenous transmitter could be blocked by specific glutamate antagonists, particularly CNQX which blocks non-NMDA glutamate type receptors.

Using in situ hybridization we have examined the expression of different glutamate receptor genes in the suprachiasmatic nucleus and surrounding areas of the hypothalamus. We find that some of the AMPA and kainate type of glutamate receptors are expressed at low levels in the SCN (van den Pol, Hermans-Borgmeyer, van den Pol, 1992).

List of recent papers published with support from the chronobiology program AFOSR.

van den Pol, A.N. (1991) Glutamate and aspartate immunoreactivity in hypothalamic presynaptic axons. Journal of Neuroscience, 11: 2087-2101.

van den Pol, A.N. (1991) The suprachiasmatic nucleus: morphological and cytochemical substrates for cellular interaction. In The Mind's Clock, D.C. Klein, R.Y. Moore, S.M. Reppert (Eds.), Oxford Univ. Press, New York, pp. 17-50.

Decavel, C. and A.N. van den Pol (1992) Converging GABA- and glutamate-immunoreactive axons make synaptic contact with identified hypothalamic neurosecretory neurons. Journal of Comparative Neurology 316: 104-116.

van den Pol, A.N., S.M. Finkbeiner, A.H. Cornell-Bell (1992) Calcium

excitability and oscillations in suprachiasmatic nucleus cells in vitro.  
Journal of Neuroscience, 12: 2648-2684.

**Abstracts.**

van den Pol, A.N., S. Finkbeiner, A. Cornell-Bell (1991) Ultradian calcium oscillations in suprachiasmatic nucleus cells. Soc. Neurosci. Abstr. 17: 25.

van den Pol, A.N., I. Hermans-Borgmeyer and S. Heinemann (1992) Glutamate receptor gene expression in hypothalamus: in situ hybridization with 7 receptor subtypes. Soc. Neurosci. Abstr. 18: In Press.

<b>Accession For</b>	
NTIS GRA&I	<input checked="checked" type="checkbox"/>
DTIC TAB	<input type="checkbox"/>
Unannounced	<input type="checkbox"/>
Justification	
By	
Distribution/	
Availability Codes	
Dist	Avail and/or Special
A-1	

## FUTURE DIRECTIONS OF THIS LAB RELATED TO AIR FORCE SUPPORT

I am approaching the time when we would like to begin writing our competitive renewal to request support for three more years of research funding related to our studies of the role of the suprachiasmatic nucleus in regulating circadian rhythms. You encouraged me on the phone to write the renewal before the end of 1992, which I will do. There are several related areas that I am very interested in. As we discussed on the phone several weeks ago, it would be a great help if you would make some recommendations as to which direction you feel might be most consistent with where you see the general program going. Perhaps we could talk at the meeting in San Antonio in October.

There are three related sets of experiments that I would like to pursue in the SCN:

1. The role of the neurotransmitter glutamate in the SCN.
2. Gene expression in living SCN cells.
3. Calcium responses and oscillations in SCN cells in vitro

1. Glutamate in the SCN: The first is the most direct extension of our current project funded by the AFOSR. As we postulated several years ago, glutamate accounts for a great deal of excitatory transmission in the SCN, and probably is the transmitter of the retinal projection to the SCN. As such it plays a very important role in resetting the clock. I have done a series of experiments with genes coding for different glutamate receptors, and find that some subtypes, but not others are strongly expressed in the SCN. This is consistent with our work on finding calcium responses of both neurons and glial cells to glutamate applied in vitro. Future experiments would include studies of what factors regulated gene expression of the glutamate receptors in the SCN and developmental changes in glutamate responses of both neurons and glia from the SCN. Experiments (in collaboration with Dr. Mike Rea) would be undertaken to examine the diurnal and circadian variation in the gene expression glutamate receptor subtypes. Glutamate is known to have an excitotoxic effect on neurons. However, SCN neurons appear resistant to the cytotoxic effects of glutamate. One aspect of this work we would pursue is why SCN neurons are resistant to glutamate toxicity. This may help us to understand the general problems of glutamate toxicity in other neurons.

2. Gene expression in living SCN cells: In general scientists who have studied gene expression kill cells or animals, and analyze the protein or mRNA for a particular gene at a single time point. What we would propose to do is examine gene expression in living cells, using computerized video microscopy and reporter genes coupled to promoters which would cause some change in the fluorescence intensity or wave length in cells in culture.

In pursuit of this general line of investigation we have constructed genes whose products would be visible in living cells. One of these genes is beta-galactosidase coupled to a strong promoter, SV40. We have successfully transfected mammalian cell lines with this bacterial gene, and have stable mammalian cell lines in culture which show a strong expression of beta-galactosidase as detected with staining with X-gal. Our next step will be to determine if we can detect the gene expression in living cells. If so, then we will transfect neuronal cells from the suprachiasmatic nucleus with the same gene construction to determine if we can get beta-galactosidase expression with this vector. A recently developed membrane permeable substrate has recently come available which becomes fluorescent in the presence of beta-galactosidase. If these preliminary experiments work, then one could couple

promoters to for various genes of interest in the SCN, for instance c-fos, transfect the cells, and study gene regulation of c-fos in living cells in culture or brain slices. This would allow studies of both the up- and down-regulation of c-fos by neurotransmitters such as GABA, glutamate, or neuroactive peptides found in the SCN.

Another tack we have followed is obtaining the gene for the enzyme that makes fireflies glow in the dark, luciferase. The gene for luciferase is abbreviated luc. We have subcloned the luc gene into different expression vectors, and then transfected cells with this. Importantly, with low light video one can detect light emitted by cells transfected with the luc gene. Because ATP is a critical co-factor in light emission from luc transfected cells, one hypothetically could transfect SCN cells with the luc gene, and then examine ultradian and circadian variations in luc in single cells or groups of cells.

3. Calcium oscillations in SCN cells and slices. By using a computer controlled video camera, we can study the behavior of individual and isolated cells in the SCN. This will allow us to ask questions about the abilities of single units of the clock to oscillate or respond to transmitter. We can also examine groups of cells, recording the interaction of a number of cells to various types of stimulation, and to each other. As new calcium dyes become available, we may be able to examine circadian patterns of intracellular calcium, which would open the door to asking questions about the unit of the clock, that is: Can a single cell show a circadian rhythm, or are a greater number needed. Several mathematical models of clock function (e.g. Pavlidis) suggest that an accurate 24-hour clock can be synthesized from a group of units showing ultradian oscillations. We would like to continue examining these ultradian calcium oscillations with video microscopy and laser confocal microscopy. These types of experiments will allow us to examine the response of single cells and groups of cells both to glutamate and to other neuroactive substances such as VIP, vasopressin, serotonin, somatostatin which are found in the SCN. Calcium itself serves as a handle to study cellular physiology with a number of calcium indicator dyes. Calcium also may serve an important role as an intermediate messenger in intracellular orchestration and circadian rhythms.

We could write a renewal application of any of these three related areas, or could write something that included all three. For instance an application entitled "Computer-video analysis of the behavior of SCN cells in vitro" could include aspects of all three sets of questions including glutamate responses, calcium imaging, and expression of genes in living SCN cells. I would worry a bit that a grant referee might suggest a more restricted focus.

Please let me know your thoughts on these future directions.

Also enclosed are a couple of color images showing cells cultured from the SCN, loaded with a calcium indicator dye, and stimulated with glutamate with a clock in the background. The images are half science, half fun. You might enjoy them.

Sincerely,

Anthony N. van den Pol  
Professor

# Calcium Excitability and Oscillations in Suprachiasmatic Nucleus Neurons and Glia *in vitro*

Anthony N. van den Pol,<sup>1</sup> Steven M. Finkbeiner,<sup>2</sup> and Ann H. Cornell-Bell<sup>3</sup>

<sup>1</sup>Section of Neurosurgery, <sup>2</sup>Section of Molecular Neurobiology, and <sup>3</sup>Department of Cell Biology, Yale University School of Medicine, New Haven, Connecticut 06510

Converging lines of evidence suggest that the hypothalamic suprachiasmatic nucleus (SCN) is the site of the endogenous biological clock controlling mammalian circadian rhythms. To study the calcium responses of the cellular components that make up the clock, computer-controlled digital video and confocal scanning laser microscopy were used with the  $\text{Ca}^{2+}$  indicator dye fluo-3 to examine dispersed SCN cells and SCN explants with repeated sampling over time.  $\text{Ca}^{2+}$  plays an important second messenger role in a wide variety of cellular mechanisms from gene regulation to electrical activity and neurotransmitter release, and may play a role in clock function and entrainment.

SCN neurons and astrocytes showed an intracellular  $\text{Ca}^{2+}$  increase in response to glutamate and 5-HT, two major neurotransmitters in afferents to the SCN. Astrocytes showed a marked heterogeneity in their response to the serial perfusion of different transmitters; some responded to both 5-HT and glutamate, some to neither, and others to only one or the other. Under constant conditions, most neurons showed irregular temporal patterns of  $\text{Ca}^{2+}$  transients. Expression of regular neuronal oscillations could be blocked by the inhibitory transmitter GABA. Astrocytes, on the other hand, showed very regular rhythms of cytoplasmic  $\text{Ca}^{2+}$  concentrations with periods ranging from 7 to 20 sec. This periodic oscillation could be initiated by *in vitro* application of glutamate, the putative neurotransmitter conveying visual input to the SCN critical for clock entrainment. Long-distance communication between glial cells, seen as waves of fluorescence moving from cell to cell, probably through gap junctions, was induced by glutamate, 5-HT, and ATP. These waves increased the period length of cellular  $\text{Ca}^{2+}$  rises to 45–70 sec. Spontaneously oscillating cells were common in culture medium, serum, or rat cerebrospinal fluid, but rare in HEPES buffer.

One source for cytoplasmic  $\text{Ca}^{2+}$  increases was an influx of extracellular  $\text{Ca}^{2+}$ , as seen under depolarizing conditions in about 75% of the astroglia studied. All neurotransmitter-induced  $\text{Ca}^{2+}$  fluxes were not dependent on voltage changes, as  $\text{Ca}^{2+}$  oscillations could be initiated under both normal and

depolarizing conditions. Since neurotransmitters could induce a  $\text{Ca}^{2+}$  rise in the absence of extracellular  $\text{Ca}^{2+}$ , the mechanisms of ultradian oscillations appear to depend on cycles of intracellular  $\text{Ca}^{2+}$  fluxes from  $\text{Ca}^{2+}$ -sequestering organelles into the cytoplasm, followed by a subsequent  $\text{Ca}^{2+}$  reduction.

In the adult SCN, fewer astrocytes are found than neurons, yet astrocytes frequently surround glutamate-immunoreactive axons in synaptic contact with SCN dendrites, isolating neurons from each other while maintaining contact with other astrocytes by gap junctions.

Neurons and glia respond to neurotransmitter application with a variety of  $\text{Ca}^{2+}$  responses; both may play a role in the function of the SCN, and their interaction may explain several aspects of mammalian clock physiology not easily explained solely on the basis of our current understanding of axonally mediated neurotransmission.

The response of suprachiasmatic nucleus (SCN) cells to glutamate and other transmitters found in SCN afferent axons includes both transient  $\text{Ca}^{2+}$  elevations and ultradian (with a period less than 24 hr) oscillations. To study these cellular responses, we used digital video and confocal laser microscopy with the  $\text{Ca}^{2+}$  indicator dye fluo-3. This video approach allows the study of the  $\text{Ca}^{2+}$  behavior of individual cells as well as the behavior of aggregates or interactive groups of cells over time.  $\text{Ca}^{2+}$  plays a crucial second messenger role in a wide variety of cellular events. The importance of  $\text{Ca}^{2+}$  is suggested by the apparent absence of circadian rhythms of 2-deoxyglucose uptake and firing rate in the SCN *in vitro* if calcium was removed from the buffer (Shibata et al., 1984, 1987). In the present study, responses of both neurons and astroglia were studied.

Several models of biological clock timekeeping are based on the interaction of cellular oscillators (Pittendrigh, 1974). The SCN, the putative site of the circadian timekeeper in mammals (Moore and Eichler, 1972; Stephen and Zucker, 1972; Rusak and Zucker, 1979; van den Pol and Powley, 1979), has tacitly been assumed to function by neuronal communication mediated by neurotransmitter release. However, recent experiments blocking sodium-dependent action potentials and related neurotransmitter release with TTX (Schwartz et al., 1987; Meijer and Rietveld, 1989; Schwartz, 1991) that failed to block timekeeping have suggested that classical  $\text{Na}^+$ -dependent axonal neurotransmission may not be required for timekeeping or for cellular orchestration within the SCN. The orchestrated metabolic rhythms of SCN cells found prior to synaptogenesis (Reppert and Schwartz, 1984) are also not easily reconciled with a

Received June 5, 1991; revised Feb. 7, 1992; accepted Feb. 11, 1992.

Research was supported by NIH Grants NS 16296 and NS 10174 and the Air Force Office of Scientific Research. We thank Dr. S. J. Smith for generous suggestions relating to digital video microscopy, Drs. M. Cooper, F. E. Dudek, and J. Miller for helpful advice, and Dr. J. C. Chisolm, J. N. Davis, and P. Thomas for helping with ratio imaging experiments.

Correspondence should be addressed to Anthony N. van den Pol, Section of Neurosurgery, Yale University School of Medicine, 333 Cedar Street, New Haven, CT 06510.

Copyright © 1992 Society for Neuroscience 0270-6474/92/122648-17\$05.00/0

clock model based solely on conventional synaptic axonal neurotransmission.

Of particular importance to circadian rhythms is the transmitter released from the optic nerves that entrains the endogenous rhythm to the ambient light cycle. Glutamate is the best transmitter candidate for mediation of visual input to the SCN, as it is released in the SCN by optic nerve stimulation (Shibata et al., 1986) and causes a phase shift in circadian rhythms (Meijer et al., 1988). Optic nerve stimulation induces alterations in electrical field potentials that can be blocked by excitatory amino acid antagonists (Cahill and Menaker, 1987). 6-Cyano-7-dinitroquinoxaline-2,3-dione, a glutamate receptor blocker, blocks the excitatory postsynaptic response to optic nerve stimulation (Kim and Dudek, 1989). In the present article, we used immunogold cytochemistry to show glial cells surrounding presynaptic axons showing high levels of glutamate immunoreactivity in the adult SCN, and we used glutamate, several glutamate agonists, 5-HT, and ATP to study the  $\text{Ca}^{2+}$  responses of SCN cells *in vitro*.

An abstract based on some of this work has been presented (van den Pol et al., 1991).

## Materials and Methods

**Cell culture.** SCN cells from 1–3-d-old neonatal rats were grown for 1–8 weeks on glass coverslips coated with collagen and polylysine or polylysine alone, or on untreated glass coverslips (van den Pol et al., 1986). SCN tissue dissected from hypothalamic slices (see below) was incubated in papain (20 U/ml; Worthington) in a buffer containing 137 mM NaCl, 5 mM KCl, 3 mM  $\text{CaCl}_2$ , 1 mM  $\text{MgCl}_2$ , 10 mM HEPES, and 25 mM glucose on an oscillating Nutator at 37°C for 45 min. Enzymatic action was stopped by the addition of 1.5 mg/ml trypsin inhibitor and 1.5 mg/ml bovine serum albumin, fraction V (Sigma). Cells were disaggregated with gentle passage through a fire-polished pipette previously coated with silicon (Prosil21, PCR, Gainesville, FL), used to reduce cell sticking and damage. Disaggregated cells were grown in low (about 2000 neurons) or high densities (about 10,000 neurons) in the middle of the coverslip. Coverslips pretreated with polylysine (540 kDa) were subsequently rinsed in five changes of sterile water. Neurons growing with confluent or nonconfluent glial cultures were used. An average of two brains were used for one glass coverslip for high density cultures. GIBCO Dulbecco's minimal essential medium (MEM) was supplemented with 10% fetal bovine serum (GIBCO and Hyclone), 50 U/ml penicillin and streptomycin and serum extender (Collaborative Research). Cultures were maintained in a Napco 6100 incubator at 37°C and 5%  $\text{CO}_2$ .

We also cultured explants of SCN made from sections of the anterior hypothalamus. The hypothalamic and preoptic area were removed from 3–4-d-old neonatal rats and cut into 300–400  $\mu\text{m}$ -thick sections held in 4°C  $\text{Ca}^{2+}$ -free buffer. Under a high-magnification Nikon stereo operating microscope, illuminated from above with a fiber optic light source or from below by substage light, we used sharpened round tubes with an inner diameter of 200 or 325  $\mu\text{m}$  to punch out the SCN. The area of the SCN can be identified by its position at the ventral surface of the hypothalamus, on either side of the third ventricle, and directly above the optic chiasm. Sections that did not show sufficient anatomical features to allow identification of the correct regions were discarded. Histological verification of these punches was done by staining the remaining tissue slice before or after fixation with 10% formalin with 0.1% propidium iodide for 20 min. Slices with the SCN punched out were examined with a Bio-Rad confocal laser scanning microscope with an argon ion laser and a Texas red filter set. On control slices, the SCN was visible as a tightly clustered group of cells stained with propidium iodide situated above the optic chiasm and at the bottom of the third ventricle. Some punches either were cultured without cell disaggregation in the Napco 6100 incubator, or alternatively were put on glass coverslips, and adhered with a thin layer of chicken plasma and thrombin, as described by Gahwiler (1981) and Wray et al. (1988). SCN tissue used for dispersed cell cultures included a small number of cells outside the border of the SCN in the region where SCN dendrites extend (van den Pol, 1980). Coverslips with an adhered SCN explant were placed

in a test tube in a Bellco cell production roller drum rotating at 10 revolutions/hr kept in a Lab-Line Imperial III incubator at 37°C.

**Digital microscopy.** For optical recording, cells were loaded with fluo-3 acetoxymethyl (AM) ester for 45 min in a HEPES buffer [10 mM HEPES, 25 mM glucose, 137 mM NaCl, 5.3 mM KCl, 3 mM  $\text{CaCl}_2$ , 1 mM  $\text{MgCl}_2$ , 1  $\mu\text{M}$  tetrodotoxin (TTX), pH 7.4], and then placed in a chamber allowing sequential perfusion of different transmitters and agonists on the stage of a Zeiss IM35 inverted microscope (Cornell-Bell et al., 1990; van den Pol et al., 1990). TTX was used to block voltage-dependent sodium channels and axon action potentials. Since the clock operates in the presence of TTX (Schwartz et al., 1987), many of our experiments parallel conditions under which the clock might operate in the absence of axonal transmission mediated by voltage-dependent sodium channels. A high potassium buffer was similar, except that KCl was increased to 56 mM, and NaCl was reduced to 86 mM. A zero-calcium buffer contained no  $\text{CaCl}_2$ , but did contain 1 mM EGTA. For some experiments studying aspartate and *N*-methyl-D-aspartate (NMDA),  $\text{MgCl}_2$  was deleted from the buffer, and 4  $\mu\text{M}$  glycine was added.

The intensity of fluorescence of fluo-3 increases in the presence of  $\text{Ca}^{2+}$ , and the dye has excellent spatial and temporal resolution. The high sensitivity was crucial for long recordings where we needed to avoid phototoxicity, and allowed us to work with very low light levels. Furthermore, fluo-3 could be detected both with fluorescent microscopy and with argon laser confocal microscopy. Ratio imaging dyes such as fura-2 that require more intense light of a shorter wavelength were unsuitable for many of our experiments due to the higher level of phototoxicity over the long recording periods with images averaged every second. Among all the available  $\text{Ca}^{2+}$  indicators, fluo-3 provides the largest optical signal per molecule and thus allows for the detection of transients in the smallest possible cytoplasmic volume. With the increased sensitivity of fluo-3, subtle changes in  $\text{Ca}^{2+}$  were more easily detected than with fura-2.

Video images were collected with a Hamamatsu 2400 SIT camera interfaced with an Imaging Technology 151 video processor and IBM AT computer, and one video frame was stored on a Panasonic 2023 laser disk recorder every sec. To reduce the possibility of phototoxicity, a computer-controlled shutter completely blocked light for 650 msec of each second, and neutral density filters were used to block 99% of the light emitted by the mercury light source when the shutter was open. Fluorescent filtration used was the same as used for fluorescein visualization. Data are expressed as a change in fluorescence over baseline fluorescence ( $\Delta F/F_0$ ). The fluorescent level of each cell under normal conditions served as its own baseline ( $F_0$ ), and was corrected for spatial heterogeneity of the video field, as well as for the video gain and offset, and differences in cell esterase activity, by including with each experiment a video record of each cell with different neutral density filters (1%, 2%, 3% transmittance). This allowed a comparison of different cells under the same experimental conditions when the data were examined as a change in  $\text{Ca}^{2+}$ -induced fluo-3 fluorescence over the baseline corrected fluorescence ( $\Delta F/F_0$ ) (Cornell-Bell et al., 1990; van den Pol et al., 1990; Cornell-Bell and Finkbeiner, 1991; Finkbeiner, 1991). As previously described with this type of perfusion apparatus, the time from turning on the switch initiating agonist flow to the point that it reached the cells was about 6 sec.

Due to the thickness of the SCN explants, the fluorescent microscope described above could not resolve cellular detail. Instead, we used the confocal scanning laser microscope described previously with a fluorescein filter set. This allowed making digital recordings of an optical section taken within a fluo-3-labeled SCN explant. The intensity of the scanning laser beam was attenuated with a 1% transmittance neutral density filter. The shutter blocking the laser was set to open immediately after the scan was initiated. As described above, different neutral density filters (1%, 3% transmittance) were used to determine corrected fluorescence values.

For the ratio imaging experiment, cells were loaded in 5  $\mu\text{M}$  fura-2 AM ester in HEPES buffer for 30 min in the incubator, and studied with a Nikon 40 $\times$  (numerical aperture, 1.3) UV-passing quartz objective with either 340 or 380 nm excitation from a xenon light source. Intensities were collected through a 480–520 band pass filter. Calibration was based on 100  $\mu\text{M}$  ionomycin in the presence of 10 mM  $\text{Ca}^{2+}$  for maximum bound dye, and chelation with EGTA for minimum. A 10- $\mu\text{m}$ -diameter aperture circle over the respective cell bodies was used for data collection.

To test whether astroglia were dye coupled, which is an indication that gap junctions exist between cells, patch-type glass pipettes with a

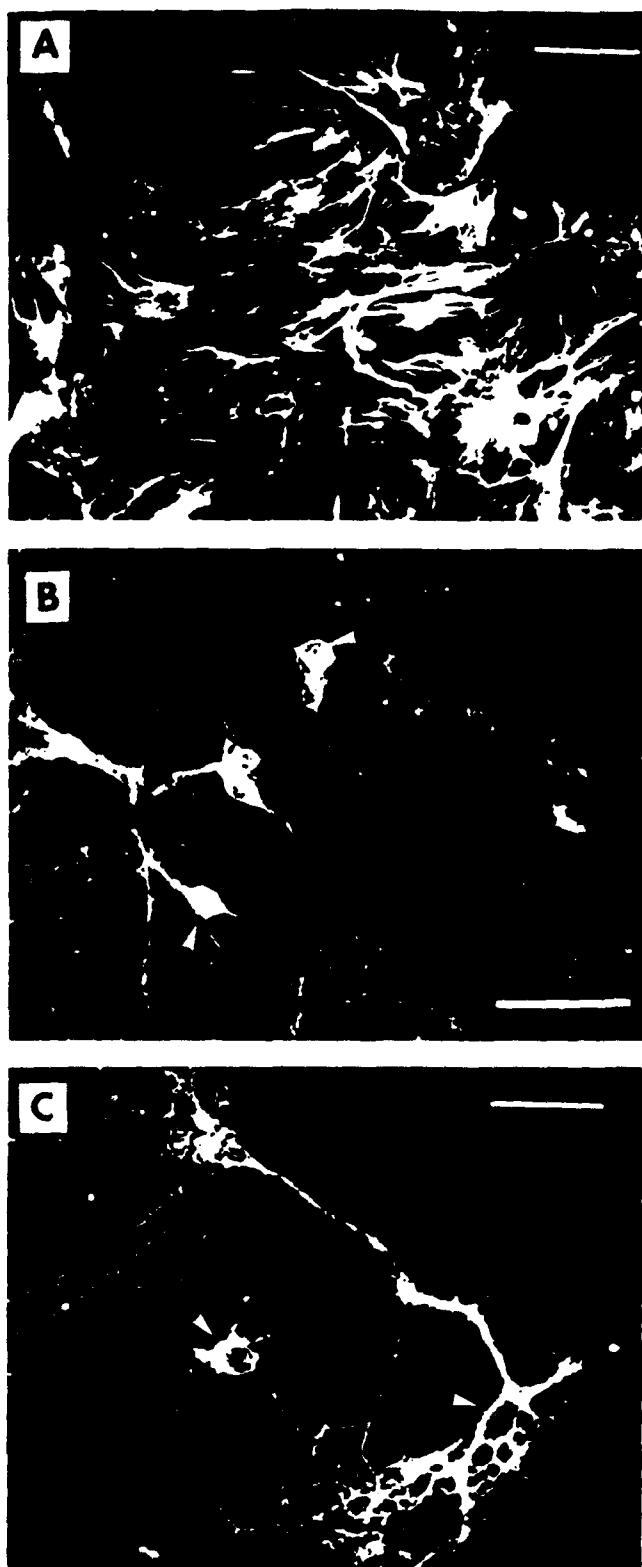


**Figure 1.** Immunocytochemistry of neurons and astroglia. *A*, On this and the other images in this figure, confocal microscopy was used to obtain images. This micrograph shows SCN glial cells stained with glial fibrillary acidic protein antiserum. *B*, Neurons are stained with neurofilament antiserum. *C*, Neurons labeled with tetanus toxin. Glial cells on which the neurons in *B* and *C* are growing are not labeled with the neuronal markers. Scale bars, 50  $\mu$ m.

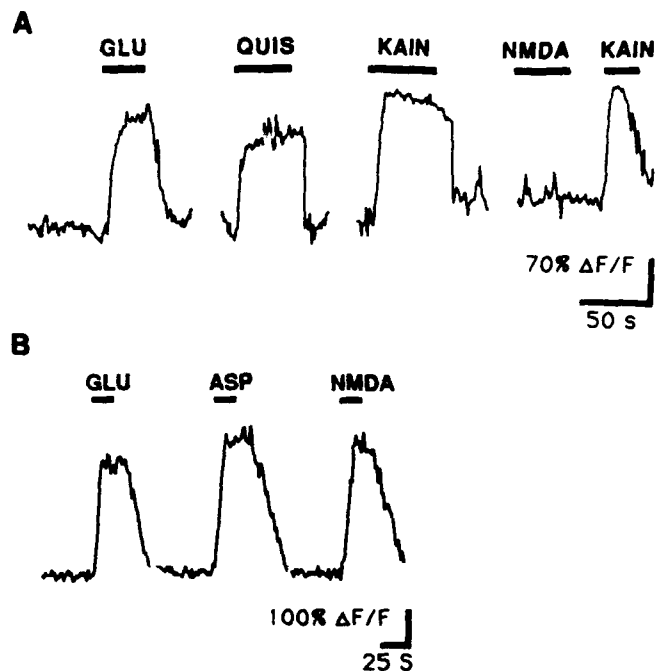


**Figure 2.** Neuron  $\text{Ca}^{2+}$  responses illustrated here are expressed as the change in fluorescence over baseline fluorescence ( $\Delta F/F$ ) as described in Materials and Methods. *A*, A single SCN neuron showed a strong increase in  $\text{Ca}^{2+}$  in response to 30  $\mu$ M glutamate, quisqualate, and kainate, but not to NMDA. *B*, An SCN neuron responds to aspartate, NMDA, and glutamate (all at 30  $\mu$ M) in the absence of magnesium and presence of 4  $\mu$ M glycine.

tip internal diameter of about 1  $\mu$ m were filled with 6-carboxyfluorescein, a small fluorescent molecule that diffuses through gap junctions. During observation on the video screen with a combination of video-intensified differential interference contrast optics and fluorescent illumination, single cells were filled with the dye by intracellular injection after a membrane seal was obtained, and 10 min later the pipette was removed.

**Immunocytochemistry.** Rabbit antiserum against glutamate was made with glutamate conjugated by glutaraldehyde to keyhole limpet hemocyanin. The antibody recognized only glutamate and not other amino acids, as determined with immunodot blot, Western blot, ELISA assays, and amino acid bound to Sepharose beads (van den Pol, 1991). After deeply anesthetizing adult male rats (250–300 gm) with Nembutal, they were perfused transcardially with 3% glutaraldehyde, and the SCN was removed, treated with 1% osmium tetroxide and 1% aqueous uranyl acetate, and embedded in Epon or Araldite. Ultrathin sections were immunostained with 10 nm colloidal gold (Janssen) as described in detail elsewhere (van den Pol, 1989, 1991; van den Pol and Decavel, 1990), and the presence of immunoreactive boutons and their anatomical relationship to nearby astrocytes was studied.

At the ultrastructural level, neurons could be differentiated from other cells by the morphological presence of synapses, dendrites, and axons, while astrocytes could be recognized by their clumps of glial filaments, absence of synapses, and by the irregular contours of astrocytic processes. To estimate the relative number of glia and neurons with stereology, electron micrographs at 60,000 $\times$  magnification were overlaid with a regular pattern of points, the number of superimpositions over different cells was counted, and cell size and the relative number of cells were determined (Palkovits, 1976).

To differentiate glia from neurons *in vitro*, morphological and cytochemical criteria, including immunostaining with antisera against the plasmalemma molecules neural cell adhesion molecule (NCAM; gift of U. Rutishauser or G. Rougon), L1 (gift of V. Lemmon), tetanus toxin-c fragment (Boehringer-Mannheim), and neurofilaments (68 kDa) (Sternberger), neuropeptides such as neurophysin, vasopressin (gift of M. Sofroniew), and vasoactive intestinal polypeptide (Incstar), and glial fibrillary acidic protein (gift of L. Eng), were used. Secondary antibodies were labeled with colloidal gold or fluorescein. Cells were imaged on

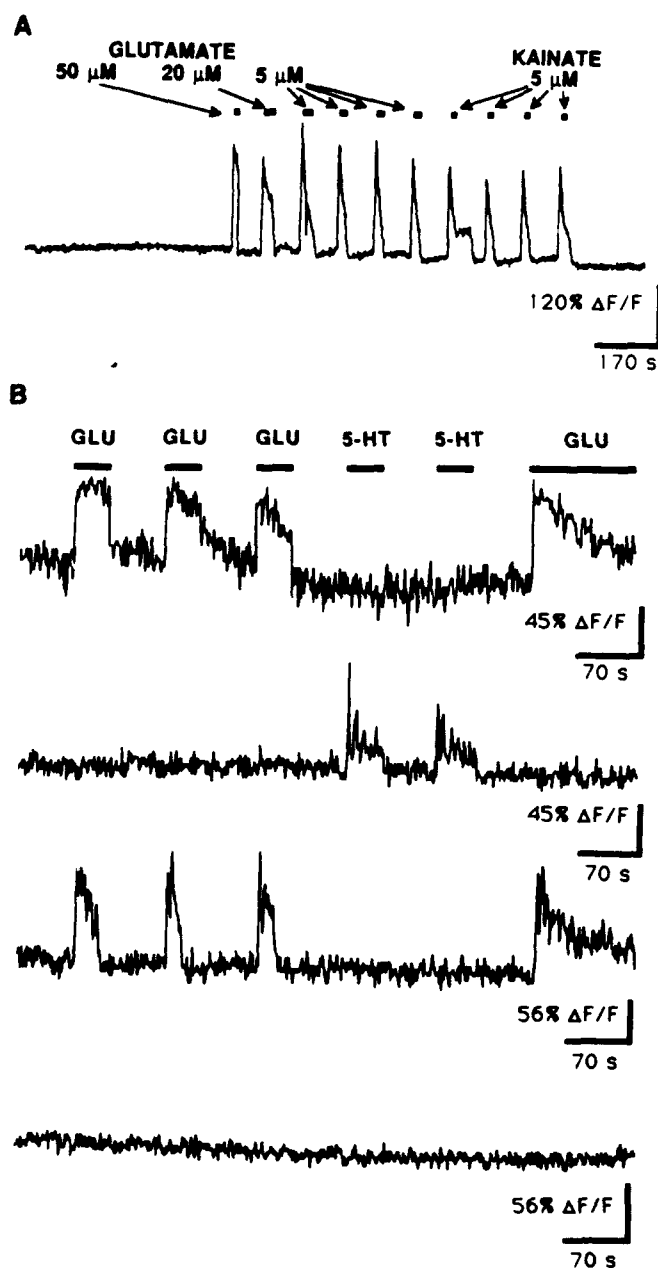


**Figure 3.** *A*, Astrocyte showed an increased intracellular  $\text{Ca}^{2+}$  in response to repeated perfusions of glutamate or kainate. *B*, Four astroglia from the same plate recorded simultaneously. Two cells showed a  $\text{Ca}^{2+}$  influx in response to glutamate, but not to 5-HT, the third cell showed a response only to 5-HT, and a fourth responded to neither of the transmitters.

either a Zeiss fluorescent microscope or a Bio-Rad confocal scanning laser microscope coupled to an Olympus upright or Zeiss inverted microscope.

## Results

Neurons had long processes and a semispherical cell body, were immunoreactive for NCAM, L1, and neurofilament protein (Fig. 1*B*), and were labeled with tetanus toxin (Fig. 1*C*). Some neurons were also immunoreactive for vasopressin or neurophysin, substances found in the SCN *in vivo*. Cells were not used until at least 5 d after culturing, a time when electron microscopy revealed that synapses were established between neurons. As-

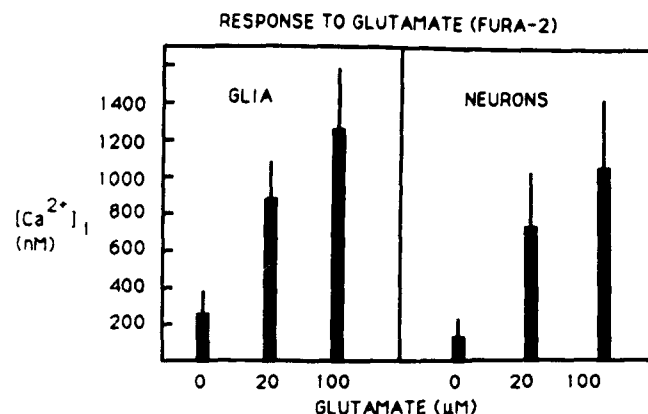


**Figure 4.** Cytoplasmic  $\text{Ca}^{2+}$  measured with fura-2 in five neurons or glia at each glutamate concentration. Error bars are SD.

trocytes had a flat, sheet-like morphology with diameters several times greater than that of neurons and exhibited positive immunostaining for glial fibrillary acidic protein antisera (Fig. 1*A*) and negative staining with L1 antiserum or neurotransmitter-related antisera including neurophysin, vasopressin, or vasoactive intestinal polypeptide.

**Transmitter response.** With optical video analysis, the majority of SCN neurons (183 of 194 cells, 94%) responded to 100  $\mu\text{M}$  glutamate.  $\text{Ca}^{2+}$  rises were also seen in many neurons at glutamate concentrations of 1–5  $\mu\text{M}$  (see Fig. 13*G,H*). Cells responded vigorously to the glutamate agonists kainate and quisqualate (Fig. 2*A*), but only a minor response to NMDA was seen with the HEPES buffer normally used. When HEPES buffer lacking  $\text{Mg}^{2+}$  and including glycine was used, SCN neurons were found that responded strongly to 30  $\mu\text{M}$  NMDA and 30  $\mu\text{M}$  aspartate (Fig. 2*B*). The estimate of the number of SCN neurons that responded to glutamate is a conservative one; neurons that showed a high initial level of fluo-3 fluorescence may have responded to glutamate with a  $\text{Ca}^{2+}$  increase not detectable with the optical constraints of the video system set to analyze faintly fluorescent cells in the same microscope field.

Astrocytes also responded to repeated administrations of 100  $\mu\text{M}$  glutamate (226 of 266 astroglia, 85%), kainate (Fig. 3*A*), and quisqualate with rapid increases in intracellular  $\text{Ca}^{2+}$ . Increases in  $\text{Ca}^{2+}$ -related fluorescence were seen in the cytoplasm of the processes and cell body, and sometimes included the cell nucleus. We did not see any strong response in astrocytes to application of either aspartate or NMDA in either the presence or absence of  $\text{Mg}^{2+}$  or glycine.

Because the percentage of SCN astrocytes that responded to glutamate was lower than the percentage of hippocampal astrocytes that responded to glutamate (100% of 323 hippocampal astrocytes), we tested whether the cells that did not respond to glutamate perhaps were unable to respond to any  $\text{Ca}^{2+}$ -inducing agents. Since 5-HT is a prevalent transmitter in afferents to the SCN from the raphe (Agajanian et al., 1969; van den Pol and Tsujimoto, 1985), we compared the glial response to glutamate and 5-HT. The response of SCN glia to serial application of different neurotransmitters was heterogeneous. In one experiment, some glia (2 of 13) showed an intracellular  $\text{Ca}^{2+}$  increase with glutamate, while others (2 of 13) in the same video field on the same coverslip responded only to 5-HT. In this group of cells, most cells (9 of 13) did not respond to either transmitter

## NEURON

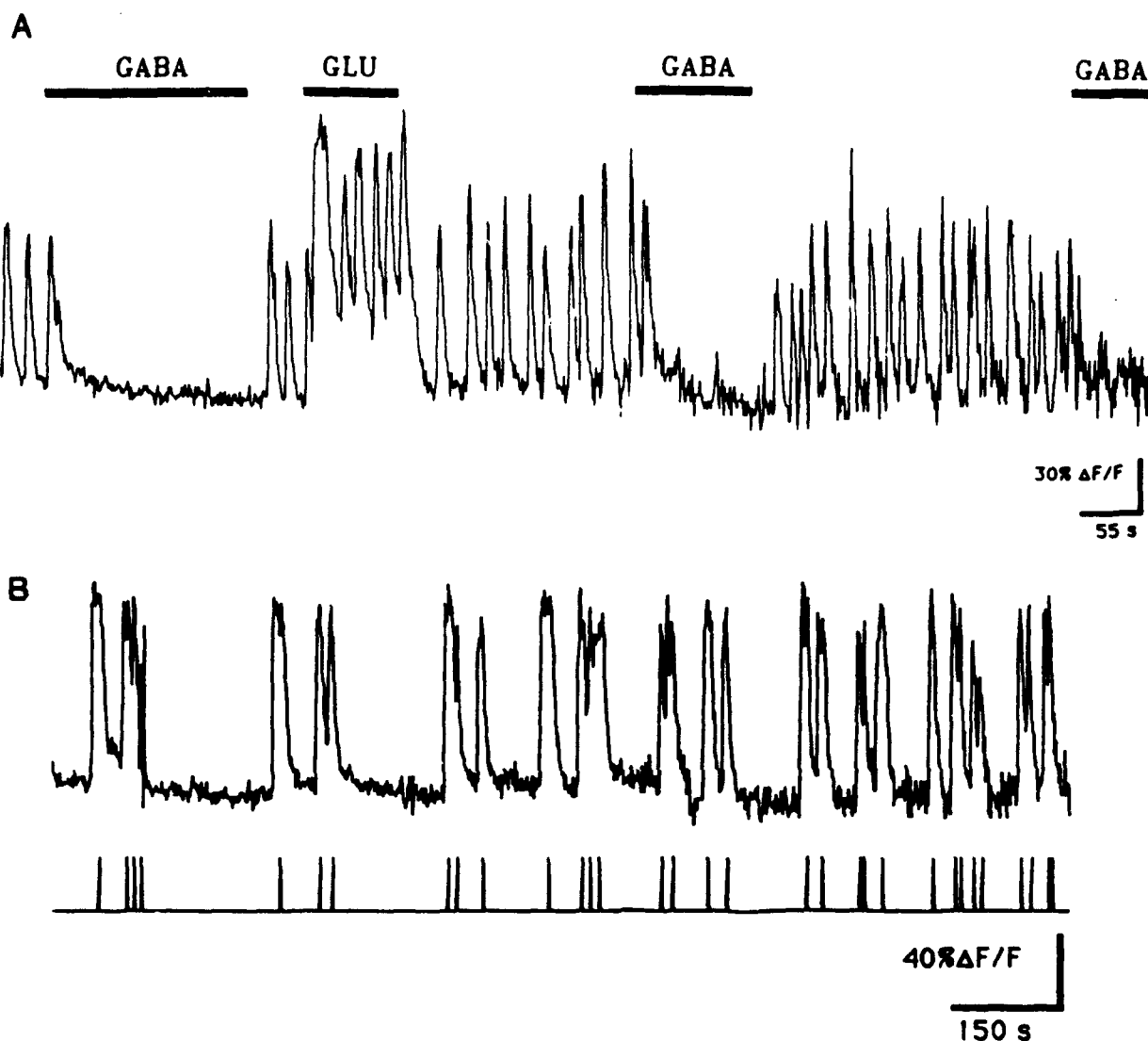


**Figure 5.** Neuron oscillations. *A*, An SCN neuron showed a spontaneous regular  $\text{Ca}^{2+}$  oscillation that could be consistently blocked with  $30 \mu\text{M}$  GABA. Glutamate raised the mean  $\text{Ca}^{2+}$  level in this cell, but oscillations continued. This cell was grown in a low neuronal culture density, and the experiments were done in the absence of TTX. *B*, A neuron showed spontaneous fluctuations in intracellular calcium in the presence of TTX. The lowest trace shows  $\text{Ca}^{2+}$  peaks in *B* as single events. The regularity of the neuron is much less than that seen in the glial cells. The variance in periodicity (expressed as the SD as a percentage of the mean) was  $4.8 \times$  greater in the neuron (62%) than in the glial cell (13%) based on cells in Figure 6*B*. This neuron and the astrocytes in Figure 6 are representative of SCN astrocytes and neurons in general in the presence of TTX.

(Fig. 3*B*). In another group of cells cultured under the same conditions, most glia (50 of 51) responded to both 5-HT and glutamate as shown by the examples in Figure 6. To examine further the heterogeneous response of astrocytes, particularly those that did not respond to glutamate, we also used ATP. ATP is released from many axon terminals (Burnstock, 1986) and has been suggested as a potent agent for increasing intracellular  $\text{Ca}^{2+}$  in astrocytes (McCarthy and Salm, 1991). In some coverslips, regions could be found where 90% of the astrocytes responded to extracellular ATP (see Fig. 7*A–C*), but a response to glutamate could not be detected. These results suggest that a clonal expansion of astrocytes with similar receptive properties may occur. Relatively little  $\text{Ca}^{2+}$  response to ATP was found in neurons.  $\text{Ca}^{2+}$  rises in the cytoplasm were seen in all responding

cells; in some cells a rapid increase in nuclear  $\text{Ca}^{2+}$  was also detected in phase with the cytoplasmic increase.

To determine how the  $\text{Ca}^{2+}$  levels in SCN cells compared with those found in other regions of the nervous system, we used the ratio imaging calcium indicator dye fura-2 and averaged the responses to glutamate for five cells at each glutamate concentration (Fig. 4). Fura-2 was not used for the long repeated video recording in most of our experiments, due to the greater cellular phototoxicity of parameters required for imaging fura-2. The baseline and stimulated values from SCN neurons and glia were in the same range as reported for cells from other brain regions (Glaum et al., 1990; Cline and Tsien, 1991).

**Calcium oscillations.** Neurons with regular oscillations were found in the absence of TTX, and could be perturbed by amino

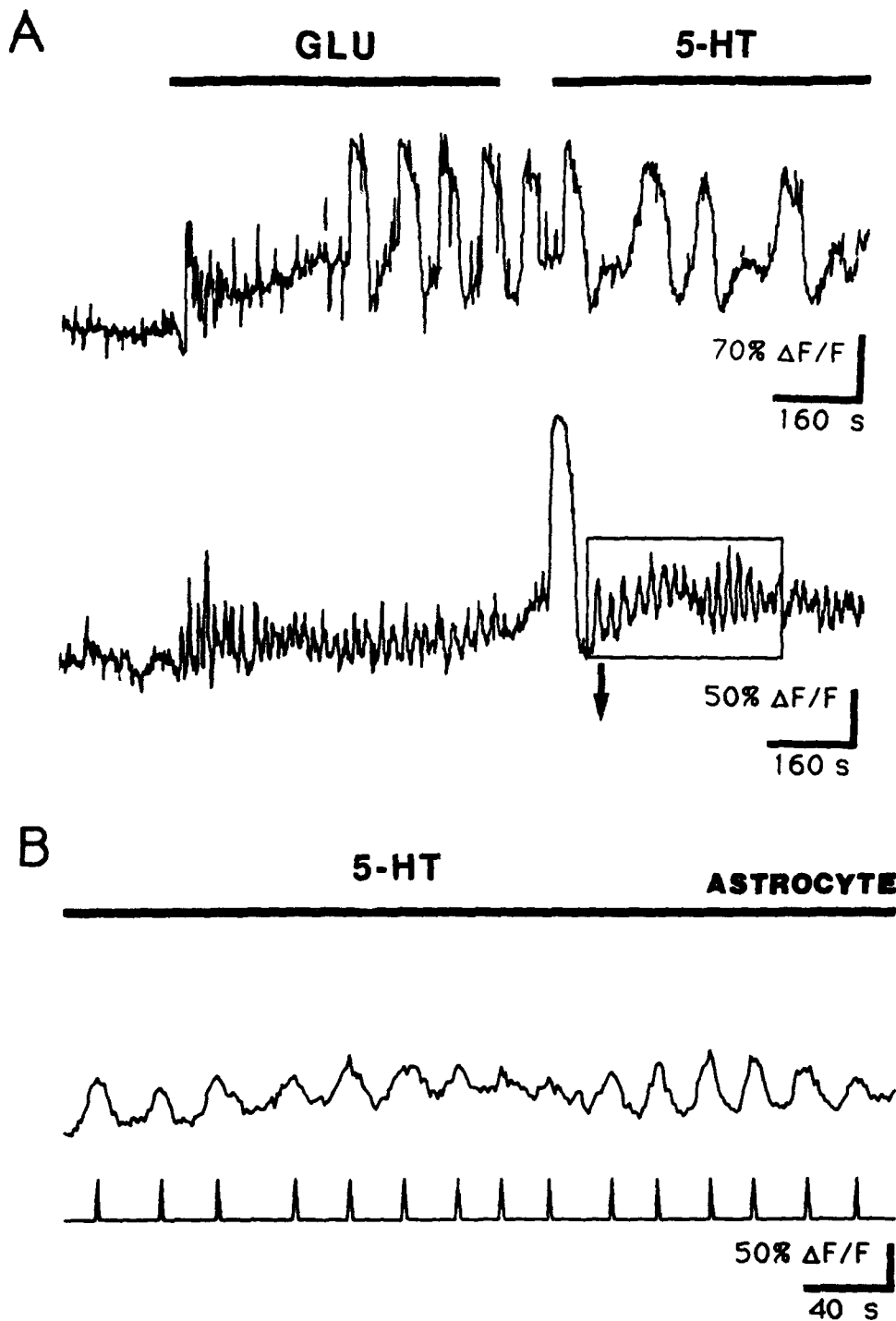


**Figure 6.** *A*, Two astrocytes responded to glutamate and then to 5-HT with a periodic oscillation of intracellular  $Ca^{2+}$ . Note the short periods of the lower cell compared to the long period of the upper cell in the presence of 5-HT. The long period in the upper cell was due to an intercellular  $Ca^{2+}$  wave originating from other glial cells, while the period of the lower cell was due to oscillations originating in that cell. These experiments were done in the presence of 1  $\mu M$  TTX. *B*, Part of the recording in the lower astrocyte in Figure 6*A* that is boxed is expanded to facilitate examination of the regularity of the periodic response. The lowest trace shows  $Ca^{2+}$  peaks in *B* as single events.

acid transmitters. An example of one neuron that showed a regular  $Ca^{2+}$  oscillation is shown in Figure 5*A*. The regular oscillation was blocked by introduction of the inhibitory transmitter GABA (Fig. 5*A*). When GABA was removed, the oscillations returned. Perfusion of glutamate raised the mean  $Ca^{2+}$  level, and the oscillations continued; in the subsequent absence of glutamate, the mean intracellular  $Ca^{2+}$  level decreased while the oscillations continued. In both neurotransmitter-stimulated and -unstimulated conditions, we found very few neurons with regular  $Ca^{2+}$  oscillations in the presence of TTX, although ir-

regular fluctuations of intracellular  $Ca^{2+}$  were not uncommon (Fig. 5*B*).

Glial cells showed stable periodic oscillations of intracellular  $Ca^{2+}$  in response to applications of neurotransmitters (Fig. 6*A, B*) in the presence or absence of TTX. The period of the oscillations varied from 7 to 20 sec. The regular oscillations of astrocytes were very common, and could easily be induced by neurotransmitter application. Glial cells showed both a  $Ca^{2+}$  rise and  $Ca^{2+}$  oscillations in response to perfusion of glutamate, 5-HT, and extracellular ATP (Fig. 7*B, C*).

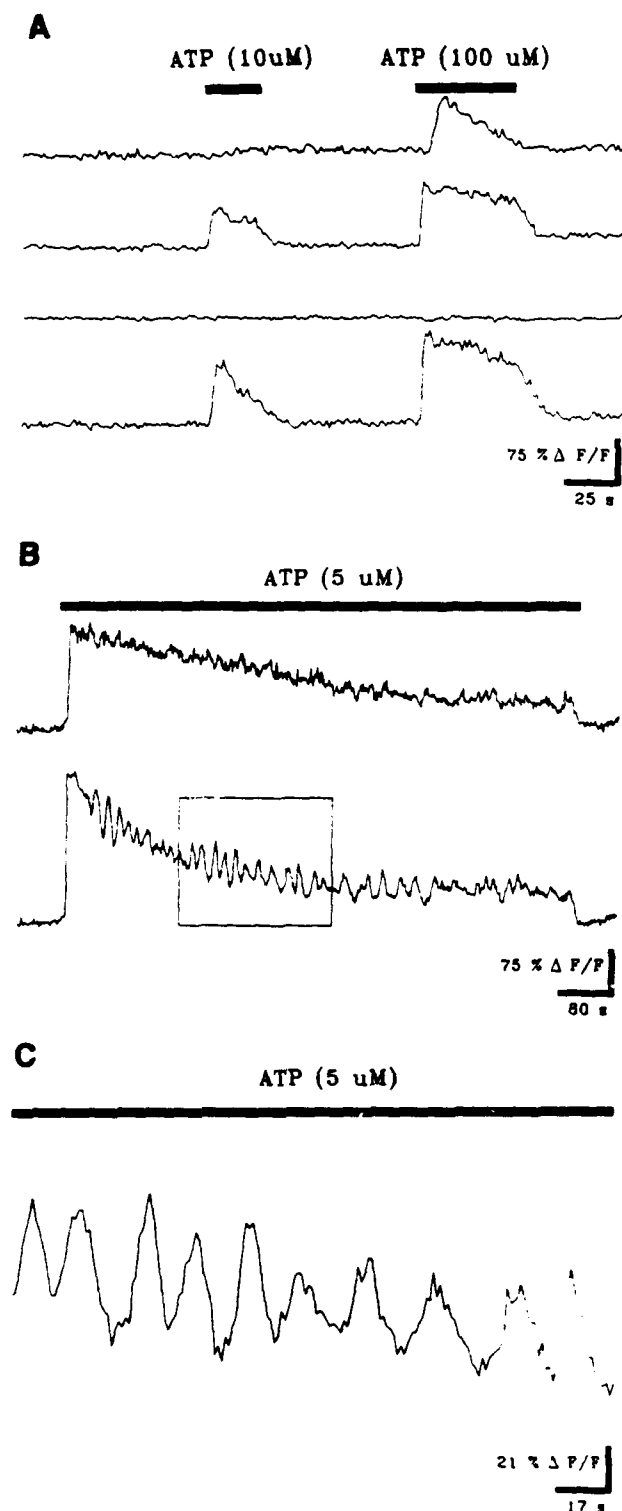


**Figure 7.** *A*, The response of four astrocytes to extracellular perfusion of ATP is shown. The *top cell* responded only to 100  $\mu$ M ATP, while the *second and fourth cells* responded to 10  $\mu$ M ATP with a small increase in intracellular  $\text{Ca}^{2+}$  and a larger increase with 100  $\mu$ M ATP. The *third cell* shows no response to ATP. *B*, Two astrocytes responded to 5  $\mu$ M ATP with an immediate increase in intracellular  $\text{Ca}^{2+}$ . They represent the majority of cells, of which 84 of 91 cells in three experiments showed a  $\text{Ca}^{2+}$  rise in response to 5 or 10  $\mu$ M ATP. The *bottom cell* shows  $\text{Ca}^{2+}$  oscillations. Both cells maintained a higher intracellular  $\text{Ca}^{2+}$  level until ATP was washed out. *C*, The boxed area in *B* is expanded to show the  $\text{Ca}^{2+}$  oscillations more clearly.

A set of three experiments was designed to classify the  $\text{Ca}^{2+}$  oscillations found in SCN astrocytes. In the first one, cells were depolarized to test whether SCN glial cells exhibited any voltage-dependent  $\text{Ca}^{2+}$  fluxes. Figure 8*A* shows an astrocyte responding to depolarizing concentrations of extracellular  $\text{K}^{+}$ . Most astrocytes (70–80%) showed a cytoplasmic  $\text{Ca}^{2+}$  rise that depended on extracellular  $\text{Ca}^{2+}$ . However, depolarization-induced  $\text{Ca}^{2+}$  oscillations were not observed. Since a significant minority of astrocytes did not respond to depolarization with a  $\text{Ca}^{2+}$  rise, cells were exposed to 5-HT while depolarized to determine if oscillations could still occur. Figure 8*B* shows an example of an astrocyte in which 5-HT-induced oscillations were relatively unaffected by depolarization. A third experiment of this series was designed to examine the  $\text{Ca}^{2+}$  origin for the transmitter-induced oscillations. Cells were perfused with 5-HT in the presence of  $\text{Ca}^{2+}$ -free/EGTA-containing buffer; Figure 8*C* shows that the  $\text{Ca}^{2+}$  involved in 5-HT-induced oscillations is primarily from intracellular sources since the response to the transmitter comes in the absence of extracellular  $\text{Ca}^{2+}$ . A minor contribution from extracellular  $\text{Ca}^{2+}$  is suggested by subtle changes in the pattern of oscillation. The period of the oscillation was slightly longer in the absence of extracellular  $\text{Ca}^{2+}$ .  $\text{Ca}^{2+}$  oscillations in  $\text{Ca}^{2+}$ -free conditions tend to be superimposed on a different intracellular  $\text{Ca}^{2+}$  baseline. In the absence of extracellular  $\text{Ca}^{2+}$ , the regular oscillations would continue for more than 10 cycles, but would eventually reduce in amplitude, possibly due to the depletion of intracellular  $\text{Ca}^{2+}$  stores.

Whereas astrocytes as a group showed heterogeneous responses to different neurotransmitters, each individual astrocyte showed a stereotyped response to a single transmitter. This is seen both in the rate of rise and fall of  $\text{Ca}^{2+}$  after single applications of transmitter as seen in the glutamate responses of cells 1 and 3 in Figure 3*B*, and in the different patterns of oscillations found with longer transmitter stimulations.

**Intercellular glial interaction.** Tracing  $\text{Ca}^{2+}$  waves between adjacent glia (Fig. 9*B*) indicated that the intercellular pathway is not random, but rather moves very specifically between certain adjacent glia, but not between others, probably due to the presence of a sufficient number of active gap junctions between communicating glial cells. The wave, seen as a slow-moving front of increased fluorescence, traveled at about 15  $\mu$ m/sec across individual cells, and from cell to cell. Ultrastructural analysis revealed large gap junctions between glia *in vitro* and *in vivo*. While neurons may not be able to communicate with one another via voltage-sensitive sodium channels and propagated axonal action potentials in the presence of TTX,  $\text{Ca}^{2+}$  waves induced in glial cells by glutamate, 5-HT, or ATP traveled intercellularly probably via gap junctions to other glial cells even in the presence of TTX (Fig. 9*A*). Intercellular waves of  $\text{Ca}^{2+}$  movement resulted in slow periodic  $\text{Ca}^{2+}$  rises in the individual cells involved in the wave, with peak-to-peak periods ranging from 45 to 70 sec, much longer than the periods of cells not showing obvious synchrony with other astrocytes. We found no slow-moving waves of  $\text{Ca}^{2+}$  traveling between neurons.

**Dye coupling.** As the  $\text{Ca}^{2+}$  wave may propagate from cell to cell by transfer of small molecules through gap junctions, we examined the dye coupling of astrocytes. Single SCN astrocytes that were intracellularly filled with carboxyfluorescein showed movement of the dye to several adjacent neighboring astrocytes in contact with the labeled cell, seen in Figure 13*B*. Not all astrocytes were dye coupled with adjacent cells, as shown in Figure 13*C*.

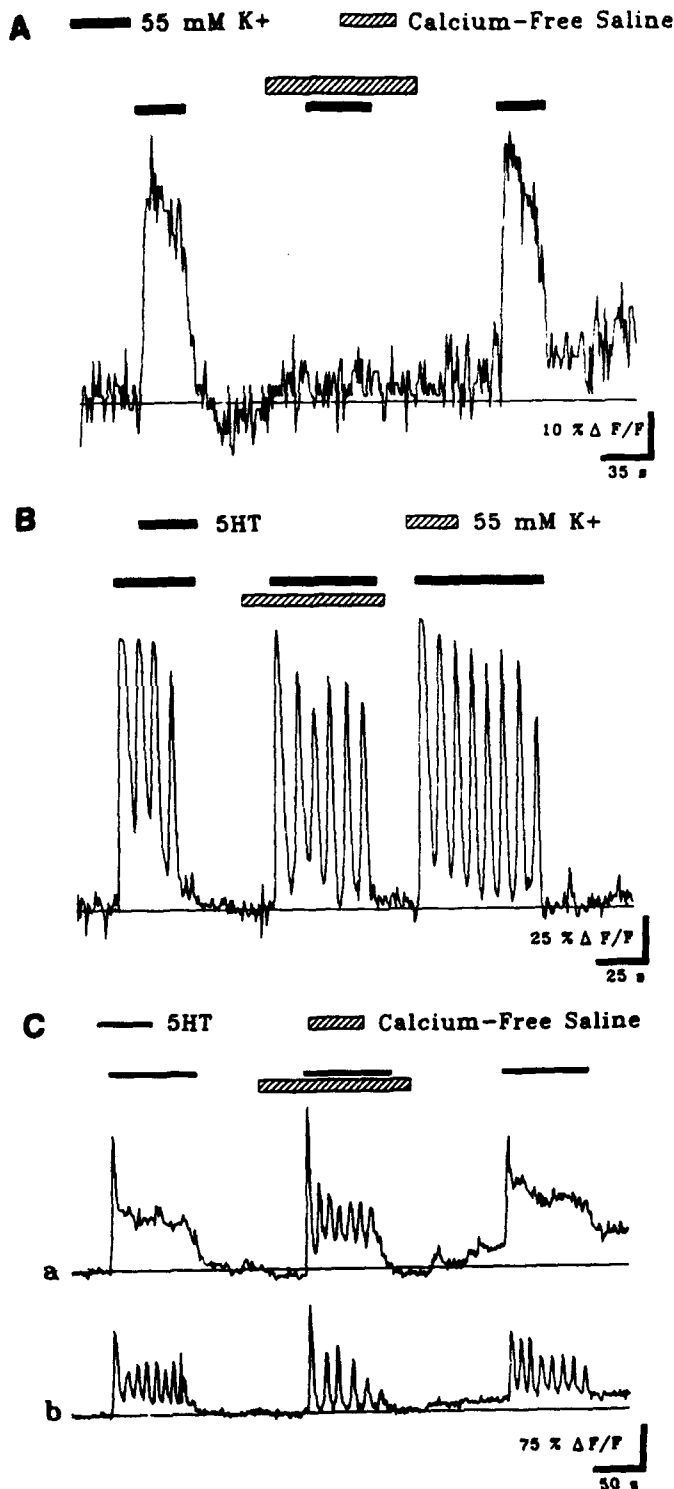


**Figure 8.** *A*, An increase in extracellular  $K^+$  caused a rise in  $Ca^{2+}$  through voltage-gated  $Ca^{2+}$  channels in the plasmalemma. No increase was seen if extracellular  $Ca^{2+}$  was removed; with later perfusion of  $Ca^{2+}$  containing buffer, cells again responded to a  $K^+$  rise. *B*, Whereas an increase in extracellular  $K^+$  did not induce a  $Ca^{2+}$  rise, 5-HT induced a  $Ca^{2+}$  rise and  $Ca^{2+}$  oscillations, in both the presence and absence of extracellular  $K^+$ . *C*, Two astrocytes showed an increase in  $Ca^{2+}$  and oscillations in  $Ca^{2+}$ -free buffer. The oscillations were not detected in the upper cell in the presence of the extracellular  $Ca^{2+}$ .

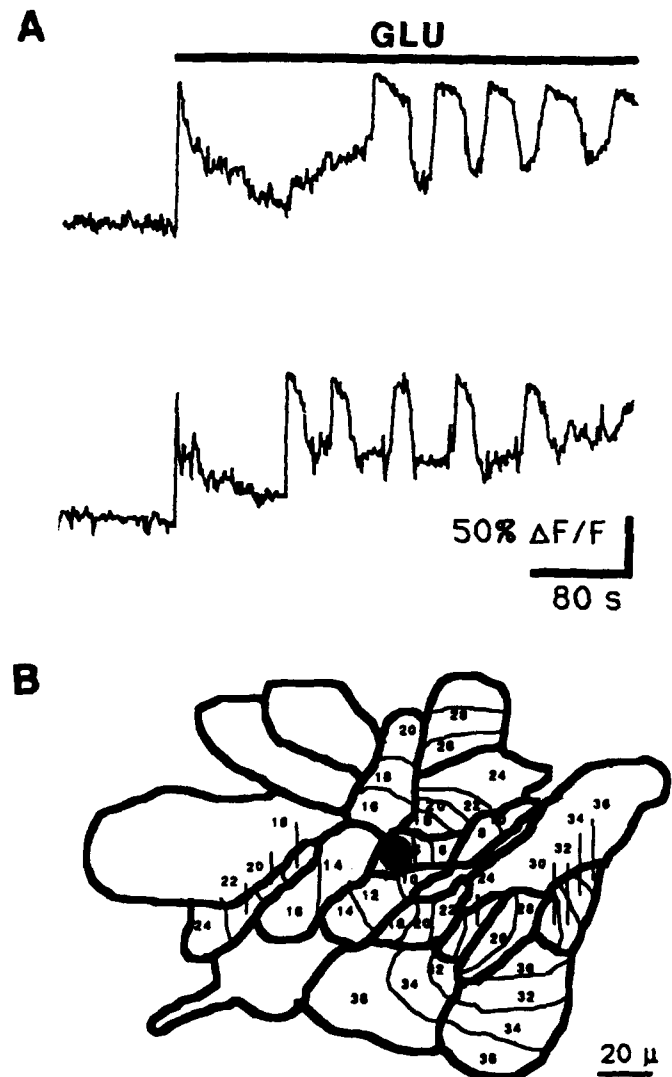


**Figure 9.** *A*, Waves of  $Ca^{2+}$  spread from one glial cell to the next adjacent one, with several seconds elapsing while the wave passed through a single cell. The intercellular wave can alter the period of the independently oscillating glial cell, increasing the length of the period. The regular rise and fall of  $Ca^{2+}$  is different in two cells from the same coverslip, showing the complex interaction between the individual oscillation and the wave dependent periodic rise and fall in cell  $Ca^{2+}$ . These experiments were done in the presence of 1  $\mu$ M TTX. *B*, An increase in intracellular  $Ca^{2+}$  started in the shaded cell (time 2), and traveled from that cell to some, but not all, of the cells in this group. Cell boundaries of single astrocytes are indicated by thick lines. Direct contact is necessary for the signal to be carried from one cell to the next. Approximate movement of the  $Ca^{2+}$  wave (shown by the thin line) at 2 sec intervals as it traveled from cell to cell is indicated by the numbers (sec).

**Serum, medium, and rat cerebrospinal fluid.** Most of the experiments were done with HEPES buffer, as commonly used with  $Ca^{2+}$  imaging. To recreate more closely the conditions under which these cells are growing, their responses to conditioned medium, nonconditioned medium, and serum were tested. The majority of cells (~95%), both neurons and glial cells, showed a  $Ca^{2+}$  rise when the medium they were growing in was reintroduced after a wash with HEPES buffer. To determine if this response was due to factors released by the cells or was due to the nonconditioned medium, three different media without serum were perfused through the chamber. All three, including

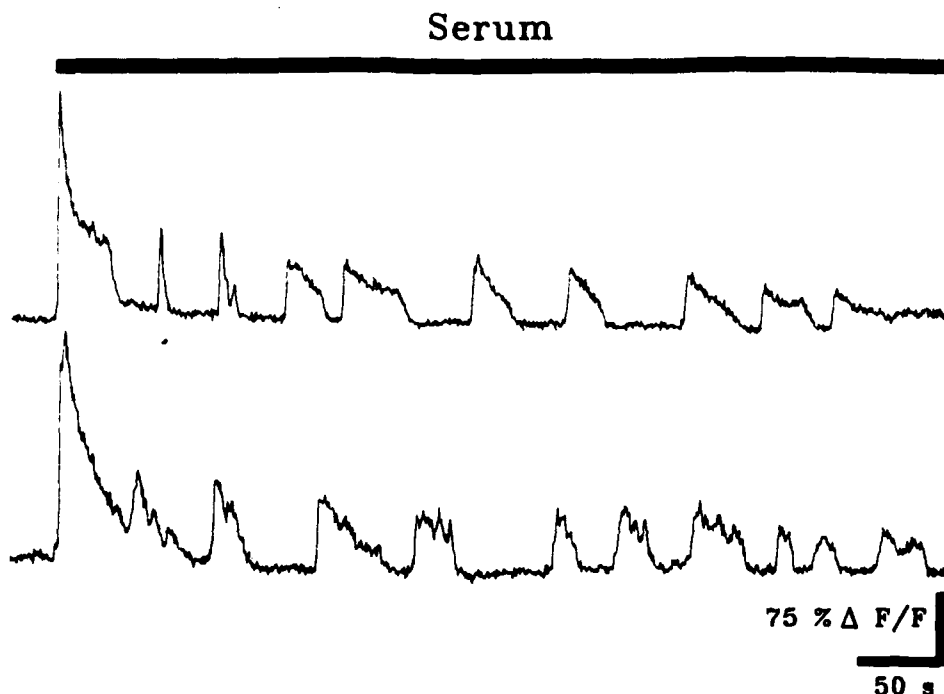


Figure 10. The addition of fetal bovine serum to the HEPES buffer induced a sharp rise in  $Ca^{2+}$  that drops down to the baseline, while  $Ca^{2+}$  oscillations continue in both of these astrocytes.

GIBCO F10, Eagle's MEM, and Dulbecco's MEM, caused an increase in  $Ca^{2+}$  levels in 95% of the cells tested ( $n > 100$ ). Similarly, fetal bovine serum (10%) when added to the HEPES buffer induced  $Ca^{2+}$  rises in 96% of the cells ( $n = 109$ ) examined (Fig. 10). Similar results were obtained with 10% horse serum. Chamber perfusion with both serum and medium also caused  $Ca^{2+}$  oscillations in glial cells.

In an attempt to recreate conditions that more closely simulate those that SCN cells might encounter in the rat brain, we used punches that contained blocks of SCN tissue that were not disaggregated with proteolytic enzymes, but instead were cultured whole. Figure 11 shows a slice used for histological verification where a part of SCN was punched out and cultured. Explants were used 4–8 d after culturing. When the fluo-3-loaded cells within the explants were examined with confocal laser microscopy, many of the astrocytes (43 of 55) showed  $Ca^{2+}$  oscillations induced by rat cerebrospinal fluid (CSF) (Fig. 12). Some glial cells showed regular oscillations that continued for the duration of the recording period with cells in the rat CSF (Fig. 13A). The top astrocyte in Figure 12 shows  $Ca^{2+}$  oscillations with an initial period of about 18 sec after introduction of CSF; as the mean  $Ca^{2+}$  level of the cell decreases, a second extended series of oscillations with a period of about 45 sec is seen for the duration of the recording period. Others showed an initial series of oscillations, followed by a return to baseline levels (Fig. 12). The thin optical sectioning capability of the confocal microscope allowed detection of nuclear responses to CSF (Fig. 13 D–F). Some astrocytes that showed regular oscillations in the cytoplasm also showed similar oscillations in the nucleus in phase with cytoplasmic  $Ca^{2+}$  levels. Prior to the addition of rat CSF, we detected no oscillations in any of the cells examined ( $n = 55$ ). Cells showing extended regular oscillations while incubated in rat CSF lost them when the CSF was replaced with HEPES buffer. Introduction of glutamate induced an additional  $Ca^{2+}$  rise and  $Ca^{2+}$  oscillations.

*Astrocytes surround presynaptic glutamate-immunoreactive boutons—ultrastructural immunocytochemistry.* Although glu-

tamate has been suggested as a primary transmitter in afferent projections to the SCN, supporting immunocytochemical evidence has been lacking. Since we found a glial response to glutamate *in vitro*, we investigated the morphological relationships between presynaptic boutons immunoreactive for glutamate and nearby astroglia in the intact adult SCN. Some axon terminals in synaptic contact with SCN perikarya and dendrites showed strong immunogold labeling with glutamate antisera. The ratio of gold particles over presynaptic axon to postsynaptic dendrite was 5:1, similar to ratios found over glutamatergic presynaptic axons in other parts of the brain (Somogyi et al., 1986; Ottersen, 1989; van den Pol, 1991). Astrocyte sheaths surrounded many synaptic complexes, including those in which the presynaptic axon exhibits a high immunoreactivity for glutamate (Fig. 14); these astrocyte processes segregate many neuronal elements from each other.

Glia in the adult SCN occur in numbers somewhat less than the number of neurons, as determined with stereological (Pal-kovits, 1976) counting of glial cells in electron micrographs from the SCN of adult male rats. Based on percentage of stereological point overlays on glia and neurons and on relative cell size in 60 random fields, the relative number of astroglia per unit volume was estimated to be about 65% of that of neurons with some variation in different regions of the SCN.

## Discussion

$Ca^{2+}$  is an important intermediary in a wide variety of cellular mechanisms. With noninvasive digital imaging of  $Ca^{2+}$  in living SCN cells, we have shown a strong neuronal and glial  $Ca^{2+}$  response to neurotransmitters. These were seen either as an increase in  $Ca^{2+}$  levels, or as a change in the patterns of ultradian oscillations.  $Ca^{2+}$  changes in the cytoplasm could serve to influence many of the intracellular systems using  $Ca^{2+}$  as a second messenger.  $Ca^{2+}$  rises detected in the cell nucleus may serve to modulate genomic expression there. The induction of *c-fos* and *c-jun* by neurotransmitters or cholera toxin may act through  $Ca^{2+}$  second messengers (Gabellini et al., 1991; Trejo and Brown,

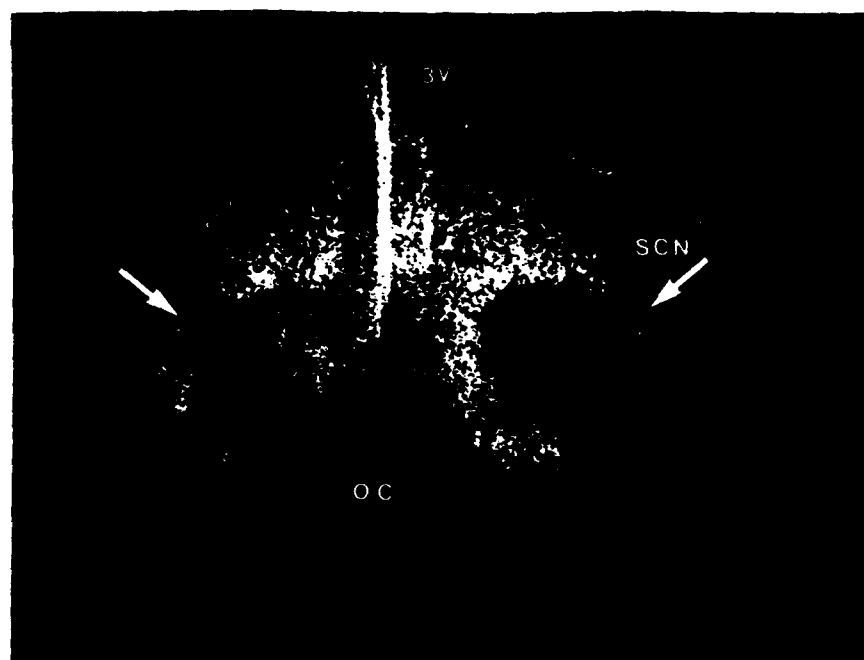


Figure 11. Laser confocal image of a propidium iodide-stained hypothalamic slice of a 3 d neonatal rat. Part of the SCN on both sides was punched out for culturing (arrows). oc, optic chiasm; 3v, third ventricle.

1991). An increase in SCN cell nuclear *c-fos* and other early-immediate gene products can be induced by photic stimulation at certain times of an animal's circadian cycle (Rea, 1989; Kornhauser et al., 1990; Rusak et al., 1990), perhaps through intracellular  $\text{Ca}^{2+}$  signaling.

**Neuron response to glutamate.** Immunocytochemical localization of high levels of glutamate in presynaptic endings in the SCN adds further support to previous suggestions that glutamate may be an important transmitter here (Shibata et al., 1986; Cahill and Menaker, 1987; Kim and Dudek, 1989). The widespread  $\text{Ca}^{2+}$  response of SCN neurons to glutamate suggests that the relative ineffectiveness of excitotoxic amino acids in killing SCN cells (Peterson and Moore, 1980) is not due either to the lack of glutamate receptors, or to a lack of an increase in intracellular  $\text{Ca}^{2+}$ , which has been suggested as one cause of cell death after exposure to high levels of excitatory amino acid agonists (Choi, 1988). Whether the reduced toxicity of glutamate in the SCN is due to a smaller number or different types of glutamate receptors, to differences in second messenger systems related to  $\text{Ca}^{2+}$ , or to differences in the astrocyte response and uptake of glutamate remains to be determined.

**Mechanism of SCN cellular  $\text{Ca}^{2+}$  oscillation.**  $\text{Ca}^{2+}$  oscillations are found outside the SCN in other cell types, and have been broadly categorized as either membrane oscillators or cytosolic oscillators according to the site where most of the  $\text{Ca}^{2+}$  fluxes occur (Berridge and Galione, 1988; Berridge and Irvine, 1989). Membrane oscillators depend on agonist-induced transmembrane voltage changes to trigger a reciprocal activation of voltage-gated  $\text{Ca}^{2+}$  and  $\text{Ca}^{2+}$ -sensitive potassium channels, resulting in a periodic  $\text{Ca}^{2+}$  influx. One example of a membrane oscillator is glucose-stimulated  $\text{Ca}^{2+}$  oscillations in pancreatic  $\beta$ -cells (Sherman et al., 1988; Grapengiesser et al., 1989; Chay, 1990). Cytosolic oscillators involve the periodic release of  $\text{Ca}^{2+}$  from an intracellular store; the mechanism may include receptor-stimulated inositol turnover, subsequent  $\text{Ca}^{2+}$  release from the endoplasmic reticulum, and specific interactions between intracellular elements such as protein kinase C, phospholipase C,

and  $\text{Ca}^{2+}$  reservoirs other than the endoplasmic reticulum. A capacitive model of cytosolic oscillators (Putney, 1986) postulates the existence of an intracellular store capable of accumulating cytosolic  $\text{Ca}^{2+}$  to a threshold level. Above threshold, additional cytosolic  $\text{Ca}^{2+}$  increases serve to stimulate a rapid release of intracellularly stored  $\text{Ca}^{2+}$ . Aspects of this idea have been incorporated into more complicated models that may explain a wider variety of features of cytosolic oscillators (Goldbeter et al., 1990). Since neurotransmitter stimulation elicits a  $\text{Ca}^{2+}$  rise in SCN glia even in the absence of extracellular  $\text{Ca}^{2+}$ , our data suggest that the neurotransmitter-induced  $\text{Ca}^{2+}$  increase, at least under our *in vitro* conditions, is primarily from intracellular stores, invoking a cytoplasmic oscillatory mechanism (Cornell-Bell et al., 1990; Jensen and Chiu, 1990) rather than a membrane oscillatory system.

Most experiments were done with HEPES buffer of minimal composition; addition of culture media, serum, or CSF to mimic more natural conditions increased the general level of activity of all cells, suggesting that a much greater level of complexity and oscillatory behavior may be occurring in the brain. Extended  $\text{Ca}^{2+}$  oscillations were found in astrocytes from SCN explants incubated in rat CSF, but not when CSF was replaced with buffer.

Regular  $\text{Ca}^{2+}$  oscillations in SCN neurons were detected less often than in astrocytes, and predominantly in the absence of TTX. Astrocyte oscillations in the presence of TTX were very regular. In contrast, neuronal oscillations tended to be sporadic and irregular in the presence of TTX in our *in vitro* conditions. This suggests that intercellular axosynaptic communication between neurons, or voltage-dependent sodium channels, may play a role in maintaining regular oscillations in neurons. Since there is a positive correlation with transmitter release and intracellular  $\text{Ca}^{2+}$ , neurons that demonstrated regular cycles of  $\text{Ca}^{2+}$  may also release their neurotransmitters in corresponding ultradian cycles. Oscillations in neurons were under neurotransmitter modulation. GABA, an inhibitory transmitter found in half (48%) of all SCN presynaptic axons (Decavel and van den Pol, 1990),

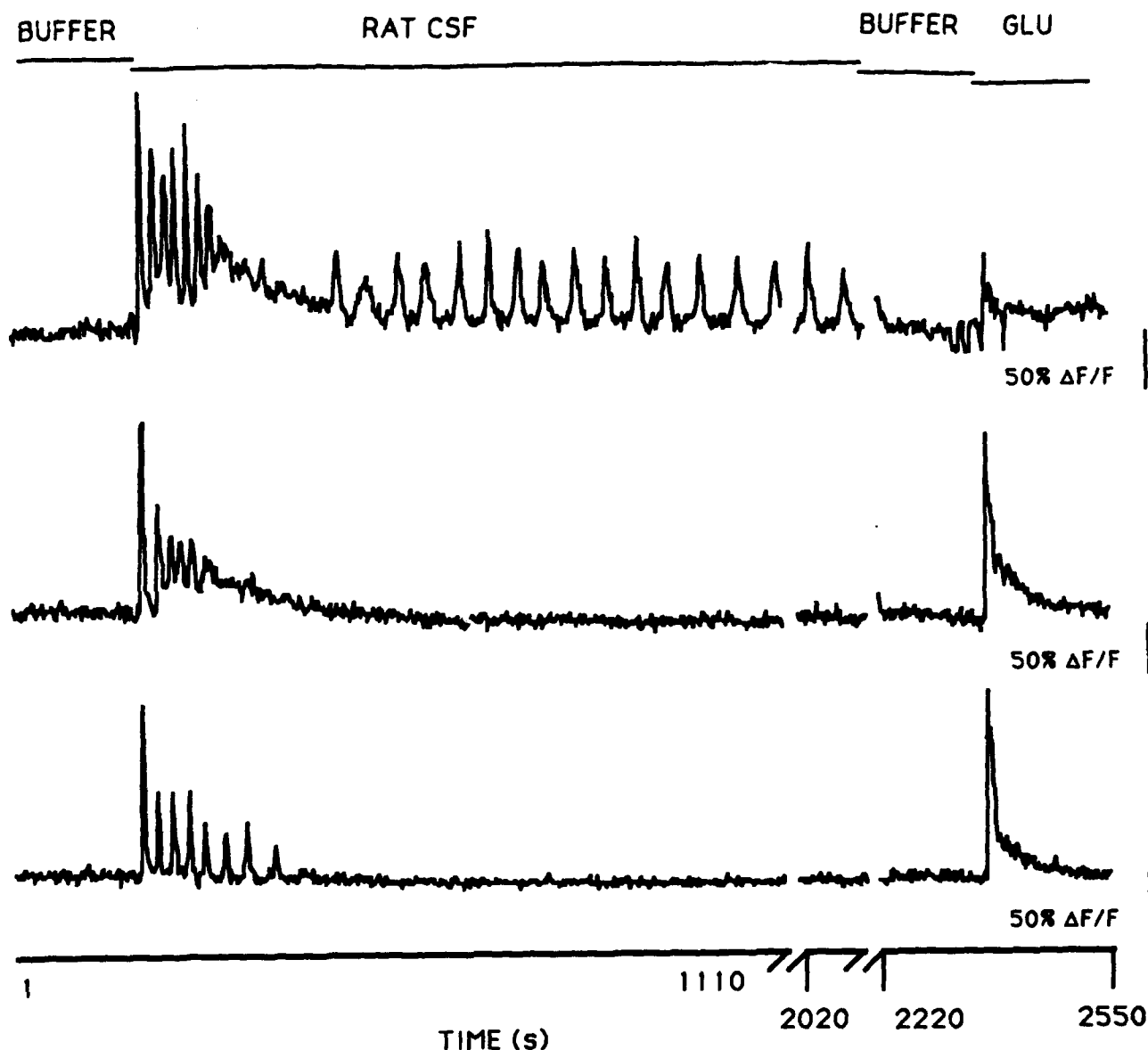


**Figure 12.** Response of three astrocytes from an SCN explant *in vitro* studied with laser confocal microscopy. During the first hundred seconds, astrocytes showed no oscillatory behavior in HEPES buffer. When rat CSF was added, all three cells showed an increase in  $\text{Ca}^{2+}$  and high-amplitude  $\text{Ca}^{2+}$  oscillations. The *top cell* continued to show  $\text{Ca}^{2+}$  oscillations throughout the time of examination. The other two cells returned to baseline  $\text{Ca}^{2+}$  levels. After 608 sec, recordings were stopped to reduce the possibility of phototoxicity of the laser beam; 500 sec later, recordings were again initiated, showing that the cell on top was still oscillating. When the rat CSF was replaced with HEPES buffer, oscillations ceased. All three cells responded with an increase in  $\text{Ca}^{2+}$  upon stimulation with  $100 \mu\text{M}$  glutamate.

**Figure 13.** *A*, A time series of 24 pseudocolored video micrographs showing a single fluo-3-labeled astrocyte (thick vertical arrow) with a regular  $\text{Ca}^{2+}$  oscillation. Green indicates higher levels of fluorescence, and pink indicates lower levels. Images were recorded 5.4 sec apart. The first image is labeled 1 and the last 24. The image sequence starts in the upper left and reads like a book, as shown by the horizontal arrow. The ultradian rhythm of this cell is very regular, seen by the strong  $\text{Ca}^{2+}$  signal in the 5th, 13th, and 21st frames;  $\text{Ca}^{2+}$  peaks were 43 sec apart. This sequence is 130 sec long and shows only a part of a sequence 10 times longer in which the cell maintained this steady rhythm. The width of the astrocyte was  $55 \mu\text{m}$ . *B*, Astrocyte during filling with carboxyfluorescein is on the left (arrow). The same cell 10 min later after the filling patch pipette was removed is seen on the right. Four adjacent cells are also labeled, suggesting dye movement through gap junctions between coupled cells. Width of the filled astrocyte was  $42 \mu\text{m}$ . *C*, Another cell in the same culture dish was filled with dye, on the left, and seen 10 min later on the right. Although many other glial cells surrounded this cell, no dye coupling was found in this case. Width of the filled astrocyte was  $40 \mu\text{m}$ . *D–F*, Confocal laser microscope was set for a thin optical section. In this series of micrographs, the nuclei (arrows) of two astrocytes show a strong response to the introduction of rat CSF to the recording chamber, similar to the response sometimes seen with introduction of neurotransmitter. Fluorescence increased in both the cytoplasm and nucleus. Dark red indicates a low level, bright red a medium level, and yellow a high level of fluorescence. *D* shows the two cells 5 sec before stimulation, representative of the previous 100 sec. *E* shows the cells 3 sec after initiation of stimulation, and *F* shows the same field 10 sec later. Width of micrograph is  $80 \mu\text{m}$ . *G*, A field of fluo-3-loaded SCN neurons prior to transmitter stimulation. *H*, The same field as shown in *G*, but at the time of stimulation with  $5 \mu\text{M}$  glutamate. All 15 neurons showed an increase in  $\text{Ca}^{2+}$  as shown by the increase in their pink coloration in this pseudocolored image. Arrows show the same two neurons in *G* and *H*. Width of micrograph is  $150 \mu\text{m}$ .

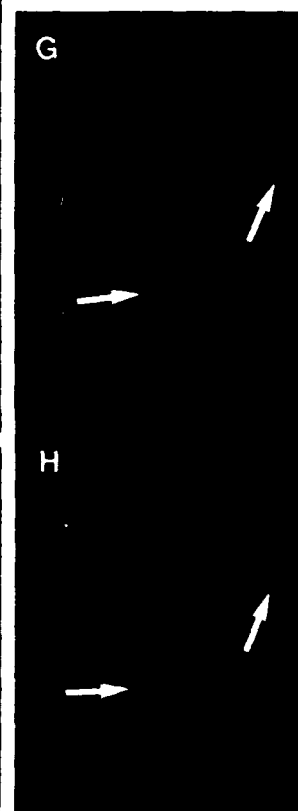
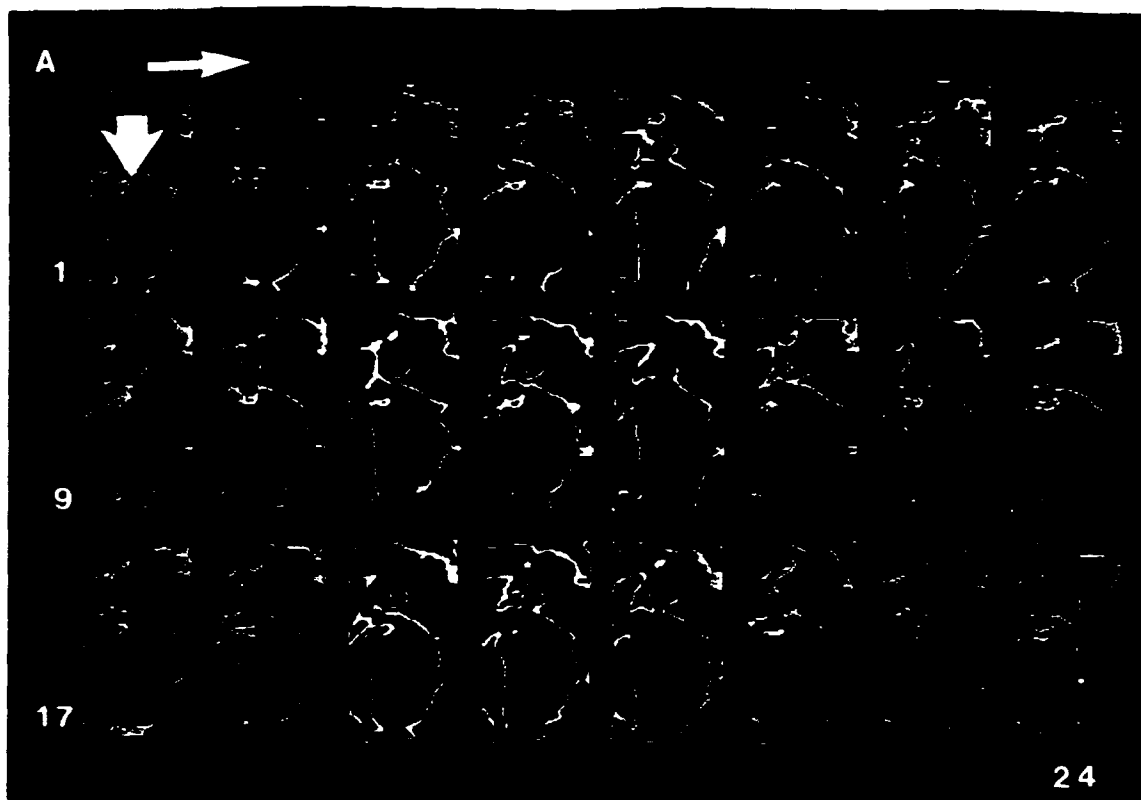




**Figure 14.** Glutamate-immunoreactive axon terminal (AX) labeled with colloidal gold particles (small arrows) makes synapse (open arrow) with dendrite (DEN). The synaptic complex is isolated from SCN neuropil by astrocyte processes (large arrows). The number of gold particles over the immunoreactive axon is eight times greater than over other cellular processes in this micrograph. Myelinated axons in the optic chiasm, probably of retinal origin, also showed glutamate immunoreactivity.

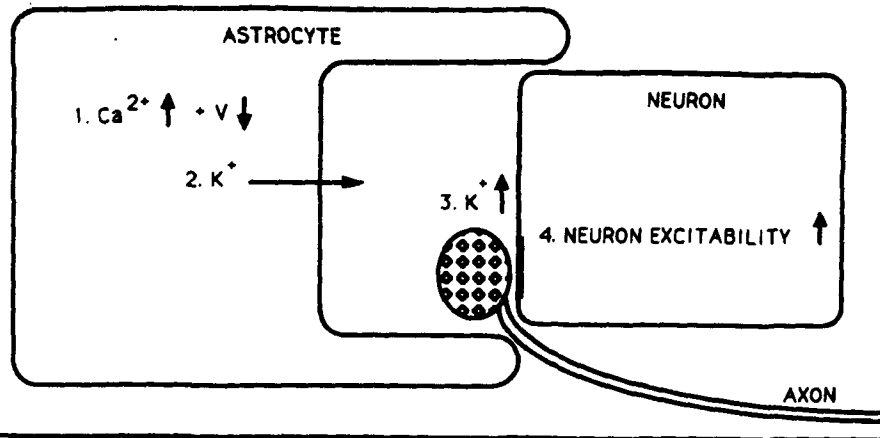
could eliminate periodic oscillations that would return in the absence of GABA, whereas glutamate set the mean intracellular  $Ca^{2+}$  of the oscillating neuron at a higher level. These amino acid transmitters, glutamate and GABA, found in large numbers of presynaptic terminals surrounded by astrocytes in the SCN, influence both the baseline level of intracellular  $Ca^{2+}$  as well as the ultradian  $Ca^{2+}$  oscillations.

That circadian rhythms may be related to ultradian oscillations is suggested by the observation that *per* mutations that eliminate or alter circadian rhythms in *Drosophila* (Konopka and Benzer, 1971) also disturb an ultradian rhythm of the flies (Kyriacou and Hall, 1980). Interestingly, the *per* gene is expressed both in neurons and in glial cells in the fly brain (Zerr et al., 1990). Recent experiments with fly genetic mosaics suggest that expression of *per* in glia without detectable expression in neurons may be sufficient for weak manifestation of circadian behavioral rhythms in *Drosophila*, although normal circadian rhythms are probably associated with *per* expression in both glia and neurons. *Drosophila* glia expressing *per* are postulated to play a role in coupling the activity of pacemaker neurons (J. Hall, personal communication; Ewer et al., 1992).

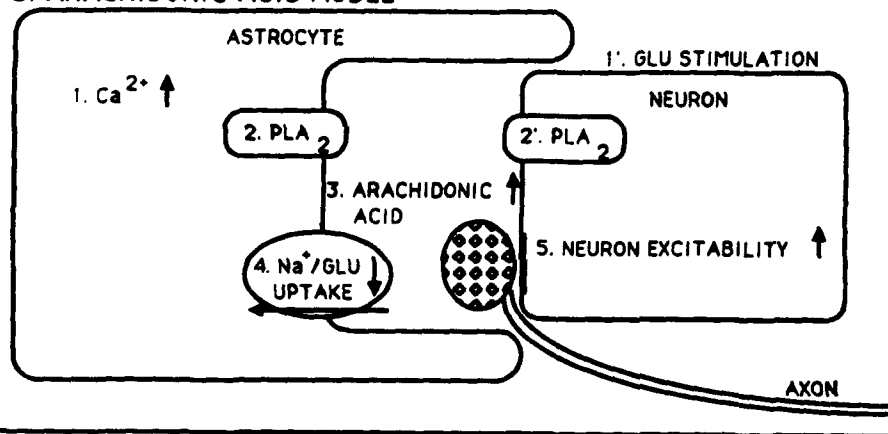
**Astrocyte modulation of neural activity.** If astrocytes are involved in SCN function, they must be in communication with neurons since the output of the clock clearly involves neuronal efferent projections (Schwartz et al., 1987; Meijer and Rietveld, 1989; Schwartz, 1991). With ultrastructural immunocytochemistry, we showed here that in the mature SCN, astrocytes are in close contact with axon terminals and surround glutamate-immunoreactive axons in synaptic contact with dendrites. We have no direct evidence that SCN astrocytes modulated neuronal activity. Three hypothetical models involving changes in intracellular  $Ca^{2+}$  and secondary changes in extracellular potassium, arachidonic acid or a metabolite, or calcium are suggested here. These models are not mutually exclusive and could underlie glial modulation of neural activity. In the potassium model (Fig. 15A), an increase in intracellular  $Ca^{2+}$  acts in concert with astrocyte depolarization induced by glutamate or other transmitters (Bowman and Kimelberg, 1984; Kettenmann and Schachner, 1985; Usowicz et al., 1989) to open enough  $Ca^{2+}$ -activated potassium channels (Quandt and MacVicar, 1986; Nowak et al., 1987; Barres et al., 1988) to significantly alter the potassium concentration of the extracellular space between astrocytes and neurons. The second model (Fig. 15B) is based on intracellular  $Ca^{2+}$  rises in glia that would directly activate phospholipase  $A_2$ , thereby liberating arachidonic acid from astrocytes (Axelrod et al., 1988; Bruner and Murphy, 1990). Similarly, arachidonic acid is released from neurons after stimulation of the NMDA receptor by glutamate (Dumuis et al., 1988). Peptide transmitters may also increase  $Ca^{2+}$ -dependent arachidonic acid release from astrocytes, leading to an increased extracellular glutamate level (Marin et al., 1991). Arachidonic acid or a metabolite inhibits the astrocyte glutamate/sodium uptake (Barbour et al., 1989). As glial uptake of neurotransmitter amino acids is a major route of transmitter inactivation, reduced uptake would lead to a net rise in extracellular glutamate concentrations, thereby influencing neuronal excitability. A third possibility (Fig. 15C) is that astrocytes may exercise some regulation of extracellular  $Ca^{2+}$  by virtue of slow synchronized  $Ca^{2+}$  uptake that could potentially influence transmitter release at synaptic junctions.  $Ca^{2+}$  uptake by astrocytes around synaptic complexes may reduce extracellular  $Ca^{2+}$ , leading to a decrease in neurotransmitter release. SCN glial cells have long regions of apposition to neurons, with an extracellular distance of less than 20 nm. The volume of the total extracellular space between a neuron and glial cell is very small ( $0.002 \mu m^3$  over a  $10 \mu m^2$  area), facilitating any neuronal response to astrocyte-mediated changes in extracellular potassium, glutamate, or calcium.

**Coupled astrocyte oscillators.** We found ultradian oscillations in both neurons and glia cultured from SCN cells. Mathematical models can be used to demonstrate that the period of an aggregate rhythm from a population of oscillators may be faster or longer than any individual oscillator in the group (Winfree, 1967), allowing a group of coupled oscillators, neurons or glia, to form an aggregate circadian rhythm. Coupling also can lead to a precise aggregate rhythm by entraining the individual oscillators that would otherwise be significantly hampered by stochastic processes (Winfree, 1967). Mathematical modeling has suggested that high-frequency oscillators with periods within the same range as those shown in the present article for SCN cells may be the basis for a low-frequency oscillator such as a circadian oscillator (Pavlidis, 1969). Since a mechanism exists for integrating  $Ca^{2+}$  transients (Lisman and Goldring, 1988), precise ultradian oscillations could form the basis for a circadian

## A. POTASSIUM MODEL



## B. ARACHIDONIC ACID MODEL



## C. CALCIUM MODEL

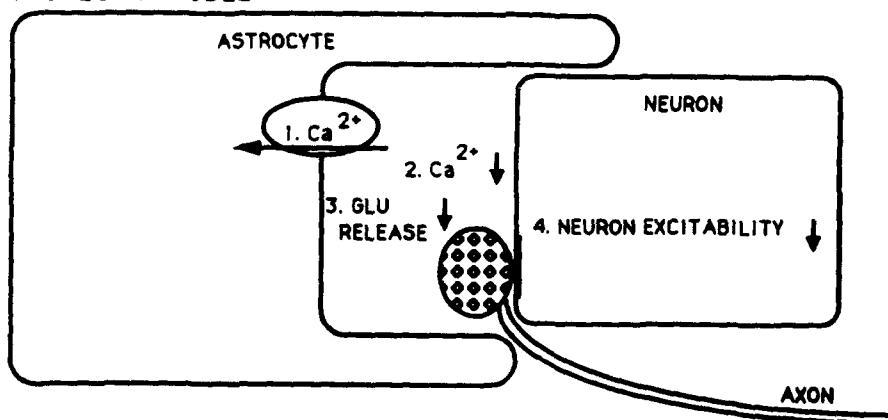


**Figure 15.** Three hypothetical models show how SCN astrocytes might modulate neuronal activity. The numbers in each model indicate the general sequence of events. Possible increases or decreases in neuronal excitability are indicated by the vertical arrows in the neurons; ion movement is indicated by horizontal arrows. Under certain temporal or concentration conditions, the direction of excitability could be postulated to be in the direction opposite to that shown.

rhythm. Coupling cellular oscillators also appears possible. For instance, liver cells are capable of synchronous and periodic  $\text{Ca}^{2+}$  secretion in response to the same agonist (Graf et al., 1987) that causes cyclical  $\text{Ca}^{2+}$  transients in single liver cells (Woods et al., 1987). Like liver cells, SCN astrocytes are extensively coupled by gap junctions, both *in vivo* and *in vitro*, and thus might couple their individual oscillations into an aggregate rhythm. On a microscopic scale, we found that the period of regular oscillations of individual astrocytes could be greatly increased by the glutamate, 5-HT, or ATP induction of intercellular waves of  $\text{Ca}^{2+}$ . These waves moving through coupled astrocytes increased the average period from about 14 sec to about

60 sec or longer, demonstrating that astrocyte intercellular communication plays a significant role in the alteration of the average period between the  $\text{Ca}^{2+}$  peaks. Waves of  $\text{Ca}^{2+}$  have been reported in other cells, where they appear to be dependent on gap junctions between cells, and may utilize inositol 1,4,5-triphosphate to carry the message across the gap junctions (Berridge and Irvine, 1989; Charles et al., 1991). That the  $\text{Ca}^{2+}$  wave may move between SCN glia through gap junctions is consistent with our confirmation in the present study of dye coupling between these cells. Substances that uncouple gap junctions eliminate the intercellular  $\text{Ca}^{2+}$  waves (Finkbeiner, 1991). The possibility that astrocytes with different transmitter responses may

have divided faster than others in culture makes it difficult to predict the relative percentage of astrocytes that might respond to transmitters in adult tissue.

**Neuron and glial role in SCN function.** The possible involvement of astroglia in SCN function has not been previously explored and, while it may appear unlikely, merits some examination. When TTX was administered to the SCN, cells of the SCN continued to keep time, but their ability to drive behavioral and physiological circadian rhythms was lost (Schwartz et al., 1987; Meijer and Rietveld, 1989; Schwartz, 1991). Similarly, TTX administration to SCN explants reduced peptide secretion, but did not alter the phase of vasopressin secretion when a rhythm could be detected after cessation of TTX (Earnest et al., 1991). Since TTX blocks sodium-dependent action potentials and axonal conduction (Katz and Miledi, 1967), SCN neurons cannot communicate with each other by conventional neurochemical transmission, yet when tetrodotoxin is removed, behavioral cycles continue as if the clock cells were keeping time but were unable to send this message to other parts of the brain. In the present study, we found that TTX does not block the regular oscillations of SCN astrocytes, and similarly has no detectable effect on long-distance intercellular communication between astrocytes. In biological clocks in other species, gap junctions have been a regular feature, and are found in cellular circadian clocks of the *Bulla* eye (Jacklet and Geronimo, 1971; Jacklet and Colquhoun, 1983) and in the avian pineal (Takahashi and Menaker, 1984), and have been postulated to mediate the function of the *Drosophila* clock gene *per* (Bargiello et al., 1987). In contrast to SCN glia, neurons of the SCN have shown little evidence for gap junctions (van den Pol, 1980). If new ways of detection are successful at demonstrating interneuronal gap junctions in the SCN, this would add another dimension to cellular interaction here.

SCN glia appear to be different than glia from the surrounding hypothalamus as shown by the strong immunoreactivity for glial fibrillary acidic protein in the SCN compared with the immediately adjacent hypothalamus (Morin et al., 1989). Furthermore, glia in other parts of the brain are estimated to occur in numbers 10 times greater than neurons (Kuffler et al., 1984). In sharp contrast, in the present study we found fewer glial cells than neurons in the SCN. SCN glia also appear to be functionally different than those in other parts of the brain. Whereas virtually all (99–100%) hippocampal astrocytes responded to glutamate under culture conditions similar to those described in the present experiment (Cornell-Bell et al., 1990), a smaller percentage of cells from SCN cultures show a  $\text{Ca}^{2+}$  response to glutamate. Those SCN astrocytes that do not respond to glutamate may respond to 5-HT or ATP; we did not compare hippocampal astrocytes with 5-HT or ATP. The communication between specific glial partners *in vitro* may be mirrored in the brain. Based on Golgi impregnations, gold sublimate staining, electron microscopy (van den Pol, 1980), cell counts, and glial fibrillary acidic protein immunostaining, single glial cells may interdigitate between neurons and surround axodendritic synaptic complexes, and thereby influence hundreds of SCN neurons. We find that not only can glutamate induce intercellular waves of  $\text{Ca}^{2+}$ , as also found in the hippocampus (Cornell-Bell et al., 1990), but of particular interest, 5-HT and ATP can also induce these waves in cultured SCN astrocytes, leading to long-distance astrocyte communication. Since the response of astrocytes to the application of these substances is heterogeneous, one may elicit waves of  $\text{Ca}^{2+}$  between subsets of glia based on their se-

lective transmitter response. The possibility of specific anatomical pathways of glial signaling, based on selective response to different transmitters, merits experimental attention, not only with regard to local circuit cellular interactions in the SCN, but also in other regions of the brain. Recent experiments on hippocampal slices have demonstrated a direct influence of presumptive glutamatergic neurons on astrocyte  $\text{Ca}^{2+}$ ; electrical stimulation of axons initiated  $\text{Ca}^{2+}$  waves in astrocytes near the axon terminals (Dani et al., in press).

Orchestrated cellular rhythms of 2-deoxyglucose uptake in the SCN are found at birth (Reppert and Schwartz, 1984). Whereas glial cells develop later than neurons in most parts of the hypothalamus, they may be found early in the SCN (Altman and Bayer, 1986) and in the adjacent optic chiasm (Vaughn and Peters, 1971), from which long astrocyte processes reach into the SCN (van den Pol, 1980). 2-Deoxyglucose rhythms are unlikely to be coordinated by synaptic interaction, which is rare at this stage of development (Moore, 1991); an alternative substrate for cellular orchestration is the gap junction present between developmentally immature cells.

In general, a primary purpose of cellular oscillators and intercellular waves of  $\text{Ca}^{2+}$  appears to be related to intercellular communication, and to increased cell synchrony. In this regard, the incorporation of this type of information could be of potential use in an area of the brain involved in timekeeping, and integration of astrocytes may lend greater stability to an oscillator based on rapidly responding neurons and astrocytes that show a slower response. Different regions of the brain appear to use similar physiological mechanisms, ion channels, and transmitters to perform different functions, in large part based on specific complex circuitry. As with other brain loci, the SCN is unique in the constellation of afferent and efferent axons, and local circuit interactions within the nucleus. Whether the ability of the SCN to drive circadian rhythms is due to some undiscovered cellular feature, or to its unique organization, remains to be determined.

The data presented here show dynamic responses and cellular communication between SCN glia induced by transmitters found in the SCN. These data suggest that the inclusion of both glial cells and neurons in models of SCN function may provide a more complete representation of cellular interaction in the biological clock. In both types of cells,  $\text{Ca}^{2+}$  may act as a critical agent mediating the influence of many neuroactive substances and orchestrating a number of intracellular mechanisms.

## References

- Aghajanian GK, Bloom FE, Sheard MH (1969) Electron microscopy of degeneration within the serotonin pathway of rat brain. *Brain Res* 13:266–273.
- Altman J, Bayer SA (1986) The development of the rat hypothalamus. *Adv Anat Embryol Cell Biol* 100:1–178.
- Axelrod J, Burch RM, Jelsema CL (1988) Receptor-mediated activation of phospholipase A2 via GTP-binding proteins: arachidonic acid and its metabolites as second messengers. *Trends Neurosci* 11:117–123.
- Barbour B, Szatkowski M, Ingledew N, Atwell D (1989) Arachidonic acid induces a prolonged inhibition of glutamate uptake into glial cells. *Nature* 342:918–920.
- Bargiello TA, Saez L, Bayliss MK, Gasic G, Young MW, Spray DC (1987) The *Drosophila* clock gene *per* affects intercellular junctional communication. *Nature* 328:686–691.
- Barres BA, Chun LLY, Corey DP (1988) Ion channel expression by white matter glia. I. Type 2 astrocytes and oligodendrocytes. *Glia* 1:10–30.

- Berridge MJ, Galione A (1988) Cytosolic calcium oscillators. *FASEB J* 2:3074-3082.
- Berridge MJ, Irvine RF (1989) Inositol phosphates and cell signalling. *Nature* 341:197-205.
- Bowman CL, Kimelberg HK (1984) Excitatory amino acids directly depolarize rat brain astrocytes in primary culture. *Nature* 311:656-659.
- Bruner G, Murphy S (1990) ATP-evoked arachidonic acid mobilization in astrocytes is via a P-purineric receptor. *J Neurochem* 55:1569-1575.
- Burnstock G (1986) Purines as cotransmitters in the adrenergic and cholinergic neurones. *Prog Brain Res* 68:193-203.
- Cahill GM, Menaker M (1987) Kynurenic acid blocks suprachiasmatic nucleus responses to optic nerve stimulation. *Brain Res* 410:125-129.
- Charles AC, Merrill JE, Dirksen ER, Sanderson MJ (1991) Intercellular signaling in glial cells: calcium waves and oscillations in response to mechanical stimulation and glutamate. *Neuron* 6:983-992.
- Chay TR (1990) Effect of compartmentalized  $Ca^{2+}$  ions on electrical bursting activity of pancreatic B-cells. *Am J Physiol* 258:C955-C965.
- Choi DW (1988) Glutamate neurotoxicity and diseases of the nervous system. *Neuron* 1:623-634.
- Cline HT, Tsien RW (1991) Glutamate-induced increases in intracellular  $Ca^{2+}$  in cultured frog tectal cells mediated by direct activation of NMDA receptor channels. *Neuron* 6:259-267.
- Cornell-Bell AH, Finkbeiner SM (1991)  $Ca^{2+}$  waves in astrocytes. *Cell* 66:12185-204.
- Cornell-Bell AH, Finkbeiner SM, Cooper MS, Smith SJ (1990) Glutamate induces calcium waves in cultured astrocytes: long-range glial signaling. *Science* 247:470-473.
- Dani J, Chernjavsky A, Smith SJ (in press) Neuronal activity triggers calcium waves in hippocampal astrocyte networks. *Neuron*, in press.
- Decavel C, van den Pol AN (1990) GABA: a dominant transmitter in the hypothalamus. *J Comp Neurol* 302:1019-1037.
- Dumuis A, Sebben M, Haynes L, Pin JP, Bockaert J (1988) NMDA receptors activate the arachidonic acid cascade system in striatal neurons. *Nature* 336:68-70.
- Earnest DJ, Digiorgio SM, Sladek CD (1991) Effects of tetrodotoxin on the circadian pacemaker mechanism in suprachiasmatic explants *in vitro*. *Brain Res Bull* 26:677-682.
- Ewer J, Frisch B, Hamblen-Coyle MJ, Rosbash M, Hall JC (1992) Expression of the *period* clock gene within different cell types in the brain of *Drosophila* adults and mosaic analysis of these cells' influence on circadian behavioral rhythms. *J Neurosci*, in press.
- Finkbeiner SM (1991) Calcium-mediated glutamate responses in cultured hippocampus, pp 1-353. PhD thesis, Yale University.
- Gabellini N, Facci L, Milani D, Negro A, Callegaro L, Skaper SD, Leon A (1991) Differences in induction of *c-fos* transcription by cholera toxin-derived cyclic AMP and  $Ca^{2+}$  signals in astrocytes and 3T3 fibroblasts. *Exp Cell Res* 19:210-217.
- Gahwiler BH (1981) Organotypic monolayer cultures of nervous tissue. *J Neurosci Methods* 4:329-342.
- Glaum SR, Holzwarth JA, Miller RJ (1990) Glutamate receptors activate  $Ca^{2+}$  mobilization and  $Ca^{2+}$  influx into astrocytes. *Proc Natl Acad Sci USA* 87:3454-3458.
- Goldbeter A, Dupont G, Berridge MJ (1990) Minimal model for signal-induced  $Ca^{2+}$  oscillations and for their frequency encoding through protein phosphorylation. *Proc Natl Acad Sci USA* 87:1461-1465.
- Graf P, vom Dahl S, Sies H (1987) Sustained oscillations in extracellular calcium concentrations upon hormonal stimulation of perfused rat liver. *Biochem J* 241:933-936.
- Grapengeter E, Glyfe E, Hellman B (1989) Three types of cytoplasmic  $Ca^{2+}$  oscillations in stimulated pancreatic B-cells. *Arch Biochem Biophys* 268:404-407.
- Jacklet J, Colquhoun W (1983) Ultrastructure of photoreceptors and circadian pacemaker neurons in the eye of a gastropod, *Bulla*. *J Neurocytol* 12:673-696.
- Jacklet JW, Geronimo J (1971) Circadian rhythm: population of interacting neurons. *Science* 174:299-302.
- Jensen AM, Chiu SY (1990) Fluorescence measurement of changes in intracellular calcium induced by excitatory amino acids in cultured cortical astrocytes. *J Neurosci* 10:1165-1175.
- Katz B, Miledi R (1967) A study of synaptic transmission in the absence of nerve impulses. *J Physiol (Lond)* 192:407-436.
- Kettenman H, Schachner M (1985) Pharmacological properties of gamma-aminobutyric acid-, glutamate-, and aspartate-induced depolarizations in cultured astrocytes. *J Neurosci* 5:3295-3301.
- Kim YI, Dudek FE (1989) Antagonism of fast excitatory postsynaptic potentials in suprachiasmatic nucleus neurons by excitatory amino acid antagonists. *Soc Neurosci Abstr* 15:1088.
- Konopka RJ, Benzer S (1971) Clock mutants of *Drosophila melanogaster*. *Proc Natl Acad Sci USA* 68:2112-2116.
- Kornhauser JM, Nelson DE, Mayo KE, Takahashi JS (1990) Photocircadian regulation of *c-fos* gene expression in the hamster suprachiasmatic nucleus. *Neuron* 5:127-134.
- Kuffler SW, Nicholls JG, Martin AB (1984) From neuron to brain. Sunderland, MA: Sinauer.
- Kyriacou CP, Hall JC (1980) Circadian rhythm mutations in *Drosophila melanogaster* affect short-term fluctuations in the male's courtship song. *Proc Natl Acad Sci USA* 77:6729-6733.
- Lisman JE, Goldring MA (1988) Feasibility of long-term storage of graded information by the  $Ca^{2+}$ /calmodulin-dependent protein kinase molecules of the postsynaptic density. *Proc Natl Acad Sci USA* 85:5320-5324.
- Marin P, Delumeau JC, Tence M, Cordier J, Glowinski J, Premont J (1991) Somatostatin potentiates the  $\alpha_1$ -adrenergic activation of phospholipase C in striatal astrocytes through a mechanism involving arachidonic acid and glutamate. *Proc Natl Acad Sci USA* 88:9016-9020.
- McCarthy KD, Salm AK (1991) Pharmacologically-distinct subsets of astroglia can be identified by their calcium response to neuroleptands. *Neuroscience* 41:325-333.
- Meijer JH, Rietveld WJ (1989) Neurophysiology of the suprachiasmatic circadian pacemaker in rodents. *Physiol Rev* 69:671-707.
- Meijer JH, van der Zee EA, Dietz M (1988) Glutamate phase shifts circadian activity rhythms in hamsters. *Neurosci Lett* 86:177-183.
- Moore RY (1991) Development of the suprachiasmatic nucleus. In: The suprachiasmatic nucleus: the mind's clock (Klein D, Moore R, Reppert S, eds), pp 391-404. Oxford: Oxford UP.
- Moore RY, Eichler VB (1972) Loss of circadian adrenal corticosterone rhythm following suprachiasmatic nucleus lesions. *Brain Res* 42:201-206.
- Morin LP, Johnson RF, Moore RY (1989) Two brain nuclei controlling circadian rhythms are identified by GFAP immunoreactivity in hamsters and rats. *Neurosci Lett* 99:55-60.
- Nowak L, Ascher P, Berwald-Netter Y (1987) Ionic channels in mouse astrocytes in culture. *J Neurosci* 7:101-109.
- Ottersen OP (1989) Quantitative electron microscopic immunocytochemistry of neuroactive amino acids. *Anat Embryol* 180:1-15.
- Palkovits M (1976) Determination of axon terminal density in the central nervous system. *Brain Res* 108:413-417.
- Pavlidis T (1969) Populations of interacting oscillators and circadian rhythms. *J Theor Biol* 22:418-436.
- Peterson GM, Moore RY (1980) Selective effects of kainic acid on diencephalic neurons. *Brain Res* 202:165-182.
- Pittendrigh CS (1974) Circadian oscillations in cells and the circadian organization of multicellular systems. In: The neurosciences: third study program (Schmitt FO, Worden FG, eds), pp 437-458. Cambridge, MA: MIT Press.
- Putney JW (1986) A model for receptor-regulated calcium entry. *Cell Calcium* 7:1-12.
- Quandt FN, MacVicar BA (1986) Calcium activated potassium channels in cultured astrocytes. *Neuroscience* 19:29-41.
- Rea M (1989) Light increases fos-related protein immunoreactivity in the rat suprachiasmatic nucleus. *Brain Res Bull* 23:577-580.
- Reppert SM, Schwartz WJ (1984) The suprachiasmatic nuclei of the fetal rat: characterization of a functional circadian clock using  $^{14}C$ -labeled deoxyglucose. *J Neurosci* 4:1677-1682.
- Rusak B, Zucker I (1979) Neural regulation of circadian rhythms. *Physiol Rev* 59:449-526.
- Rusak B, Robertson HA, Wisden W, Hunt SP (1990) Light pulses that shift rhythms induce gene expression in the suprachiasmatic nucleus. *Science* 248:1237-1240.
- Schwartz WJ (1991) Further evaluation of the tetrodotoxin-resistant circadian pacemaker in the suprachiasmatic nuclei. *J Biol Rhythms* 6:149-158.
- Schwartz WJ, Gross RA, Morton MT (1987) The suprachiasmatic nuclei contain a tetrodotoxin-resistant circadian pacemaker. *Proc Natl Acad Sci USA* 84:1694-1698.
- Sherman A, Rinzel J, Keizer J (1988) Emergence of organized bursting

- in clusters of pancreatic B-cells by channel sharing. *Biophys J* 54: 411-425.
- Shibata S, Shiratsuchi A, Liou SY, Ueki S (1984) The role of calcium ions in circadian rhythm of suprachiasmatic nucleus neuron activity in rat hypothalamic slices. *Neurosci Lett* 52:181-184.
- Shibata S, Liou SY, Ueki S (1986) Influence of excitatory amino acid receptor antagonists and of baclofen on synaptic transmission in the optic nerve to the suprachiasmatic nucleus in slices of rat hypothalamus. *Neuropharmacology* 25:403-409.
- Shibata S, Newman GC, Moore RY (1987) Effects of calcium ions on glucose utilization in the rat suprachiasmatic nucleus *in vitro*. *Brain Res* 426:332-338.
- Somogyi P, Halasy K, Somogyi J, Storm-Mathisen J, Ottersen OP (1986) Quantification of immunogold labelling reveals enrichment of glutamate in mossy and parallel fibre terminals in cat cerebellum. *Neuroscience* 19:1045-1050.
- Stephan FK, Zucker I (1972) Circadian rhythms in drinking behavior and locomotor activity of rats are eliminated by hypothalamic lesions. *Proc Natl Acad Sci USA* 69:1583-1586.
- Takahashi JS, Menaker M (1984) Multiple redundant circadian oscillators within the isolated avian pineal gland. *J Comp Physiol* 154: 435-440.
- Trejo JA, Brown JH (1991) *c-fos* and *c-jun* are induced by muscarinic receptor activation of protein kinase C but are differentially regulated by intracellular calcium. *J Biol Chem* 266:7876-7882.
- Usonicz MM, Gallo V, Cull-Candy SG (1989) Multiple conductance channels in type-2 cerebellar astrocytes activated by excitatory amino acids. *Nature* 339:380-383.
- van den Pol AN (1980) The hypothalamic suprachiasmatic nucleus of rat: intrinsic anatomy. *J Comp Neurol* 191:661-702.
- van den Pol AN (1989) Neuronal imaging with colloidal gold. *J Microsc* 155:27-59.
- van den Pol AN (1991) Glutamate and aspartate immunoreactivity in hypothalamic presynaptic axons. *J Neurosci* 11:2087-2101.
- van den Pol AN, Decavel C (1990) Synaptic interaction between chemically defined neurons: dual ultrastructural immunocytochemical approaches. In: *Methods for the analysis of neuronal microcircuits and synaptic interactions* (Bjorklund A, Hokfelt T, Wouterlood F, van den Pol AN, eds), pp 199-272. Amsterdam, Elsevier.
- van den Pol AN, Powley T (1979) A fine-grained anatomical analysis of the role of the rat suprachiasmatic nucleus in circadian rhythms of feeding and drinking. *Brain Res* 160:307-326.
- van den Pol AN, Tsujimoto K (1985) Neurotransmitters of the hypothalamic suprachiasmatic nucleus: immunocytochemical analysis of 25 neuronal antigens. *Neuroscience* 15:1049-1086.
- van den Pol AN, di Porzio U, Rutishauser U (1986) Growth cone localization of NCAM on central nervous system neurons *in vitro*. *J Cell Biol* 102:2281-2294.
- van den Pol AN, Wuarin JP, Dudek FE (1990) Glutamate, the dominant excitatory transmitter in neuroendocrine regulation. *Science* 250:1276-1278.
- van den Pol AN, Cornell-Bell A, Finkbeiner S (1991) Ultradian calcium oscillations in suprachiasmatic nucleus cells. *Soc Neurosci Abstr* 17:25.
- Vaughn JE, Peters A (1971) The morphology and development of neuroglial cells. In: *Cellular aspects of growth and differentiation* (Pease DC, ed), pp 103-140. Los Angeles: University of California Press.
- Winfree AT (1967) Biological rhythms and the behavior of populations of coupled oscillators. *Theor Biol* 16:15-42.
- Woods NM, Cuthbertson RKS, Cobbold PH (1987) Agonist-induced oscillations in the cytoplasmic free calcium concentration in single rat hepatocytes. *Cell Calcium* 8:79-100.
- Wray S, Gahwiler BH, Gainer H (1988) Slice cultures of LHRH neurons in the presence and absence of brainstem and pituitary. *Peptides* 9:1151-1175.
- Zerr DM, Hall JC, Rosbash M, Siwicki KK (1990) Circadian fluctuations of period protein immunoreactivity in the CNS and the visual system of *Drosophila*. *J Neurosci* 10:2749-2762.

# Glutamate and Aspartate Immunoreactivity in Hypothalamic Presynaptic Axons

Anthony N. van den Pol

Section of Neurosurgery, Yale University School of Medicine, New Haven, Connecticut 06510

Within the hypothalamus, a large number of neuroactive substances are found, many first detected in this part of the brain. Excitatory amino acids, recognized as important transmitters in other parts of the brain, have received little attention here. To study glutamate immunoreactivity at the ultrastructural level in the hypothalamus, postembedding colloidal gold or silver-intensified gold was used. Antisera raised against glutamate conjugated with glutaraldehyde to key-hole limpet hemocyanin were specific for glutamate, tested with a battery of tests including immunodot blot, ELISA assays, Western blot, and Sepharose epoxy-conjugated amino acids. Antisera did not cross-react with other amino acids and related compounds, with proteins containing glutamate, or with polyglutamate.

A population of presynaptic boutons in the suprachiasmatic, arcuate, ventromedial, supraoptic, and parvocellular and magnocellular paraventricular nuclei showed strong immunoreactivity for glutamate. Highly labeled presynaptic axons generally made asymmetrical Gray type 1 synaptic contacts with dendrites or cell bodies and had up to eight times more immunogold particles per unit area than postsynaptic dendrites. Axon terminals exhibiting strong glutamate immunoreactivity had large numbers of round, clear vesicles adjacent to the synaptic specialization together with a few larger, dense-core vesicles. The largest number of gold particles over axons were located in regions containing the small clear vesicles. Axons in general had about three times more gold particles over them than did the postsynaptic dendrites. Staining of single boutons in adjacent serial ultrathin sections with glutamate or GABA antisera showed that non-GABAergic terminals had a higher level of glutamate staining than did axons immunoreactive for GABA. In control experiments, immunostaining with glutamate antiserum could be blocked by solid-phase absorption of the antiserum with glutamate conjugated with glutaraldehyde to proteins.

Aspartate was also detected with immunocytochemistry in some presynaptic boutons in the medial hypothalamus. To compare the response of neurons to aspartate and glutamate, calcium-imaging dyes were used in combination with

digital video microscopy. Whereas almost all neurons showed a rise in intracellular  $Ca^{2+}$  in response to glutamate, many but not all of the same cells also showed a  $Ca^{2+}$  rise of smaller magnitude in response to aspartate.

These ultrastructural immunocytochemical data, taken in conjunction with biochemical and electrophysiological experiments, suggest that glutamate, and to a lesser extent aspartate, may play an important neurotransmitter role in a wide variety of hypothalamic circuits.

While much previous cytochemical work in the hypothalamus has concentrated on neuroactive peptides and other neurotransmitters, little has focused on excitatory amino acids (Poulain and Wakerly, 1982; Silverman and Pickard, 1983; Swanson and Sawchenko, 1983; Renaud et al., 1985; Renaud, 1987; Sladek and Armstrong, 1987; Swanson, 1987; Hokfelt et al., 1989; Ganong and Martini, 1990). In other areas of the brain where neurons have been reported to utilize an amino acid as a neurotransmitter, high levels of that amino acid are found in the presynaptic axon terminals (Storm-Mathisen et al., 1983; Ottersen and Storm-Mathisen, 1984; van den Pol, 1985; Somogyi et al., 1986; van den Pol and Gorcs, 1988). The present article employs extensively characterized antiserum against glutamate to study the ultrastructural distribution of hypothalamic presynaptic axonal endings that contain high concentrations of immunoreactive glutamate. The antibody used binds to glutamate fixed with glutaraldehyde, but not to glutamate when it is part of the normal amino acid structure of proteins or peptides. These studies are based on postembedding immunogold staining, which allows better ultrastructural preservation than preembedding immunostaining and facilitates a semiquantitative comparison of the intensity of immunolabeling over different ultrastructural profiles.

Glutamate has been suggested as the major excitatory amino acid neurotransmitter in a number of neural loci including the hippocampus, cortex, spinal cord, and cerebellum (Curtis and Johnston, 1974; Storm-Mathisen et al., 1983; Tait and Storm-Mathisen, 1984; Somogyi et al., 1986; Conti et al., 1987) and may be the primary agent in fast excitatory neurotransmission throughout the CNS (Iversen, 1984). Glutamate is taken up into axon terminals in slices and synaptosomes and can be released in a calcium-dependent manner by electrical stimulation or high potassium (De Belleruche and Bradford, 1972; Mulder and Snyder, 1974; Vargas et al., 1977; Nicholls and Sihra, 1986). Its role as the primary excitatory neurotransmitter of motoneurons at neuromuscular junctions in some invertebrates is well established (Atwood, 1976; Bicker et al., 1988). A growing body of physiological evidence suggests that, as in other regions of the brain (Curtis and Johnston, 1974), hypothalamic cells respond

Received Sept. 25, 1990; revised Jan. 29, 1991; accepted Feb. 8, 1991.

I thank Ms. A. Schneider for excellent histological assistance and Drs. R. Vogt, C. Decavel, and S. Finkbeiner for immunoblotting, staining, and video analysis suggestions. This work was supported by NIH Grants NS 10174 and NS 16296 and by the Air Force Office of Scientific Research.

Correspondence should be addressed to A. N. van den Pol, Section of Neurosurgery, Yale University School of Medicine, 333 Cedar Street, New Haven, CT 06510.

Copyright © 1991 Society for Neuroscience 0270-6474/91/112087-15\$03.00/0

to glutamate (Moss et al., 1972; Bioulac et al., 1978; Arnauld et al., 1983) and are activated by glutamate agonists, and the postsynaptic responses of most hypothalamic neuroendocrine neurons can be blocked by glutamate antagonists (Gribkoff and Dudek, 1988; van den Pol et al., 1990). The present study seeks to localize high concentrations of excitatory amino acids, particularly glutamate, in presynaptic hypothalamic axons.

## Materials and Methods

### Antibody production

Prior to use as an antigen, the purity of glutamate was tested by high-performance liquid chromatography and was found to exhibit a high degree of purity. Glutamate was conjugated with glutaraldehyde to keyhole limpet hemocyanin (KLH). Free glutamate and free glutaraldehyde were removed by dialysis in several changes of phosphate buffer.

The glutamate-glutaraldehyde-KLH antigen complex was mixed with complete Freund's adjuvant and injected both sub- and intracutaneously into the backs of several albino rabbits. After 5 weeks, a boost was given with the same antigen in incomplete Freund's adjuvant.

Sera were tested with glutamate conjugated with glutaraldehyde to bovine serum albumin (BSA) on nitrocellulose; staining of glutamate was compared with staining of GABA, aspartate, glycine, and glutamine. The serum with the greatest titer and least cross-reactivity (GLU-2) was used for further analysis, affinity purification, and immunocytochemical staining.

**Affinity purification.** Raw glutamate antiserum showed a slight cross-reaction on nitrocellulose with aspartate and a weaker cross-reaction with glutamine. To reduce this cross-reaction, BSA was coupled to cyanogen bromide activated Sepharose 4B, treated with glutaraldehyde, and conjugated to aspartate, glutamine, GABA, and glycine. Any remaining glutaraldehyde binding sites were saturated with lysine and ethanolamine. Glutamine antiserum was run down a column of BSA conjugated with glutaraldehyde to these heterologous amino acids to remove cross-reacting antibodies.

### Glutamate antiserum specificity

**Nitrocellulose dot blots.** Three approaches to antigen blots on nitrocellulose were used. The first required amino acids to be independently conjugated to BSA with glutaraldehyde; the resultant complexes were spotted on nitrocellulose and stained with the glutamate antisera using biotinylated goat anti-rabbit IgG followed by avidin-biotin-peroxidase complexes (ABC method of Hsu et al., 1981) used at half the concentrations recommended by the supplier (Vector Labs). Rabbit antiserum against aspartate (gift of Dr. T. Gorcs) was tested in a similar manner. Specificity was also tested with glutaraldehyde-activated polylysine nitrocellulose onto which spots of amino acids could be placed as described by Hodgson et al. (1985).

Immunodot blots were also tested with the peroxidase anti-peroxidase (PAP) procedure of Sternberger (1986). Glutamate was bound with glutaraldehyde to bovine serum albumin. Other putative neuroactive amino acids were also used to test cross-reactivity; these included aspartate, GABA, glycine, and taurine. Equimolar concentrations of the substances were blotted on nitrocellulose with a pore size of 0.22  $\mu$ m using a Biorad 96-well dot-blot apparatus. Nitrocellulose was then treated overnight with 5% milk and 1% lysine to reduce nonspecific immunoglobulin sticking. Nitrocellulose strips were incubated in the glutamate antiserum at a 1:2000 dilution for 2 hr, washed with phosphate buffer, incubated in secondary goat anti-rabbit immunoglobulin for 45 min, washed, and incubated in rabbit peroxidase anti-peroxidase. Nitrocellulose strips were then incubated in diaminobenzidine with hydrogen peroxide.

**ELISA tests for cross-reactivity.** To quantify further the potential cross-reactions of the antiserum, a test was applied allowing use of spectrophotometry of 96-well plastic plates. Ninety-six-well plates (Dynatech Immulon) were used to allow simultaneous comparison of a large number of different substances and repetitive samples of a single substance. Different amino acids conjugated by glutaraldehyde to bovine serum albumin (BSA) were adsorbed to 96-well plastic plates. Glutamate antiserum was used at dilutions of 1:1000 in a buffer containing 0.2% Triton X-100, 1.5% sodium chloride, 0.1% BSA, and 0.05 M Tris. Primary antiserum was detected with affinity-purified goat anti-rabbit immunoglobulin (Flow Labs) conjugated to horseradish peroxidase, fol-

lowed by visualization with orthophenaline diamine (OPD), as described in detail elsewhere (van den Pol and Gorcs, 1988).

To determine the density of the OPD reaction product, optical absorbance at 492 nm was measured with a BioRad EIA 96-well reader interfaced with a lab microcomputer.

**Western blots.** To test whether the glutamate antibody bound to any other protein from the hypothalamus, or to any other glutaraldehyde-treated protein, Western blots of extracted hypothalamic protein were used. Identical 1-cm strips of nitrocellulose were cut from a wide Western blot and prepared under the following conditions: (1) glutamate plus glutaraldehyde, (2) glutaraldehyde alone, (3) GABA plus glutaraldehyde, (4) no glutaraldehyde (the first four lanes were all stained with the primary glutamate antibody GLU-2), (5) GABA plus glutaraldehyde (stained with GABA antibody), and (6) glutamate plus glutaraldehyde (stained with second glutamate antibody).

Strips were stained with the PAP method as described above for the immunodot blot specificity test. Diaminobenzidine or nickel-intensified diaminobenzidine was used to detect reactivity.

**Sepharose beads.** The amino end of glutamate or GABA was conjugated by a long-carbon-chain epoxy linker to Sepharose beads. Beads were immunostained with either glutamate antiserum or GABA antiserum (Incstar), followed by fluorescein-conjugated secondary goat anti-rabbit immunoglobulin antiserum.

### Postembedding immunocytochemistry

Rats were heavily anesthetized with Nembutal and perfused transcardially with physiological saline, followed by 3% glutaraldehyde in 0.1 M phosphate buffer. After 3 hr of postfixation, 75- $\mu$ m-thick sections were cut on a Vibratome, treated with 1% osmium tetroxide for 45 min, and 1% uranyl acetate for 30 min, and embedded in Araldite. Ultrathin pale gold sections were cut on a Reichert Ultracut microtome and picked up on Formvar-coated and carbon-stabilized nickel or gold grids.

Postembedding staining with 10-nm colloidal gold (Janssen Pharmaceutical) was performed as we have previously described (van den Pol, 1984, 1985; van den Pol and Gorcs, 1988; van den Pol and Decavel, 1990). Briefly, either sections were incubated overnight in the primary antiserum (1:3000 to 1:10,000), followed by several washes, and then by 10-nm colloidal gold (1:75) adsorbed to goat anti-rabbit immunoglobulin (Janssen Pharmaceutical), or sections were treated with sodium metaperiodate for 12 min, primary antiserum (1:3000 to 1:6000) for 2 hr, and then with colloidal gold. All staining was done at room temperature in a humidified environment.

**Silver-intensified gold.** To increase the size and visibility of the metallic particles after immunolabeling on ultrathin sections, some grids were placed in a silver physical developer described in detail elsewhere (Liesegang, 1911; Danacher, 1981; Holgate et al., 1983; van den Pol, 1985, 1986b) or in the physical developer from Janssen Pharmaceutical. Grids were placed on drops of silver solution for 3–4 min, and then washed in distilled deionized water several times (van den Pol, 1989).

**Serial ultrathin section staining with different antisera.** To study single axonal boutons stained with GABA or glutamate antisera, serial ultrathin sections were cut from the magnocellular region of the paraventricular nucleus and picked up on different gold grids. Alternate sections were stained for glutamate or for GABA with the colloidal gold procedures described above. The GABA antiserum has been tested with immunodot blot and shows no cross-reaction with glutamate.

**Digital imaging of calcium.** To examine the response of hypothalamic neurons to glutamate and aspartate, hypothalamic neurons from fetal rats (embryonic days 17–21) were grown on glass coverslips coated with polylysine. Ten days after plating, cells were loaded with the calcium-sensitive dye fluo-3 acetoxymethyl ester or calcium green acetoxymethyl ester (Molecular Probes) and studied with digital video microscopy as described elsewhere (Cornell-Bell et al., 1990; van den Pol et al., 1990). Experiments examining the responses to glutamate, NMDA, and aspartate were done with a HEPES buffer (10 mM HEPES, 25 mM glucose, 3 mM calcium chloride, 137 mM sodium chloride, 5.3 mM potassium chloride, 5 mM glycine). Neurons were grown in higher densities than we previously used (van den Pol et al., 1990) in minimal essential medium (Gibco) without added glutamine. A Hamamatsu 2400 SIT video camera was interfaced with an Imaging Technology Inc. 151 video processor and an IBM AT microcomputer. A computer-controlled shutter kept the cells in darkness except during the times when video frames were being recorded.

GLUTAMATE AB	ASPARTATE AB
GLU	ASP
GABA	TAU
ASP	GLU
GLY	GLY
TAU	GABA
BSA (NO GA)	CYS
BSA	GA
BSA/TBG	BSA

**Figure 1.** Different amino acids were conjugated with glutaraldehyde to BSA and applied in 2- $\mu$ l quantities to nitrocellulose strips. Glutamate antiserum stained only the glutamate-containing spot and did not stain other amino acids linked to the same carrier protein. Similarly, aspartate antibody stained only the aspartate-containing spot. GA, glutaraldehyde; BSA, bovine serum albumin; TBG, thyroglobulin.

## Results

### Antiserum characterization

**Immunoblot blot.** With the dot blot test for cross-reactivity, only the spot containing glutamate bound with glutaraldehyde to BSA gave a strong positive reaction. No appreciable reaction was detected with the same protein carrier bound with glutaraldehyde to aspartate, GABA, glycine, taurine, native BSA, or glutaraldehyde activated BSA (Fig. 1). The antiserum did not bind to the dipeptide aspartyl glutamate. Lysine was used to block activated glutaraldehyde binding sites, and reactivity with this amino acid was not seen. A different antibody against aspartate reacted only with the aspartate-containing spot (Fig. 1).

**Western blots.** The tests for specificity with the glutamate antiserum on the Western blots (Fig. 2) control for several factors. This antiserum did not bind to any detectable protein in its native state or after glutaraldehyde cross-linking. It also did not bind to a different neurotransmitter amino acid (GABA) conjugated with glutaraldehyde to any detectable protein. As expected, the antiserum bound to hundreds of different proteins of different molecular weights that had been treated with glutaraldehyde and glutamate.

**ELISA analysis.** The ELISA-type assay allowed a quantitative assessment of possible cross-reactivity of the glutamate antiserum. A number of substances were tested for possible cross-reactivity. Percentage of cross-reactivity was determined by comparison of the absorbance of 0.1 M of the substance being tested with the absorbance of different concentrations of glutamate standards tested at the same time, as described in more detail for glycine antisera (van den Pol and Gorcs, 1988). No significant cross-reaction was found with any of the primary amino acid neurotransmitter candidates, including GABA, glycine, or aspartate, nor with any other amino acid or compound

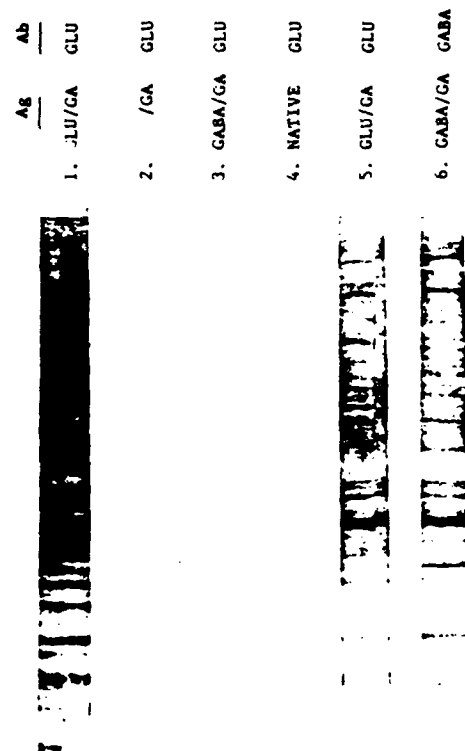


**Figure 2.** Western blots of hypothalamic protein. The lane on the left shows the glutamate antibody bound to a large number of proteins of different molecular weights fixed with glutaraldehyde (GA) and bound with glutamate (GLU). The second lane shows the glutamate antibody did not bind to proteins fixed with glutaraldehyde in the absence of glutamate, to proteins fixed with glutaraldehyde and bound to GABA (lane 3), or to native unfixed proteins (lane 4). Lane 5 shows that a different glutamate antiserum (from Dr. T. Gorcs) reacts to proteins fixed with glutaraldehyde and bound to glutamate. Lane 6 shows the GABA antibody (Incstar) with a similar pattern of binding to lanes 1 and 5. Ag, antigen; Ab, antibody.

(Table 1). A slight cross-reactivity with D-glutamate (2.9%) was detected; because D-glutamate is not found in any quantity in the brain, this should not pose a problem. A general level of binding in the 0.1–0.3% range was found for most glutaraldehyde-conjugated amino acids.

**Fixation dependency.** To determine if the glutamate recognition was dependent on the glutaraldehyde fixative, several other conjugation procedures were tried. As expected, 10% paraformaldehyde substituted for 10% glutaraldehyde did not bind sufficient glutamate and was not detected by the antibody. On the other hand, 10% acrolein substituted for 10% glutaraldehyde bound glutamate, and the glutamate antiserum discriminated glutamate–acrolein–BSA from other amino acids bound similarly with acrolein and BSA; the binding affinity for acrolein-conjugated glutamate was only a small fraction of that for glutaraldehyde-conjugated glutamate (Table 1). The glutamate antiserum did not bind to glycine, GABA, or aspartate conjugated by acrolein.

**Sepharose beads.** The glutamate antiserum bound only to the glutamate–epoxy Sepharose, and not to the GABA–epoxy Sepharose (Fig. 3). That the GABA conjugation had been suc-

Table 1. Cross-reactivity of affinity-purified glutamate antiserum

Amino acid	Cross-reactivity
Alanine	
$\beta$ -Alanine	
D-Aspartate	
L-Aspartate	
Carnosine	
Cysteine	
Ethanolamine	
GABA	
D-Glutamate	2.9%
L-Glutamate	100 %
(Acetyl)-glutamate	
Glutamine	
(Acetyl)-glutamine	
Glycine	
(Acetyl)-glycine	
Homo-carnosine	
Lysine	
Methionine	
Phenylalanine	
Proline	
Serine	
Taurine	
Tris	
Tryptophan	
Valine	
Polyamino acids	
Poly-aspartate	
Poly-glutamate	
Poly-glycine	
Peptides	
Aspartate-glycine	
Glutamate-alanine	
Glycine-glycine-valine	
Glutamate-glutamine	
Different conjugation procedures	
Glutamate (paraformaldehyde conjugation)	
Glutamate (acrolein conjugation)	2.5%
Aspartate (acrolein conjugation)	
GABA (acrolein conjugation)	
Glycine (acrolein conjugation)	

Baseline cross-reactivity was 0–0.3% unless otherwise indicated.

cessful was indicated by positive immunostaining of the GABA-conjugated Sepharose with GABA antiserum.

#### Immunocytochemical staining

In all hypothalamic nuclei studied, including the magnocellular and parvocellular paraventricular (see Figs. 4A,B; 7), ventromedial (Fig. 4C), supraoptic (Fig. 5A), arcuate (Fig. 5B), and suprachiasmatic (Fig. 6) nuclei, and throughout the lateral hypothalamic area, glutamate-immunoreactive axon terminals were found making synaptic contact with dendrites and neuronal perikarya. Presynaptic axonal endings that had the strongest labeling with immunogold particles generally had asymmetrical Gray type I synaptic specializations (Figs. 4, 5). Small, clear, round vesicles with a diameter of about 45–50 nm were found

in the axon, often clustered near the point of synaptic contact. The highest level of gold labeling per unit area was in regions containing synaptic vesicles (Figs. 4–7). Mitochondria generally had a higher level of gold labeling in immunoreactive presynaptic axons than found in mitochondria in the postsynaptic dendrite. The level of label in astrocytic processes was consistently very low.

Medium-size dense-core vesicles with a diameter of about 60 nm were often found in axonal endings filled with small, clear vesicles that were immunoreactive for glutamate in all the regions studied, as shown in an example from the paraventricular nucleus (Fig. 4B). While the small, clear vesicles were often tightly apposed to the presynaptic side of the synaptic membrane specialization, dense-core vesicles were found farther back or lateral to the membrane specialization. While single thin sections did not always reveal dense-core vesicles in axonal endings, serial sections through boutons generally showed some dense-core vesicles in each bouton.

To determine the identity of the neuropil elements with the greatest glutamate immunoreactivity, 30 micrographs with a final magnification of 60,000 $\times$  were studied in the paraventricular nucleus. To reduce the probability of focusing on metabolic glutamate, cell bodies and their proximal dendrites that might use glutamate for protein synthesis or for other perikaryal metabolic processes were excluded from this analysis. In 28 of 30 electron micrographs, from over 500 neuropil profiles including axons, dendrites, dendritic spines, and glial processes, axon terminals showed the highest level of glutamate immunoreactivity.

Because axons in general showed a variable level of immunoreactivity, single boutons on serial sections were stained for either GABA or glutamate to determine if axons with low levels of glutamate were GABAergic; glutamate in GABAergic neurons is needed for the enzyme glutamate decarboxylase to synthesize GABA. Axons that showed the most intense staining with glutamate antisera (Fig. 7A) generally did not stain for GABA (Fig. 7B), while axons that were clearly GABA immunoreactive (Fig. 7C) showed a lower level of staining for glutamate (Fig. 7D). In a comparison of serial sections through 27 boutons stained alternately for GABA or glutamate using a stereological approach described elsewhere (Somogyi et al., 1986; Ottersen, 1989; Decavel and van den Pol, 1990), those boutons that were not GABA immunoreactive (mean, 1 particle) showed a mean of  $23.6 \pm 2.2$  ( $\pm$ SEM) particles/ $\mu\text{m}^2$  after glutamate staining, while those immunoreactive for GABA (mean, 23 particles) showed less (mean,  $13.6 \pm 2.8$  particles/ $\mu\text{m}^2$ ) glutamate immunoreactivity. The difference in the intensity of labeling for glutamate in GABAergic and non-GABAergic axons was statistically significant ( $p < 0.05$ ), with GABA-immunoreactive terminals showing 74% fewer particles.

To compare the intensity of immunostaining in axons and dendrites, the number of gold particles per unit area was counted. Twenty axons from the paraventricular nucleus had a mean of  $10.7 \pm 2.6$  gold particles compared to their postsynaptic dendrites of  $3.5 \pm 0.8$  for the same area. By paired  $t$  test the difference was statistically significant ( $p < 0.01$ ). Of 20 axodendritic synapses, 18 had a larger number of gold particles in the presynaptic axon than in the postsynaptic dendrite, one had an equal number, and one had a more strongly labeled dendrite. In these comparisons, axons were used irrespective of the type of synaptic specialization they made. Some axons making asymmetrical synaptic specializations had up to eight times more

gold particles per unit area than their postsynaptic dendrite and were the most immunoreactive structures found in the neuropil.

Whereas the primary focus of the present article is on glutamate, aspartate is another possible excitatory amino acid transmitter. Immunostaining with aspartate antisera in the paraventricular and arcuate nuclei showed strong staining in some axons, and little or no staining in others (Fig. 8). Some neuronal perikarya and proximal dendrites also showed aspartate immunoreactivity (Fig. 8).

#### Calcium response to aspartate and glutamate

Under the culture conditions used in the present experiment, many neurons responded to aspartate with a dose-dependent increase in intracellular  $\text{Ca}^{2+}$  (Fig. 9). Neurons showed a greater response to glutamate than to an equimolar concentration of aspartate (Fig. 9), regardless of the serial order of amino acid perfusion. Cells that responded to 10 and 100  $\mu\text{M}$  aspartate also responded to 10 and 100  $\mu\text{M}$  NMDA (Fig. 9, cells TL1–3). Some cells showed little or no response to aspartate or NMDA, but did show an intracellular  $\text{Ca}^{2+}$  rise in response to 10  $\mu\text{M}$  glutamate (cells TL4, TL6). In most cells, the intracellular  $\text{Ca}^{2+}$  rise was followed by a fall after removal of the transmitter or agonist (cells TL1–4, TL6). However, a few cells (e.g., cell TL5) showed an increase in intracellular  $\text{Ca}^{2+}$  rise in response to aspartate, which stayed elevated throughout the time course of the experiment.

#### Perikaryal immunostaining

Neuron perikarya showed greater immunoreactivity than adjacent glia in the same section (Fig. 10). In the arcuate nucleus, counts of silver-intensified gold particles showed that glial cells had a mean of  $6.7 \pm 0.8$  particles/ $\mu\text{m}^2$  while neurons had  $20.3 \pm 0.7$  particles/ $\mu\text{m}^2$  over the same area, a statistically greater number ( $t$  test;  $t = 13.7$ ;  $\text{df} = 22$ ;  $p < 0.001$ ). Similarly, neurons in the paraventricular nucleus showed a stronger immunoreactivity than nearby glial cells, as reported in the magnocellular supraoptic nucleus (Meeker et al., 1989). Neuronal perikarya throughout the hypothalamus have a higher level of labeling than found in the neuropil in general. The density of immunogold staining over perikarya varied with cell type; cell bodies of magnocellular neurosecretory neurons were more strongly labeled than other cells of the medial hypothalamus.

#### Control immunostaining in hypothalamus

After absorption of the respective homologous antiserum with glutamate or aspartate conjugated by glutaraldehyde to bovine serum albumin, only background nonspecific labeling was observed. Absorption with GABA conjugated to bovine serum albumin did not block staining with glutamate antiserum. Post-embedding control immunostaining with GABA antisera on the same sections labeled only a subset of axons that made symmetrical synapses as described before (van den Pol, 1985, 1986a, 1989) and, in general, did not stain axons that made asymmetrical synaptic junctions. Postembedding staining with peptide antisera against neuropeptides or luteinizing hormone-releasing hormone stained only granules in a small population of axons and did not give the staining patterns seen with post-embedding immunogold studies with amino acid antisera.

Silver intensification of gold facilitated detection of the particles (Fig. 4). Control grids intensified in silver physical developer but not immunolabeled with gold showed no labeling with the development times used here. Extended incubation of grids

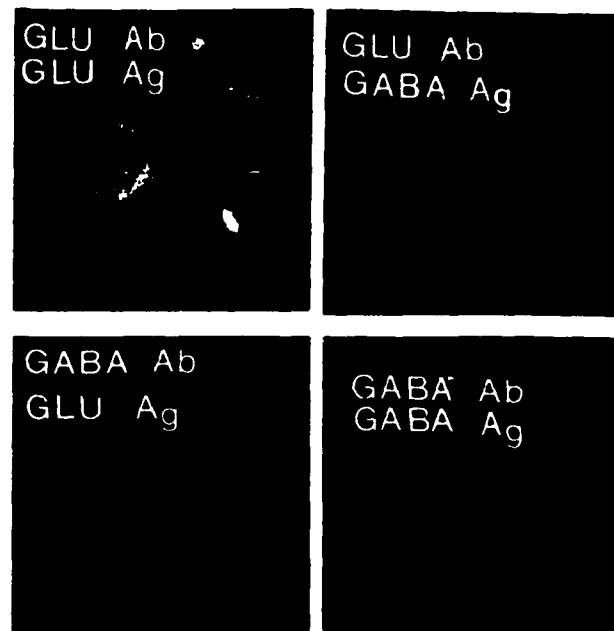


**Figure 3.** Glutamate (GLU) or GABA antigens (Ag) were conjugated to Sepharose beads. Glutamate antisera (Ab) stained only the glutamate-conjugated beads (top left) and did not stain the GABA-containing beads (top right). GABA antisera, on the other hand, stained only GABA-containing beads, but not glutamate-containing beads.

in the physical developer eventually led to a random precipitation of different-sized silver particles over all tissue and non-tissue areas of an ultrathin section.

#### Discussion

**Glutamate as a hypothalamic transmitter.** Although the finding of high levels of a suspected neurotransmitter antigen in presynaptic axon terminals does not by itself prove that the substance is released as a neurotransmitter, it is a necessary piece of evidence in this regard. That glutamate acts as a hypothalamic neurotransmitter in neuroendocrine circuits has received support from electrophysiological recordings. Application of glutamate to magnocellular neurons invariably causes an increase in the firing rate of stimulated neurons (Moss et al., 1972; Bioulac et al., 1978; Arnould et al., 1983), similar to other neurons in the brain (Curtis and Johnston, 1974; Iversen, 1984). Broad-spectrum excitatory amino acid antagonists such as kynurenic acid and gamma *D*-glutamylglycine block the action of the endogenous transmitter released by electrical stimulation of afferent projections to the supraoptic (Gribkoff and Dudek, 1988, 1990) and paraventricular nuclei (Wuarin and Dudek, 1988) and block most spontaneous excitatory postsynaptic potentials in these nuclei. Similarly, the non-NMDA glutamate receptor antagonist 6-cyano-7-dinitroquinoxaline-2,3-dione (CNQX) consistently blocked the majority of the excitatory response to electrical stimulation of the afferent axons projecting to the paraventricular and arcuate nuclei (van den Pol et al., 1990).

The data in the present study suggest glutamate as the primary candidate for the specific excitatory amino acid released by neuronal endings whose actions are blocked by general excitatory amino acid antagonists. Aspartate, localized in some hypothalamic axons, causes a smaller intracellular  $\text{Ca}^{2+}$  rise than does glutamate in many of the same cells tested. Cells cultured from

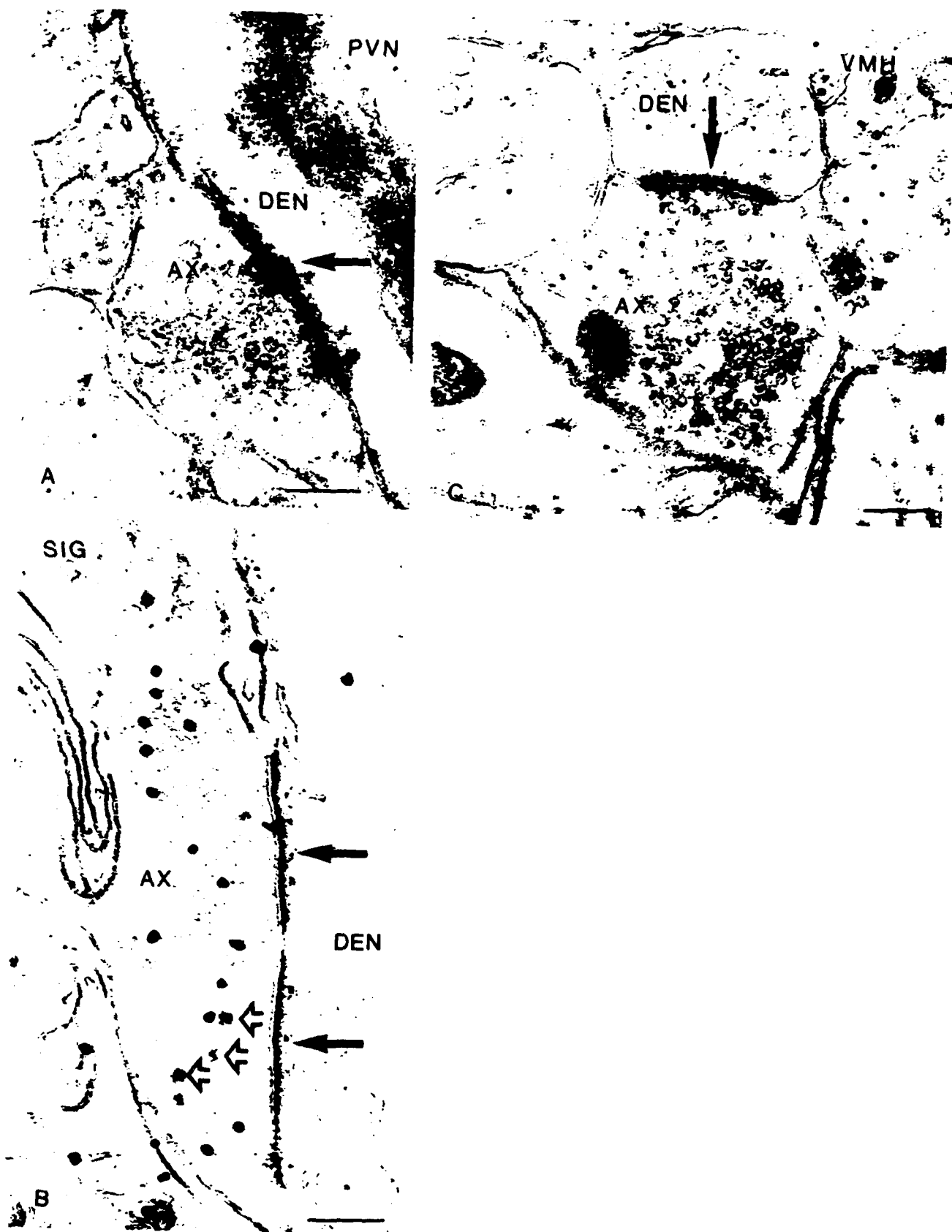


**Figure 4.** Glutamate immunoreactivity is found in the paraventricular nucleus (PVN) in axon terminals. *A*, Round, clear vesicles are found in large numbers at the site of synaptic junction (arrow) in axons (AX) immunolabeled for glutamate with 10-nm colloidal gold. These are presynaptic to dendrites (DEN) with a much lower level of gold labeling. *B*, Silver-intensified gold (SIG) particles label a PVN presynaptic axon that is immunoreactive for glutamate. Silver intensification makes the metallic particles an order of magnitude larger. Dense-core vesicles in glutamate-immunoreactive axons are noted by open arrows, synapse by solid arrow. *C*, Ventromedial nucleus (VMH) glutamate immunoreactivity is shown by gold labeling of axon (AX) that makes synaptic contact (arrow) with small dendrite. Scale bars: *A*, 0.18  $\mu\text{m}$ ; *B*, 0.22  $\mu\text{m}$ ; *C*, 0.19  $\mu\text{m}$ .

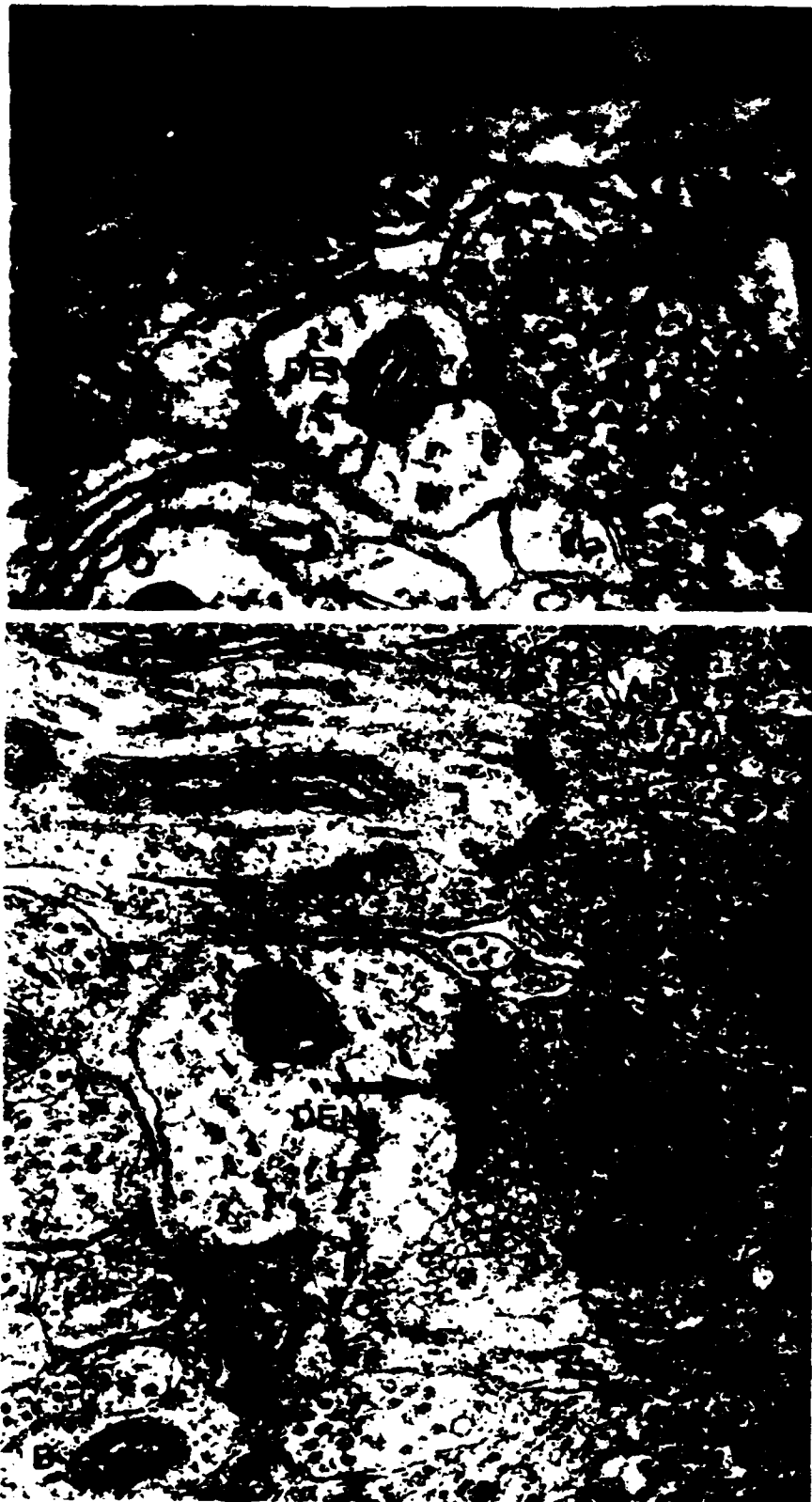


**Figure 5.** Supraoptic (SON; *A*) and arcuate (ARC; *B*) nucleus glutamate immunoreactivity. Immunoreactive axons (AX) exhibit a strong level of gold labeling compared with a postsynaptic dendrite (DEN) in both the SON and the ARC. Synaptic specializations are indicated by arrows. Scale bars, *A*, 0.14  $\mu$ m; *B*, 0.20  $\mu$ m.

the mediobasal hypothalamus showed a heterogeneous group of responses to glutamate, aspartate, and NMDA. In a previous experiment, we found that almost all cells in culture responded to glutamate, kainate, and quisqualate, but only a minor response was seen to NMDA (van den Pol et al., 1990). By chang-

ing several of the culture conditions, increasing the cell density, and eliminating extra glutamine, we found a more widespread response to NMDA. Exactly which factors may facilitate NMDA receptor expression is not clear; one of several possibilities is that the absence of glutamine, which can be converted to glu-



**Figure 6.** Suprachiasmatic nucleus (SCN) axon (AX). An axon in the SCN is heavily labeled with 10 nm gold particles (arrows). This photomicrograph is shown at low magnification to demonstrate the high immunoreactivity of this axon compared with the lower level of glutamate immunoreactivity found over the other axons, dendrites, and glial processes here. Scale bar, 0.24  $\mu$ m.

glutamate and thereby influence cell survival (Goldberg et al., 1988) and amino acid receptor expression, may have facilitated the increase in the NMDA response. Whether aspartate acts solely at the NMDA receptor (Patneau and Mayer, 1990) or at several receptor sites (Watkins and Evans, 1981) of hypothalamic neurons remains to be determined.

Substances that block the action of nonexcitatory amino acid

neurotransmitters may alter the firing rate of hypothalamic neurons, but are relatively ineffective in blocking the actions of the endogenous transmitter released by electrical stimulation (Gribkoff and Dudek, 1990).

The source of glutamate-containing axons is unclear, but they probably arise from many loci. Some of the axons in the suprachiasmatic nucleus with high glutamate immunoreactivity

may arise from the retina (Hendrickson et al., 1972; Moore and Lenn, 1972). Electrical stimulation of the optic nerve releases glutamate, but not GABA (Liou et al., 1986), and glutamate mimics the release of the retinal transmitter. The glutamate receptor antagonist kynurenic acid blocks the postsynaptic response to optic nerve stimulation as measured by field potentials (Shibata et al., 1986; Cahill and Menaker, 1987) and intracellular recording (Kim and Dudek, 1989). Behavioral experiments have shown that injections of glutamate into the suprachiasmatic nucleus, the putative site of the mammalian biological clock, cause a phase shift in activity cycles (Meijer et al., 1988).

That mediobasal hypothalamic neurons contain glutamate receptors is illustrated by experiments showing massive neuronal damage to cells and dendrites of the arcuate nucleus, but not to adjacent axons, after peripheral administration of monosodium glutamate to young rodents and primates (Olney and Sharpe, 1969; Olney et al., 1971). Damage to this region of the brain via the excitotoxic effects of large doses of glutamate occurs together with disturbances in the regulation of the endocrine system and caloric balances controlled by this region of the brain. Focal injections of excitatory neurotoxins including ibotenate and kainate have been reported to kill cells in the paraventricular nucleus, with some difference in toxicity among the different cell types (Zhang and Ciriello, 1985; Herman and Wiegand, 1986). That cells in some regions of the hypothalamus seem more resistant to neurotoxic glutamate analogs than cells elsewhere (Peterson and Moore, 1980; Hastings et al., 1985) may be due to different types of receptors, differences in second-messenger systems, or different levels of ion channel activation. This resistance may also be due to fewer receptors, as shown by lower levels of receptor binding by glutamate agonists in the hypothalamus than in cortical areas (Monaghan and Cotman, 1982; Rainbow et al., 1984; Cotman et al., 1987). Evidence showing that a recently isolated novel glutamate receptor (GluR5) is expressed more strongly in the hypothalamus than in other areas of brain such as the hippocampus may explain some of the differences in response to glutamate (Bettler et al., 1990).

**Immunocytochemical specificity.** Because the amino end of glutamate is bound by glutaraldehyde, the antibody probably requires a free carboxy terminal to bind to. A different antibody against glutamate (Madl et al., 1986) can react with glutamate as part of the carboxy terminal of the tubulin protein, but not to tubulin lacking the glutamate at the carboxy terminal (McDonald et al., 1989).

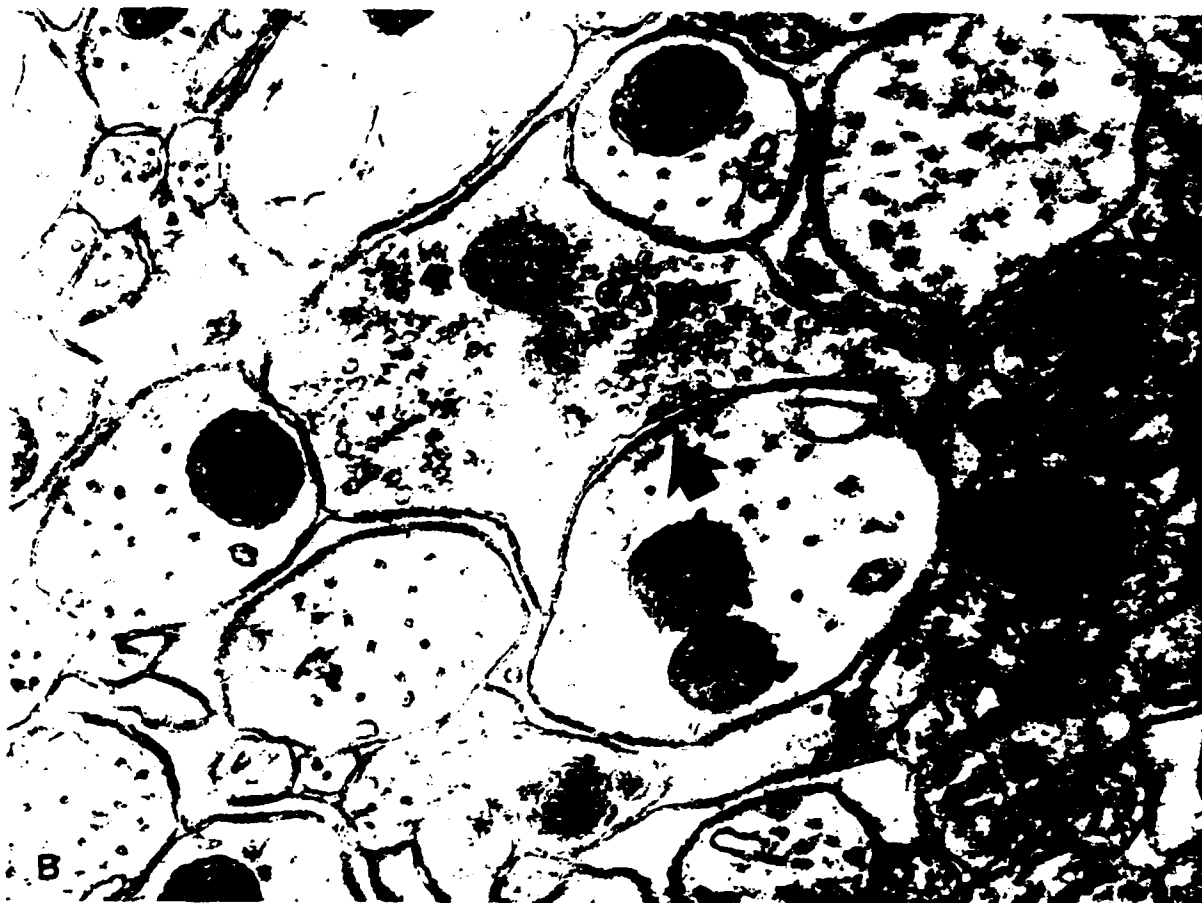
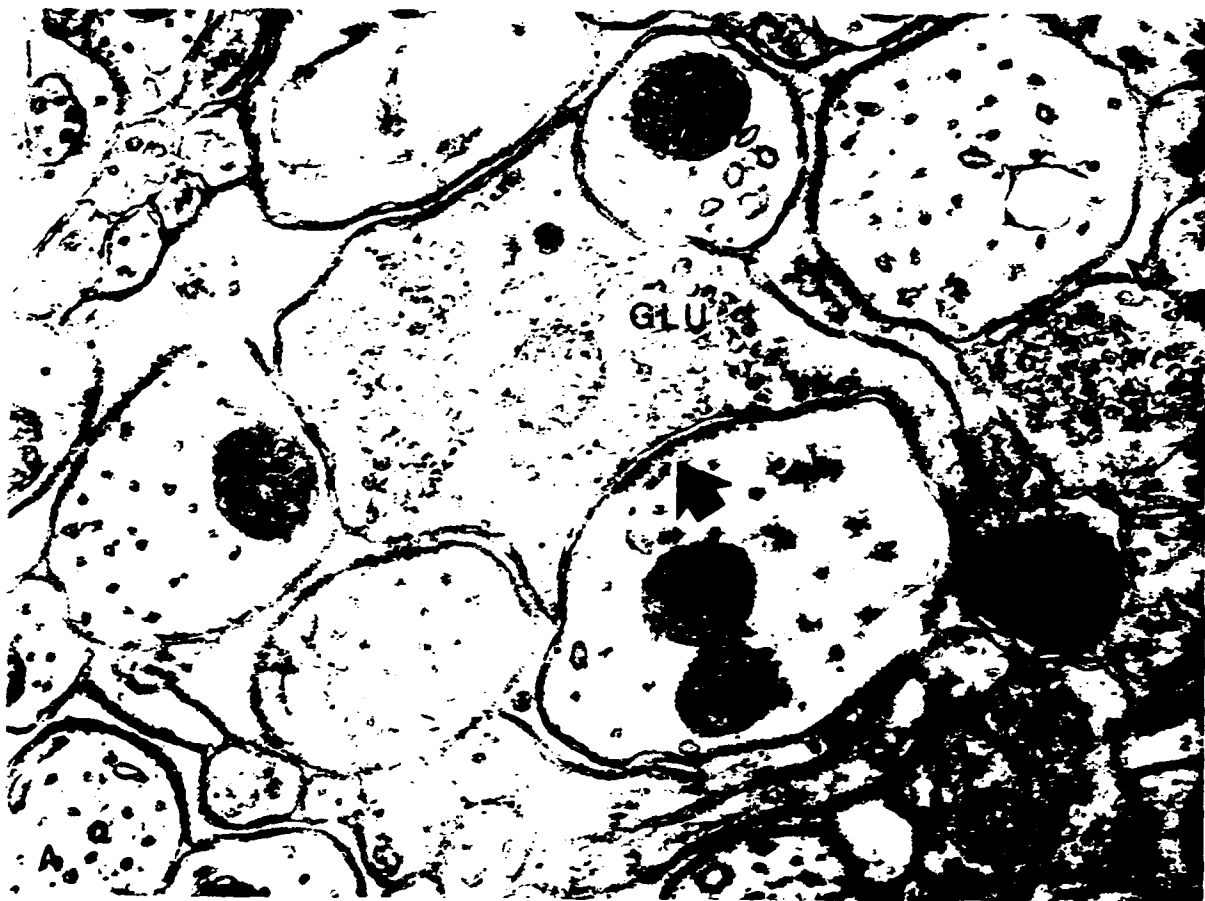
When paraformaldehyde, a common fixative for microscopy, was substituted for glutaraldehyde with either immunodot blots or with the ELISA assay, the antibody used in the present study did not bind. This may have been due to paraformaldehyde not sufficiently cross-linking the glutamate to the protein matrix, and thus the glutamate was washed out. This is important in terms of the immunocytochemical localization in brain tissue. Most common fixatives for electron microscopy employ combinations of paraformaldehyde and glutaraldehyde that result in excellent fixation (see references in Peters et al., 1976). How-

ever, in the present case, where immunocytochemical localization of the glutamate is desired, paraformaldehyde would compete with glutaraldehyde for the available intracellular glutamate, and the paraformaldehyde-glutamate dimer would be subsequently washed out of the tissue. This is a particular problem because paraformaldehyde penetrates into tissue faster and is often used in an excess molarity compared with glutaraldehyde. Acrolein works better than paraformaldehyde, but still results in the loss of 97.5% of the signal. Because we found similar results with another antiserum against glycine conjugated by glutaraldehyde to thyroglobulin (van den Pol and Gorcs, 1988), one might expect most antibodies made against an amino acid conjugated by glutaraldehyde to a protein carrier molecule would react in a similar fashion, and therefore, caution should be exercised against using paraformaldehyde during tissue fixation if maximal amino acid antigen retention is important.

**Cellular localization of glutamate immunoreactivity.** An uneven distribution of a neurochemical is sometimes used as one criterion for its function as a neurotransmitter. When different brain regions are compared, a twofold difference in glutamate content can be detected (Curtis and Johnston, 1974). This uneven distribution is greatly magnified at the subcellular level, with presynaptic axons showing an average of three times and up to eight times more gold particles than dendrites postsynaptic to those axons. In comparison, hypothalamic axons immunoreactive for GABA had 10–20 times more gold particles over the presynaptic axon than over the postsynaptic dendrite (van den Pol, 1985, 1986a). The finding of different ratios of labeling is consistent with the role of glutamate both in neurotransmission and in metabolic activities including protein synthesis. GABA, on the other hand, which is not incorporated into proteins and does not have known significant roles other than neurotransmission, would be expected to have a higher ratio of labeling in immunoreactive axons compared to other elements of the neuropil. Glutamate immunoreactivity is high in axons of neural circuits known to be excitatory and postulated to use glutamate as a neurotransmitter. In the cerebellar cortex, excitatory terminals of mossy fibers and parallel fibers had higher levels of immunoreactivity than axon terminals from a known inhibitory cell, the Golgi cell (Somogyi et al., 1986). Similarly, in the hippocampus, mossy fibers that synapse on pyramidal cells have been postulated to use glutamate as a neurotransmitter (Storm-Mathisen et al., 1983). With the glutamate antiserum used in the present study, we confirmed the high level of glutamate in mossy fibers relative to other elements of the neuropil. The ratios of glutamate in some axons of the hypothalamic neuropil in the present study compare favorably with similar ratios found in excitatory axons of the cerebellum for which glutamate is the primary neurotransmitter candidate (Somogyi et al., 1986).

Asymmetrical synapses are often considered to be indicative of excitatory endings, while symmetrical synapses are thought to be inhibitory (see discussion in Peters et al., 1976). Data from the present study are in general agreement with this; however,

**Figure 7.** Dual staining with glutamate (GLU) and GABA antisera. *A*, Large numbers of gold particles are found over an axon making an asymmetrical synaptic contact (solid arrow) and over a bouton not making synaptic contact (open arrow). *B*, The same axons are not labeled when GABA antiserum is substituted for glutamate antiserum. Arrows are same as in *A*. *C*, As a further control, on the same ultrathin section used in *B*, high densities of gold labeling immunoreactive GABA can be found over many axons making symmetrical synaptic contact (arrow). *D*, Glutamate staining of the same bouton from the same section as illustrated in *A* shows fewer gold particles. Scale bar, 0.15  $\mu$ m.





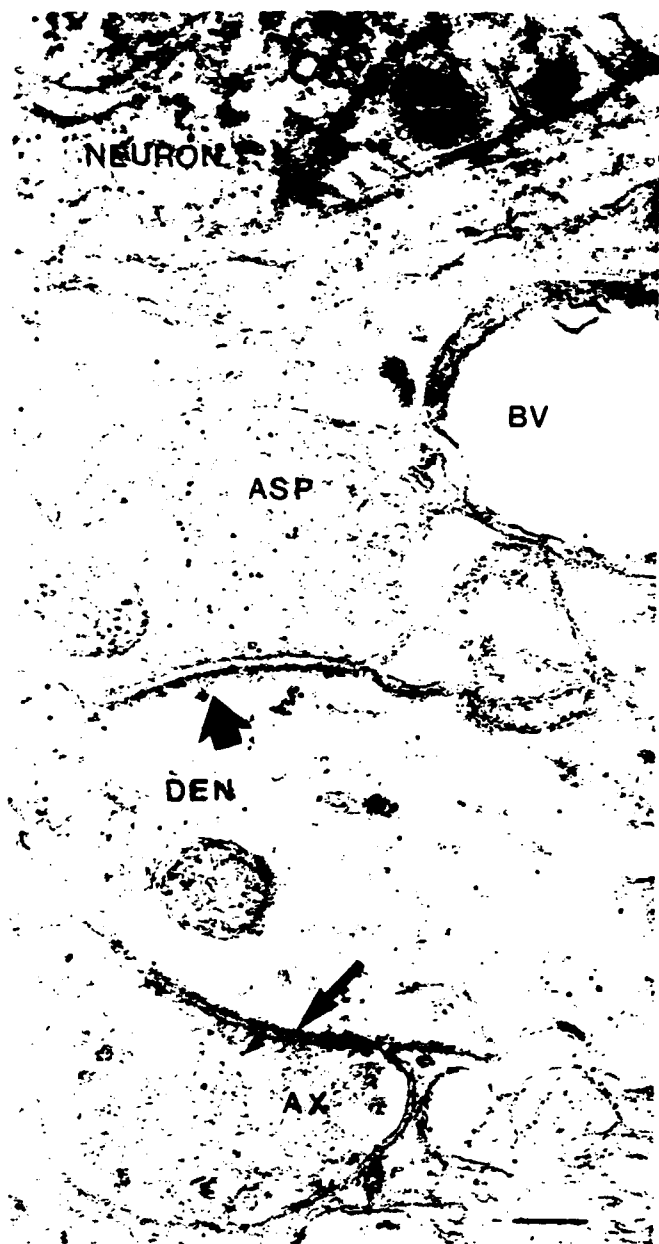


**Figure 8.** Aspartate (ASP) immunoreactivity in the paraventricular nucleus. One axon (ASP) makes an asymmetrical synapse on a dendrite (DEN) that is slightly labeled. A second axon (AX) shows little label. The lumen of the blood vessel (BV) is almost clear of gold particles. At the top of the micrograph, the cell body of a magnocellular neuron is labeled (NEURON). Scale bar, 150 nm.

some presynaptic axons with strong glutamate immunoreactivity, and no GABA immunoreactivity, appeared to make symmetrical synapses. This could in part be due to the plane of the ultrathin section relative to the orientation of the synaptic cleft. However, we have also found a small percentage (1–3%) of hypothalamic boutons strongly immunoreactive for GABA that make strikingly asymmetrical synaptic endings (Decavel and van den Pol, 1990). Together, these data would support the general probability of the inhibitory transmitter GABA being contained in boutons making symmetrical synapses and the excitatory transmitter glutamate in boutons making asymmet-

#### CALCIUM RESPONSE TO ASPARTATE, NMDA, GLUTAMATE

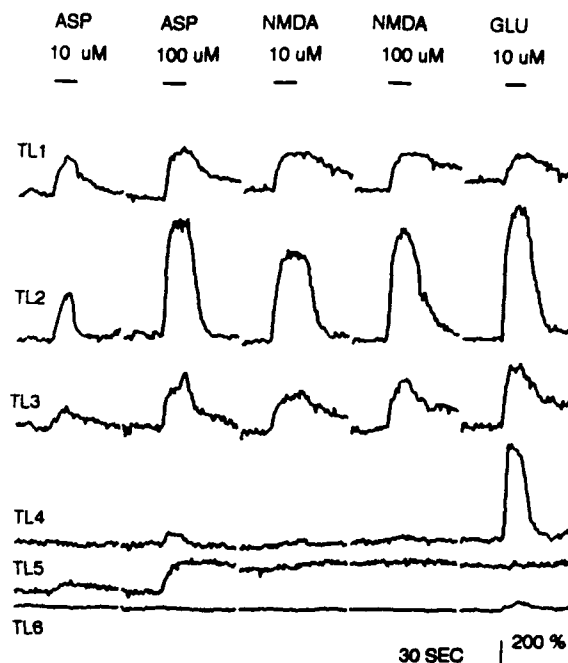


**Figure 9.** Recordings were made simultaneously from six hypothalamic cells (TL1–6) loaded with fluo-3. Recordings were normalized to the baseline fluorescence from each cell and are presented as a change in fluorescent intensity over baseline fluorescence ( $\Delta F/F$ ), allowing comparisons between cells from the same video field (Cornell-Bell et al., 1990). Each of the six cells was tested for 400 sec. For each application, recordings were made for 20 sec prior to application, during 15 sec of transmitter perfusion (shown by the lines at top) and for a 45 sec recovery period. To reduce possible phototoxicity and allow for a longer recovery period between transmitter application, an additional 60-sec recovery period was used, during which the computer-controlled shutter allowing excitation from the mercury light was kept closed (shown by short gaps in the traces). Each trace represents the average of eight video frames. The shutter was closed during the part of the second when the video signal was not being averaged. A 1% transmittance neutral-density filter was used to reduce the intensity of the excitation light.

rical synapses, but also indicate that any single bouton in the hypothalamus cannot be classified as excitatory or inhibitory simply by its synaptic morphology.

Our finding of strong glutamate immunoreactivity in some axonal endings is consistent with some data showing high-affinity uptake of radiolabeled excitatory amino acids into axon terminals (Taxt and Storm-Mathisen, 1984). That the presence of glutamate in axons is not primarily due to its role in general metabolism is suggested by *in vitro* studies of hippocampal slices. After depletion of the metabolic pool of glutamate in neuronal cell bodies, the glutamate in axon terminals still showed a robust immunoreactivity (Ottersen and Storm-Mathisen, 1985); stimuli such as high potassium or veratridine in the presence of calcium, which depolarize neurons and induce release of neurotransmitters, caused a loss of axonal glutamate immunoreactivity (Cotman et al., 1987). In some regions of the brain, glia have been shown to take up glutamate (Ehinger and Falck, 1971). In the present study, glial processes had a much lower level of labeling than did neuronal processes in the same section. This indicates that, even with a high uptake mechanism in glia, the internal pool of glutamate is not as high in glia as in neurons.

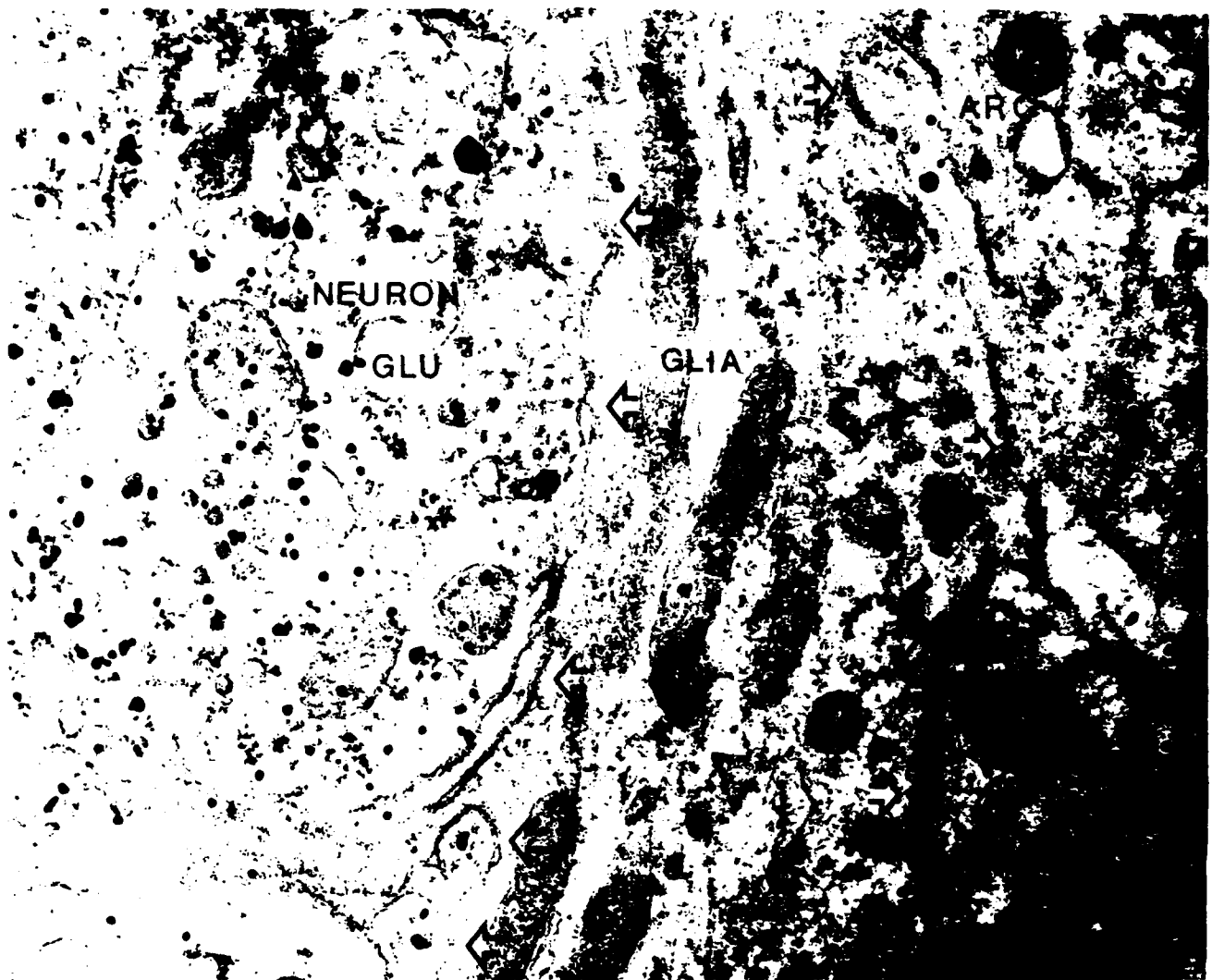


**Figure 10.** Neuron in the arcuate nucleus (ARC) is heavily immunolabeled with glutamate antiserum (GLU) and silver-intensified gold particles (NEURON), while in the adjacent glial cell (GLIA), much less labeling is seen. The boundaries of the glial cell are shown with open arrows. Scale bar, 225 nm.

As with the detection of other antigens with postembedding immunogold procedures (Somogyi and Hodgson, 1985; van den Pol, 1985; Somogyi et al., 1986; Ottersen, 1987), gold particles do not reveal all the antigens in a particular cell; however, the number of gold particles per unit area is roughly proportional to the total number of molecules (Ottersen, 1987). The absence of gold labeling in some elements of the neuropil does not necessarily indicate the absence of the amino acid. Rather, it indicates a relatively low level of glutamate in that particular cell compared with the high levels of glutamate in some axons. Had stronger concentrations of antibody or longer times of incubations been used, it is probable that more immunogold particles would be found over structures that might have less or no label with the procedures used in the present study.

Medium-size dense-core vesicles are found in many axon terminals that demonstrate a strong immunoreactivity for glutamate. Similarly, in hypothalamic axons that show high levels of GABA immunoreactivity, medium-size dense-core vesicles are invariably found in the same terminal (Decavel and van den

Pol, 1990). Because most evidence indicates that these dense-core vesicles contain neuroactive peptides or proteins, the possibility exists that cells with axons that contain high levels of either GABA or glutamate routinely synthesize peptides or proteins that are transported to the axonal ending and probably released, suggesting that colocalization of peptides with amino acid transmitters may be the rule rather than the exception in the hypothalamus. Substance P has been identified as one peptide that is colocalized in a putative glutamatergic neuron of the dorsal root ganglion (Battaglia and Rustioni, 1988).

In conclusion, data from the present experiment, together with electrophysiological data revealing a widespread response to glutamate by hypothalamic neurons, the simulation of the effects of endogenous transmitter release by glutamate, the blockade of normal excitatory neurotransmission by glutamate receptor blockers, and the cytological data that hypothalamic neurons are susceptible to glutamate-like excitatory neurotoxins, support the hypothesis that excitatory amino acids, particularly glutamate, play a major role in excitatory neurotransmission throughout the hypothalamus.

## References

- Arnauld E, Cirino M, Layton BS, Renaud LP (1983) Contrasting actions of amino acids, acetylcholine, noradrenaline, and leucine enkephalin on the excitability of supraoptic vasopressin-secreting neurons. *Neuroendocrinology* 36:187-196.
- Atwood HL (1976) Organization and synaptic physiology of crustacean neuromuscular systems. *Prog Neurobiol* 7:291-391.
- Battaglia G, Rustioni A (1988) Coexistence of glutamate and substance P in dorsal root ganglion neurons of the rat and monkey. *J Comp Neurol* 277:302-312.
- Bettler B, Boulter J, Hermans-Borgmeyer I, O'Shea-Greenfield A, Deneris ES, Moll C, Borgmeyer U, Hollman M, Heinemann S (1990) Cloning of a novel glutamate receptor subunit, GluR5: expression in the nervous system and during development. *Neuron* 5:583-595.
- Bicker G, Schafer S, Ottersen OP, Storm-Mathisen J (1988) Glutamate-like immunoreactivity in identified neuronal populations of insect nervous systems. *J Neurosci* 8:2108-2122.
- Bioulac B, Dufy B, DeVitry F, Fleury H, Tixier-Vidal A, Vincent JD (1978) Effects of acetylcholine, sodium glutamate, and GABA on the discharge of supraoptic neurons in the rat. *Brain Res* 154:159-162.
- Cahill GM, Menaker M (1987) Kynurenic acid blocks suprachiasmatic nucleus responses to optic nerve stimulation. *Brain Res* 410:125-129.
- Conti F, Rustioni A, Petrusz P, Towle AC (1987) Glutamate-positive neurons in the somatic sensory cortex of rats and monkeys. *J Neurosci* 7:1887-1901.
- Cornell-Bell AH, Finkbeiner SM, Cooper MS, Smith SJ (1990) Glutamate induces calcium waves in cultured astrocytes: long-range glial signaling. *Science* 247:470-473.
- Cotman CW, Monaghan DT, Ottersen OP, Storm-Mathisen J (1987) Anatomical organization of excitatory amino acid receptors and their pathways. *Trends Neurosci* 10:273-280.
- Curtis DR, Johnston GAR (1974) Amino acid transmitters in the mammalian central nervous system. *Ergeb Physiol* 69:97-189.
- Danscher G (1981) Histochemical demonstration of heavy metals. A revised version of the sulphide silver method suitable for both light and electron microscopy. *Histochemistry* 71:1-16.
- De Belleruche JS, Bradford HF (1972) Metabolism of beds of mammalian cortical synaptosomes: response to depolarizing influences. *J Neurochem* 19:585-602.
- Decavel C, van den Pol AN (1990) GABA: a dominant transmitter in the hypothalamus. *J Comp Neurol* 302:1019-1037.
- Ehinger B, Falck B (1971) Autoradiography of some suspected neurotransmitter substances: GABA, glycine, glutamic acid, histamine, dopamine, and L-dopa. *Brain Res* 33:157-172.
- Ganong WF, Martini L (1990) *Neuroendocrinology*, 1990. *Front Neuroendocrinol* 11:1-5.
- Goldberg MP, Monyer H, Choi DW (1988) Hypoxic neuronal injury *in vitro* depends on extracellular glutamine. *Neurosci Lett* 94:52-57.
- Gribkoff VK, Dudek FE (1988) The effects of the excitatory amino acid antagonist kynurenic acid on synaptic transmission to supraoptic neuroendocrine cells. *Brain Res* 442:152-156.
- Gribkoff VK, Dudek FE (1990) The effects of excitatory amino acid antagonists on synaptic responses of supraoptic neurons in slices of rat hypothalamus. *J Neurophysiol* 63:60-71.
- Hastings MH, Winn P, Dunnett SB (1985) Neurotoxic amino acid lesions of the lateral hypothalamus: a parametric comparison of the effects of ibotenate, N-methyl-D,L-aspartate and quisqualate in the rat. *Brain Res* 360:248-256.
- Hendrickson AE, Wagoner N, Cowan WM (1972) An autoradiographic and electron microscopic study of retino-hypothalamic connections. *Z Zellforsch* 135:1-26.
- Herman JP, Wiegand SJ (1986) Ibotenate-induced cell death in the hypothalamic paraventricular nucleus: differential susceptibility of magnocellular and parvocellular neurons. *Brain Res* 383:367-372.
- Hodgson AJ, Penke B, Erdei A, Chubb IW, Somogyi P (1985) Antisera to gamma amino butyric acid. I. Production and characterization using a new model system. *J Histochem Cytochem* 33:229-239.
- Hokfelt T, Elde R, Fuxe K, Johansson O, Ljungdahl A, Goldstein M, Luft R, Efendic S, Nilsson G, Terenius L, Ganten D, Jeffcoate SL, Rehfeld J, Said S, Perez de la Mora M, Possani L, Tapia R, Teran L, Palacios R (1978) Aminergic and peptidergic pathways in the nervous system with special reference to the hypothalamus. In: *The hypothalamus* (Recihlin S, Balderssarini RJ, Martin JB, eds), pp 69-135. New York: Raven.
- Holgate CS, Jackson P, Cowen PN, Bird CC (1983) Immunogold-silver staining: new method of immunostaining with enhanced sensitivity. *J Histochem Cytochem* 31:938-944.
- Hsu S, Raine L, Fanger H (1981) Use of avidin-biotin-peroxidase complex (ABC) in immunoperoxidase techniques: a comparison between ABC and unlabeled antibody (PAP) procedures. *J Histochem Cytochem* 29:577-580.
- Iversen LL (1984) Amino acids and peptides, fast and slow chemical signals in the nervous system? *Proc R Soc Lond [Biol]* 221:245-260.
- Kim YI, Dudek FE (1989) Antagonism of fast excitatory postsynaptic potentials in suprachiasmatic nucleus neurons by excitatory amino acid antagonists. *Soc Neurosci Abstr* 15:1088.
- Liesegang R (1911) Die Kolloidchemie der histologischen Silberfärbungen. *Kolloid Beihefte* 3:1-46.
- Liou SY, Shibata S, Iwasaki K, Ueki S (1986) Optic nerve stimulation-induced increase of release of <sup>3</sup>H-glutamate and <sup>3</sup>H-aspartate but not <sup>3</sup>H-GABA from the suprachiasmatic nucleus in slices of rat hypothalamus. *Brain Res Bull* 16:527-531.
- Madi JE, Larson AA, Beitz AJ (1986) Monoclonal antibody specific for carbodiimide-fixed glutamate: immunocytochemical localization in the rat CNS. *J Histochem Cytochem* 34:317-326.
- McDonald AJ, Beitz AJ, Larson AA, Kuriyama R, Sellitto C, Madi JE (1989) Co-localization of glutamate and tubulin in putative excitatory neurons of the hippocampus and amygdala: an immunohistochemical study using monoclonal antibodies. *Neuroscience* 30:405-421.
- Meeker RB, Swanson DJ, Hayward JN (1989) Light and electron microscopic localization of glutamate immunoreactivity in the supraoptic nucleus of the rat hypothalamus. *Neuroscience* 33:157-167.
- Meijer JH, van der Zee EA, Dietz M (1988) Glutamate phase shifts circadian activity in hamsters. *Neurosci Lett* 86:177-183.
- Monaghan DT, Cotman CW (1982) The distribution of [<sup>3</sup>H] kainic acid binding sites in rat CNS as determined by autoradiography. *Brain Res* 252:91-100.
- Moore RY, Lenn NJ (1972) A retinohypothalamic projection in the rat. *J Comp Neurol* 146:1-14.
- Moss RL, Urban I, Cross BA (1972) Microelectrophoresis of cholinergic and aminergic drugs on paraventricular neurons. *Am J Physiol* 223:310-318.
- Mulder AH, Snyder SH (1974) Potassium-induced release of amino acids from cerebral cortex and spinal cord slices of the rat. *Brain Res* 76:297-308.
- Nicholls DG, Sihra TS (1986) Synaptosomes possess an exocytotic pool of glutamate. *Nature* 321:772-774.
- Olney JW, Sharpe LG (1969) Brain lesions in an infant rhesus monkey treated with monosodium glutamate. *Science* 166:386-388.
- Olney JW, Ho OL, Rhee V (1971) Cytotoxic effects of acidic and sulfur containing amino acids on the infant mouse central nervous system. *Exp Brain Res* 14:61-70.
- Ottersen OP (1987) Postembedding light- and electron microscopic immunocytochemistry of amino acids: description of a new model system allowing identical conditions for specificity testing and tissue processing. *Exp Brain Res* 69:167-174.
- Ottersen OP (1989) Quantitative electron microscopic immunocytochemistry of neuroactive amino acids. *Anat Embryol* 180:1-15.
- Ottersen OP, Storm-Mathisen J (1984) Glutamate- and GABA-containing neurons in the mouse and rat brain, as demonstrated with a new immunocytochemical technique. *J Comp Neurol* 229:374-392.
- Ottersen OP, Storm-Mathisen J (1985) Different neuronal localization of aspartate-like and glutamate-like immunoreactivities in the hippocampus of rat, guinea-pig and senegalese baboon (*Papio papio*), with a note on the distribution of gamma-aminobutyrate. *Neuroscience* 16:589-606.
- Patneau DK, Mayer ML (1990) Structure-activity relationships for amino acid transmitter candidates acting at N-methyl-D-aspartate and quisqualate receptors. *J Neurosci* 10:2385-2399.
- Peters A, Palay SL, Webster H (1976) Fine structure of the nervous system, pp 1-406. Philadelphia: Saunders.
- Peterson GM, Moore RY (1980) Selective effects of kainic acid on diencephalic neurons. *Brain Res* 202:165-182.
- Poulain DA, Wakerley JB (1982) Electrophysiology of hypothalamic magnocellular neurons secreting oxytocin and vasopressin. *Neuroscience* 4:773-808.
- Rainbow TC, Wiczorek CM, Halpain S (1984) Quantitative autoradiography of binding sites for [<sup>3</sup>H] AMPA, a structural analogue of glutamic acid. *Brain Res* 309:173-177.

- Renaud LP (1987) Magnocellular neuroendocrine neurons: update on intrinsic properties, synaptic inputs and neuropharmacology. *Trends Neurosci* 10:498-502.
- Renaud LP, Bourque CW, Day TA, Ferguson AV, Randle JC (1985) Electrophysiology of mammalian hypothalamic supraoptic and paraventricular neurosecretory cells. In: *The electrophysiology of the secretory cell* (Poisner AM, Trifaro J, eds), pp 165-194. Amsterdam: Elsevier.
- Shibata S, Liou SY, Ueki S (1986) Influence of excitatory amino acid receptor antagonists and of baclofen on synaptic transmission in the optic nerve to the suprachiasmatic nucleus in slices of rat hypothalamus. *Neuropharmacology* 25:403-409.
- Silverman JA, Pickard GE (1983) The hypothalamus. In: *Chemical neuroanatomy* (Emson PC, ed), pp 295-336. New York: Raven.
- Sladek CD, Armstrong WE (1987) Effect of neurotransmitters and neuropeptides on vasopressin release. In: *Vasopressin* (Gash DM, Boer GJ, eds), pp 275-333. New York: Plenum.
- Somogyi P, Hodgson AJ (1985) Antiserum to gamma amino butyric acid. III. Demonstration of GABA in Golgi-impregnated neurons and in conventional electron microscopic sections of cat striate cortex. *J Histochem Cytochem* 33:249-257.
- Somogyi P, Halasy K, Somogyi J, Storm-Mathisen J, Ottersen OP (1986) Quantification of immunogold labelling reveals enrichment of glutamate in mossy and parallel fibre terminals in cat cerebellum. *Neuroscience* 19:1045-1050.
- Sternberger LA (1986) *Immunocytochemistry*. New York: Wiley.
- Storm-Mathisen J, Leknes AK, Bore AT, Vaaland JL, Edminson P, Haug FM, Ottersen OP (1983) First visualization of glutamate and GABA in neurones by immunocytochemistry. *Nature* 301:517-520.
- Swanson LW (1987) The hypothalamus. In: *Handbook of chemical neuroanatomy. Integrated systems of the CNS, Pt 1, Hypothalamus, hippocampus, amygdala, retina* (Bjorklund A, Hokfelt T, Swanson LW, eds), pp 1-124. Amsterdam: Elsevier.
- Swanson LW, Sawchenko PE (1983) Hypothalamic integration: organization of the paraventricular and supraoptic nuclei. *Annu Rev Neurosci* 6:269-324.
- Taxt T, Storm-Mathisen J (1984) Uptake of D-aspartate and L-glutamate in excitatory axon terminals in hippocampus: autoradiographic and biochemical comparison with gamma-aminobutyrate and other amino acids in normal rats and in rats with lesions. *Neuroscience* 11:79-100.
- van den Pol AN (1984) Colloidal gold and biotin-avidin conjugates as ultrastructural markers for neural antigens. *Quart J Exp Physiol* 69:1-33.
- van den Pol AN (1985) Dual ultrastructural localization of two neurotransmitter-related antigens: colloidal gold labeled neurophysin immunoreactive supraoptic neurons receive peroxidase labeled glutamate decarboxylase or gold labeled GABA immunoreactive synapses. *J Neurosci* 5:2940-2954.
- van den Pol AN (1986a) Gamma-aminobutyrate, gastrin releasing peptide, serotonin, somatostatin, and vasopressin: ultrastructural immunocytochemical localization in presynaptic axons in the suprachiasmatic nucleus. *Neuroscience* 17:643-659.
- van den Pol AN (1986b) Tyrosine hydroxylase immunoreactive neurons throughout the hypothalamus receive glutamate decarboxylase immunoreactive synapses: a double pre-embedding immunocytochemical study with particulate silver and HRP. *J Neurosci* 6:877-891.
- van den Pol AN (1989) Neuronal imaging with colloidal gold. *J Microsc* 155:27-59.
- van den Pol AN, Decavel C (1990) Synaptic interaction between chemically defined neurons: dual ultrastructural immunocytochemical approaches. In: *Methods for the analysis of neuronal microcircuits and synaptic interactions* (Bjorklund A, Hokfelt T, Wouterlood F, van den Pol AN, eds), pp 199-272. Amsterdam: Elsevier.
- van den Pol AN, Gorcs T (1988) Glycine and glycine receptor immunoreactivity in brain and spinal cord. *J Neurosci* 8:472-492.
- van den Pol AN, Wuarin JP, Dudek FE (1990) Glutamate, the dominant excitatory transmitter in neuroendocrine regulation. *Science* 250:1276-1278.
- Vargas O, de Lorenzo CD, Orrego F (1977) Effects of elevated extracellular potassium on the release of labelled noradrenaline, glutamate, glycine,  $\beta$ -alanine and other amino acids from rat brain cortex slices. *Neuroscience* 2:383-390.
- Watkins JC, Evans RH (1981) Excitatory amino acid transmitters. *Annu Rev Pharmacol Toxicol* 21:165-204.
- Wuarin JP, Dudek FE (1988) Kynurenate antagonism of fast EPSP's in paraventricular neurons. *Soc Neurosci Abstr* 14:1178.
- Zhang T-X, Ciriello J (1985) Kainic acid lesions of paraventricular nucleus neurons reverse the elevated arterial pressure after aortic baroreceptor denervation in the rat. *Brain Res* 358:334-338.

GLUTAMATE-RECEPTOR GENE EXPRESSION IN HYPOTHALAMUS:  
IN SITU HYBRIDIZATION WITH 7 RECEPTOR SUBTYPES.

A.N. van den Pol\*, I. Hermans-Borgmeyer, S. Heinemann.  
Sect. Neurosurgery, Yale Med.Sch., New Haven, CT 06510,  
Lab Molec. Neurobiol., Salk Inst., La Jolla, CA 92186.

Glutamate has received relatively little attention for its contribution to hypothalamic regulation. To examine the expression of glutamate receptor subtypes, we used in situ hybridization with <sup>35</sup>S-labeled RNA probes complementary to mRNA coded by seven of the glutamate receptor genes. GluR1 and -R2 were expressed in many hypothalamic areas including, but not restricted to, the ventromedial, arcuate, and dorsomedial nuclei, and in the preoptic area and mammillary region. GluR4 was weakly expressed in the supraoptic, paraventricular, and arcuate nuclei. GluR5 and -R6 labeling was detected in the suprachiasmatic nucleus, with a greater label density over the ventrolateral part which receives retinal input. Although detectable in other CNS regions, we found little GluR3 or -R7 label in hypothalamus. Controls with unrelated probes not expected in the hypothalamus were negative. Since the receptors may manifest different physiological properties, these data suggest a variety of cellular responses to glutamate may exist in the hypothalamus, and together with other data, underline the widespread role of glutamate in hypothalamic and neuroendocrine regulation.

In Press. Society for Neuroscience Abstracts (1992)